

Mechanisms of Type IV Collagen Targeting to Developing Basement Membranes

by

Ranjay Jayadev

Department of Pharmacology and Cancer Biology
Duke University

Date: _____

Approved:

David Sherwood, Supervisor

Xiao-Fan Wang

Harold Erickson

Brenton Hoffman

Terry Lechler

Bernard Mathey-Prevot

Dissertation submitted in partial fulfillment of
the requirements for the degree of Doctor of Philosophy
in the Department of Pharmacology and Cancer Biology
in the Graduate School of Duke University

2019

ABSTRACT

Mechanisms of Type IV Collagen Targeting to Developing Basement Membranes

by

Ranjay Jayadev

Department of Pharmacology and Cancer Biology
Duke University

Date: _____

Approved:

David Sherwood, Supervisor

Xiao-Fan Wang

Harold Erickson

Brenton Hoffman

Terry Lechler

Bernard Mathey-Prevot

An abstract of a dissertation submitted in partial fulfillment of
the requirements for the degree of Doctor of Philosophy
in the Department of Pharmacology and Cancer Biology
in the Graduate School of Duke University

2019

Copyright by
Ranjay Jayadev
2019

Abstract

Basement membranes (BMs) are cell-associated extracellular matrices that support tissue integrity, signaling, and barrier properties. Type IV collagen is critical for the mechanical and signaling functions of BM. However, due to the challenge of imaging of BMs *in vivo*, the lethal phenotypes of null mutations of many BM components, and the expanded gene families of BM receptors and matrix components in vertebrates, how collagen is directed to BMs *in vivo* is not clear. Here, I exploited the visual tractability and small BM receptor and matrix families of the nematode *C. elegans*, using live-cell imaging of endogenous localization, conditional knockdown, misexpression, and RNAi screening techniques to investigate how the sole *C. elegans* type IV collagen molecule is recruited to the BMs of growing gonadal and pharyngeal organs during larval development. In Chapter 1, I review BM composition and functions, identify gaps in our understanding of how collagen is directed to BMs, and introduce *C. elegans* as a model to study type IV collagen incorporation into BMs *in vivo*. In Chapter 2, I discover that the α subunits of the matrix receptor integrin dictate distinct modes of collagen IV recruitment to the *C. elegans* pharyngeal and gonadal BMs. In Chapter 3, I explore the roles of the matricellular proteins nidogen, agrin, perlecan, and SPARC in the targeting of collagen to pharyngeal and gonadal BMs. In Chapter 4, I identify potentially novel regulators of type IV collagen synthesis, trafficking, secretion,

and incorporation into BMs through a genome-scale RNAi screen. Finally, in Chapter 5, I discuss the implications of these findings to our understanding of type IV collagen incorporation into BMs *in vivo*.

Dedication

To my mother Rani, and my partner John, whose unwavering support and unconditional love have been instrumental in my personal growth.

Contents

Abstract	iv
List of Tables.....	xi
List of Figures	xii
Acknowledgements	xv
1. Introduction.....	1
1.1 Basement membrane composition	3
1.1.1 Laminin.....	3
1.1.2 Type IV Collagen.....	4
1.1.3 Other extracellular proteins	5
1.1.4 Matrix receptors.....	5
1.2 Functions of basement membranes in polarity, differentiation, signaling, and tissue maintenance	6
1.3 Active and dynamic roles for basement membranes in shaping and connecting tissues.....	10
1.4 Basement membranes in disease	13
1.5 Gaps in our understanding of basement membrane assembly and type IV collagen incorporation into basement membranes.....	15
1.6 Using <i>C. elegans</i> as a model to study collagen IV targeting to basement membranes in vivo.....	18
2. α -integrins dictate distinct modes of type IV collagen recruitment to basement membranes.....	21
2.1 Introduction.....	21

2.2	Results	24
2.2.1	The pharynx and gonad are basement membrane-encased growing organs supported by type IV collagen	24
2.2.2	The pharyngeal basement membrane is collagen-rich, but laminin-poor, compared to the gonadal basement membrane	28
2.2.3	Laminin is required for collagen recruitment to the gonadal but not pharyngeal basement membrane	30
2.2.4	INA-1/PAT-3 integrin mediates collagen recruitment to the gonadal basement membrane in a laminin-dependent manner	33
2.2.5	The PAT-2/PAT-3 integrin heterodimer promotes collagen recruitment to the pharyngeal basement membrane independent of laminin	38
2.2.6	The PAT-2 intracellular domain dictates basement membrane recruiting activity of integrins in the pharynx	43
2.2.7	RAP-3 is a pharyngeal-specific activator of PAT-2/PAT-3 integrin	44
2.3	Discussion	54
2.4	Acknowledgements	62
3.	Roles of the matricellular proteins nidogen, agrin, perlecan, and SPARC in type IV collagen recruitment to basement membranes	64
3.1	Introduction	64
3.2	Results	66
3.2.1	Agrin, perlecan, and nidogen are individually required for the recruitment of collagen to the posterior pharyngeal basement membrane	66
3.2.2	Nidogen and agrin function in a distinct pathway from perlecan in recruiting collagen to the posterior pharyngeal basement membrane	72
3.2.3	SPARC is required for collagen recruitment to the pharyngeal but not gonadal basement membrane	74

3.3	Discussion.....	78
3.4	Acknowledgements.....	81
4.	A genome-scale RNAi screen to identify novel regulators of type IV collagen synthesis, trafficking, and incorporation into basement membranes	82
4.1	Introduction.....	82
4.2	Results	83
4.2.1	Screen design	83
4.2.2	Candidate novel regulators of type IV collagen	84
4.3	Discussion.....	90
4.4	Acknowledgements.....	94
5.	Discussion.....	95
5.1	Integrins mediate distinct modes of type IV collagen incorporation into basement membranes	97
5.2	The matricellular proteins nidogen, agrin, and perlecan, have tissue-specific functions in collagen recruitment to basement membranes.....	101
5.3	A genome-scale RNAi screen to uncover novel regulators of collagen targeting to basement membranes.....	103
6.	Conclusion.....	105
	Appendix A.....	107
A.1	Materials and Methods	107
A.1.1	C. elegans strains.....	107
A.1.2	Transgene construction	107
A.1.2.1	mNeonGreen (mNG)/mKate2 knock-ins	107

A.1.2.2	rap-3 knock-out.....	109
A.1.2.3	myo-2p::pat-2::mNG::unc-54 3'utr	110
A.1.2.4	myo-2p::ina-1[EX]::pat-2[CTMD]::mNG::unc-54 3'utr	110
A.1.2.5	myo-2p::rap-3 ^{G12V} ::mNG::unc-54 3'utr	110
A.1.2.6	inx-8p::rap-3::mNG::unc-54 3'utr	111
A.1.3	Transgenic strains.....	111
A.1.4	RNAi	112
A.1.5	Imaging.....	113
A.1.6	Image analysis, processing, and quantification	114
A.1.7	Statistical analysis.....	115
	References	116
	Biography.....	132

List of Tables

Table 1: Targeted screen of vertebrate integrin-associated proteins with <i>C. elegans</i> orthologs.....	47
Table 2: Candidate novel regulators of type IV collagen synthesis, trafficking, secretion, and incorporation into basement membranes	86
Table 3: <i>C. elegans</i> strains used in this study	107

List of Figures

Figure 1: Basement membrane (BM) localization and composition.	2
Figure 2: BM function in polarity and signaling.....	8
Figure 3: BMs form barriers between tissues.	10
Figure 4: BMs shape and connect tissues and provide mechanical support.	12
Figure 5: The <i>C. elegans</i> pharynx and gonad are growing basement membrane (BM)- encased organs.	25
Figure 6: BM type IV collagen supports the growing pharynx and gonad.	27
Figure 7: The pharyngeal BM is collagen-rich, while the gonadal BM is laminin-rich.....	29
Figure 8: Collagen recruitment to the gonadal BM is dependent on laminin.	31
Figure 9: Collagen recruitment to the pharyngeal BM is independent of laminin.	32
Figure 10: Dystroglycan is not required for laminin or collagen recruitment to the gonadal BM.	34
Figure 11: The integrin α subunits INA-1 and PAT-2 and the integrin β subunit PAT-3 are expressed in the gonadal sheath.....	35
Figure 12: The INA-1/PAT-3 integrin heterodimer is required for laminin-dependent collagen recruitment to the gonadal BM.	36
Figure 13: Loss of integrin does not perturb collagen secretion.....	37
Figure 14: Reduction of <i>pat-2</i> results in increased INA-1 levels at the gonadal sheath surface.....	39
Figure 15: Knockdown of targeted matrix receptors does not affect collagen recruitment to the gonadal BM.	39
Figure 16: All three integrin subunits—INA-1, PAT-2, and PAT-3—but not dystroglycan are expressed in the pharynx.	40

Figure 17: The PAT-2/PAT-3 integrin heterodimer is required for laminin-independent collagen recruitment to the pharyngeal BM.....	41
Figure 18: PAT-2 is sufficient for collagen recruitment to the pharyngeal BM.....	42
Figure 19: Knockdown of targeted matrix receptors does not affect collagen recruitment to the pharyngeal BM.	42
Figure 20: The intracellular domain of PAT-2 controls the activity of PAT-2/PAT-3 in the pharynx to promote collagen recruitment.....	45
Figure 21: Loss of rap-3 affects pharyngeal but not gonadal BM collagen levels.....	48
Figure 22: RAP-3 is expressed in the larval and adult pharynx, but not the gonad.....	48
Figure 23: Loss of rap-3 does not affect pharyngeal BM laminin levels.....	49
Figure 24: Expression of constitutively active RAP-3 in results in an increase in pharyngeal BM collagen levels.	50
Figure 25: RAP-3 and PAT-2/PAT-3 integrin function together to promote pharyngeal BM collagen recruitment.....	51
Figure 26: RAP-3 does not regulate PAT-2 or PAT-3 levels.....	52
Figure 27: Ectopic gonadal expression of RAP-3 increases BM collagen but not laminin levels.	53
Figure 28: Model for distinct modes of collagen recruitment to the pharyngeal and gonadal BMs.	56
Figure 29: Perlecan is required for collagen requirement to the anterior and posterior pharyngeal basement membrane (BM), but not the gonadal BM.	68
Figure 30: Nidogen is required for the recruitment of collagen to the posterior pharyngeal BM but not the gonadal BM.	70
Figure 31: Agrin is required for collagen recruitment to the posterior pharyngeal BM, but not the gonadal BM.....	71
Figure 32: Agrin and nidogen function together to recruit collagen to the pharyngeal BM.	73

Figure 33: Nidogen and agrin function in a distinct pathway from perlecan in the recruitment of collagen to the pharyngeal BM. 75

Figure 34: SPARC is required for collagen recruitment to the pharyngeal BM. 77

Figure 35: SPARC is not required for collagen recruitment to the gonadal BM. 78

Figure 36: Representative phenotypes observed in the screen. 87

Acknowledgements

This work could not have been possible without the support and contributions of so many individuals. First and foremost, to my advisor David Sherwood: thank you for being so invested in my scientific growth and challenging me to push through every obstacle to develop my project to its fullest potential. Thank you to everyone who has been a part of the Sherwood laboratory for the past seven years — you have helped me grow as a scientist and as a person. To Qiuyi Chi: you have been like a mother away from home to me. Thank you for being a patient and kind listening ear, and your guidance with virtually every molecular biology project I have undertaken in the laboratory. Laura Kelley: thank you for your mentorship when I first joined the lab, and your friendship over the years. I truly value your support with not only my science, but also with my struggles in adulting. Sandra Vergara: thank you for being a wonderful friend and scientific influence in my life. Thank you for sharing your extensive worm knowledge with me, and for opening up your home, goats, and cats to me when I needed it most. Shelly McClatchey: thank you for being a wonderful benchmate and senior graduate student at the lab. I have truly appreciated our daily conversations about science and life. Wei Zou: I admire your dedication and passion for science. Thank you for being an amazing mentor to me when I was a novice worm wrangler. Eric Hastie: thank you for always being there to listen to me vent, but never judging me.

Aastha Garde: I appreciate our frequent conversations about science, music, and life. Your vibrancy and positivity continue to inspire me. Sara Payne: thank you for being a wonderful friend. I enjoy our scientific discussions and our daily exchange of cute animal videos. Meghan Morrissey: you are an amazing scientist. Thank you for your helpful suggestions with my projects over the years. To Dan Keeley and Kacy Gordon: Thank you for the helpful feedback on my project, and for your contributions to some of my experiments over the years. To the rest of my labmates past and present: Dan Costa, Isabel Kenny, Claire Gianakas, Lara Linden, Lauren Lohmer, Matt Clay, Zheng Wang, Dave Matus, and Adam Schindler—thank you for making the Sherwood Lab such a wonderful and personable environment to conduct science in. To my dissertation committee members Xiao-Fan Wang, Harold Erickson, Bernard Mathey-Prevot, Brent Hoffman, and Terry Lechler: I am very grateful for your enthusiasm, engagement, and thoughtful feedback through every stage of my graduate school career.

Several mentors have guided me in my scientific development. To Dan Kiehart and Blanche Capel: thank you for letting me work on rotation projects in your labs. To Snezhana Oliferenko: thank you for welcoming me into your lab as I transitioned from undergraduate studies to grad school. I truly admire your creativity and passion for science, and your enthusiasm for my scientific pursuits means the world to me. To Maki Murata-Hori: I fell in love with science in the two years I spent in your lab as an undergraduate researcher. Thank you so much for your unwavering support. To

Cynthia He: I appreciate your enthusiasm with my undergraduate research endeavors, and your advice in preparing for grad school.

I am very grateful to have met and made wonderful friends that have supported me over the years. To Angel Martin, Christine Daniels, Ariana Eily, and Kathryn Walder: thank you for being my tribe in grad school. You love me unconditionally and have supported me through the ups and downs. I am in awe of all of your scientific achievements and you inspire me daily. To Hanif Samad, Gary Kwong, and Kevin Tessensohn: You are my closest friends and I have leaned on you wonderful people over the years in many ways. Thank you for supporting me all the way from Singapore! To Shyanhuey Low, Shazmina Rafee, Vinayaka Srinivas, Bianca Victorio, Adrian Ng, Ivan Yow, Dan Zhang, Aleksandar Vjestica, and Gu Ying: thank you for being wonderful friends and labmates in Singapore. I love you all. To my high school friends Shawn Ng, Clarence Chung, Keith Tan, Ing Ann Yeo, Samuel Lai, Gerard Yip, Amir Hussain, and Taffy Cheung: it is hard to believe that I've known you folks for 20 years now. I am so grateful to have all of you in my life even after all of these years and you inspire me in so many ways. To my other Singaporean tribe: Shiyun Koh, Fei Koon Chan, Huiling Lee, Huizhen See, Jiayan Neo, Liyu Tan, Shaopin Toh, Yewtze Liew, Huimin Teo, and Huimin Han—thank you for your continued friendship over the past 15 years.

To my lovely friends at the Duke International House, Lisa Giragosian, Paige Vinsion, Seun Olanosu, Esra Mason, and Alan Kendrick: thank you for all that you do

for international students at Duke. I feel privileged for the many opportunities to serve at IHouse over the years, and IHouse has been an amazing resource in helping me navigate through grad school as a foreigner. Many thanks to Jamie Smith, Jo Bernhardt, Anne Lacey, and Carol Richardson for your invaluable help as graduate school administrators.

None of my work would have been possible without the support of my family. To my mother Rani: you have been a rock in my life. Thank you for your love and support and all of the sacrifices you have made for me to have a better life. To my grandmother Sumathy Das: I could not have made it here without your love and support and everything you have done for me growing up. To my grandfather Palpoo Shanmugha Das: you are not here with us now, but we will never forget your hard work and sacrifices in building a better life for our family. I know you are watching over all of my scientific pursuits today. To my aunt Rejiny and uncle Renjit: you have given me so much and have supported my mother and I through some hard times. I cherish you both dearly. To my cousin Roy: I hope you are smiling from up above. I miss you.

Most of all, to my chosen family, John Sewell: thank you so much for being on this journey with me. You are selfless, loving, and kind, and have stood by me always. Thank you for making me laugh when I needed it most. Thank you for all the sacrifices you've made for me. You are my best friend and partner in life. I love you.

1. Introduction

Chapter One was modified from a primer published in Current Biology entitled “Basement Membranes” (Jayadev and Sherwood 2017). The authors of this minireview are Ranjay Jayadev and David R. Sherwood.

Basement membranes (BMs) are thin, dense sheets of specialized, self-assembled extracellular matrix that surround most animal tissues (Figure 1, top; (Pozzi et al. 2017; Yurchenco 2011)). The emergence of BMs coincided with the origin of multicellularity in animals, suggesting that they were essential for the formation of tissues (Fidler et al. 2017; Grau-Bové et al. 2017). Their sheet-like structure derives from two independent polymeric networks—one of laminin and one of type IV collagen (Figure 1, bottom). These independent collagen and laminin networks are thought to be linked by several additional extracellular matrix proteins, including nidogen and perlecan (Figure 1, bottom; (Yurchenco 2011)). BMs are usually cell-associated and are anchored to cell surfaces through interactions with adhesion receptors and sulfated glycolipids (Figure 1, bottom; (Yurchenco and Patton 2009)). Various combinations of other proteins, glycoproteins, and proteoglycans—including fibulin, hemicentin, SPARC, agrin, and type XVIII collagen—are present in BMs, creating biochemically and biophysically distinct structures that serve a wide variety of functions (Sekiguchi and Yamada 2018). BMs have traditionally been viewed as static protein assemblies that provide structural

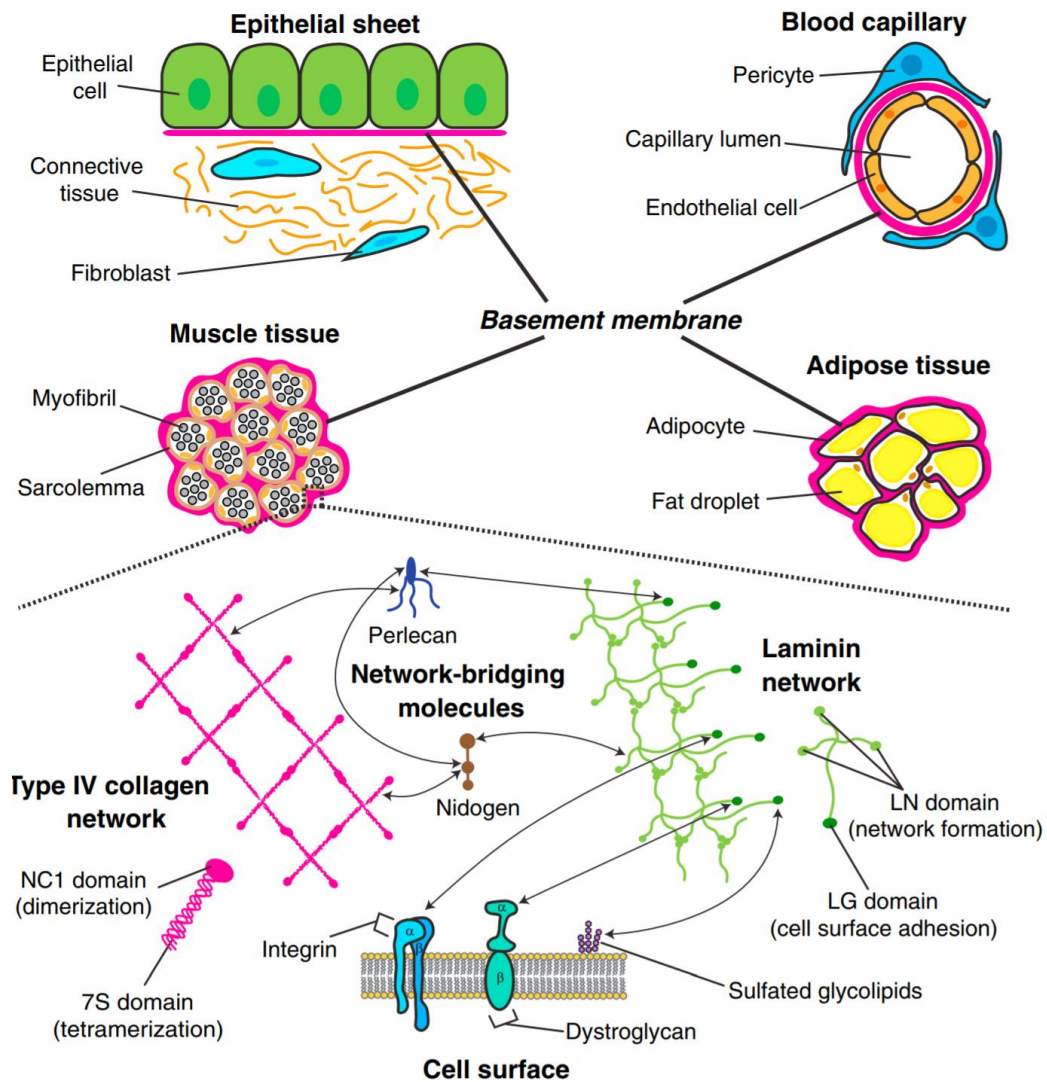


Figure 1: Basement membrane (BM) localization and composition.

(Top) BMs underlie or surround most tissues, including epithelial, endothelial, muscle, and adipose tissues. (Bottom) The self-assembling polymeric networks of type IV collagen and laminin provide BMs with their core structure and these networks associate with each other through interactions (indicated by arrows) with bridging adaptor proteins, such as perlecan and nidogen. The laminin network is closely associated with cell surfaces through interactions (arrows) with integrins and dystroglycan receptors as well as sulfated glycolipids. Figure originally appeared in (Jayadev and Sherwood 2017) and is adapted with permission.

support to tissues. However, recent studies have begun to uncover dynamic, active roles for BMs in many developmental processes (Jayadev and Sherwood 2017; Morrissey and Sherwood 2015). In this chapter, I first outline the composition of BMs. Then, I discuss established and emerging roles of BMs in development, tissue construction, and tissue homeostasis. Next, I briefly outline the roles of BMs in human diseases. Finally, I discuss gaps in our understanding of how type IV collagen is incorporated into BMs and introduce *C. elegans* as a model to study collagen integration in developing BMs *in vivo*.

1.1 Basement membrane composition

1.1.1 Laminin

Studies in the model organisms *Drosophila*, *C. elegans*, and mice support the idea that laminin is the foundational building block for the initial formation of BMs (Urbano et al. 2009; Matsubayashi et al. 2017; Huang et al. 2003; Pöschl et al. 2004). Laminin is a secreted heterotrimeric protein made up of an α , β , and γ subunit (Aumailley et al. 2005; Miner and Yurchenco 2004). Laminin trimers self-assemble into a polymeric sheet-like lattice that is tightly associated with the cell surface (Figure 1, bottom). In *Drosophila* and *C. elegans*, two genes encode α subunits and single genes encode the β and γ subunits, which combine to form two heterotrimers (Clay and Sherwood 2015; Isabella and Horne-Badovinac 2015a). In mammals, five α , four β , and three γ chains have been identified; these assemble into at least 16 heterotrimeric complexes that are often

expressed in tissue-specific manners (Hohenester and Yurchenco 2013). In addition to being secreted locally, laminin can be secreted from distant sites and incorporated into BMs from the interstitial fluid. For example, *C. elegans* sublateral nerves are covered by a laminin α 2-containing BM, even though the neurons do not express laminin subunits (Huang et al. 2003). Similarly, the mouse neural tube BM contains the laminin α 5 subunit that is not expressed by the neural tube cells (Copp et al. 2011).

1.1.2 Type IV Collagen

Following laminin assembly, an independent self-assembling, covalently cross-linked type IV collagen network is laid onto BMs (Figure 1, bottom). Type IV collagen is highly conserved among animals, and its emergence in unicellular ancestors was thought to be a requirement for the formation of BMs and appearance of complex tissues in animals (Fidler et al. 2018; Grau-Bové et al. 2017). Type IV collagen is a heterotrimer made up of two α 1 and one α 2 chains that wind around each other into a long and rigid 400nm triple helix (Fidler et al. 2018). The stiff triple helical structure together with covalent cross-linking in the form of disulfide and sulfilimine bonds between type IV collagen molecules bestows BMs mechanical resistance to tensile forces (Fidler et al. 2018; Vanacore et al. 2009). *Drosophila* and *C. elegans* possess two type IV collagen genes and produce a single collagen heterotrimer made up of two α 1 and one α 2 chains (Clay and Sherwood 2015; Isabella and Horne-Badovinac 2015a). Vertebrate genomes,

however, encode six collagen chains— $\alpha 1$ to $\alpha 6$ —that assemble into three distinct heterotrimers ((Khoshnoodi et al. 2008). Similar to laminin, type IV collagen may be produced and incorporated into BMs locally or from distant sources (Graham et al. 1997; Kedinger et al. 1998; Pastor-Pareja and Xu 2011).

1.1.3 Other matricellular proteins

Various other proteins associate with the laminin and type IV collagen networks in BM. The glycoprotein nidogen and the heparan sulfate proteoglycan perlecan are thought to link the two networks together, due to their high affinity for both laminin and collagen (Yurchenco 2011). The proteoglycans collagen XVIII and agrin, and glycoproteins SPARC and fibulin-1 are also often associated with BMs (Sekiguchi and Yamada 2018). Recent proteomic analyses of isolated BMs have identified over a hundred proteins associated with BMs—many of which are tissue specific—highlighting the complexity and diversity of BMs (Randles et al. 2017).

1.1.4 Matrix receptors

Cell culture studies have indicated that BMs adhere to cell surfaces by interacting with various adhesion receptors and lipids. Laminin interacts with the BM receptors integrin and dystroglycan through LG domains present in α subunits (Figure 1, bottom; (Hohenester and Yurchenco 2013; Yurchenco and Patton 2009)). Laminin has also been

shown to directly bind to sulfated glycolipids on the cell surface of cultured Schwann cells (Li et al. 2005). Comparatively little is known about whether type IV collagen is directly anchored to cell surfaces. Discoidin domain receptors (DDRs) are unique collagen binding receptor tyrosine kinases. The kinase activity and downstream signaling of DDRs is activated by collagen binding. In particular, the kinase activity of DDR1 promotes collagen synthesis (Leitinger 2014). However, it is unclear whether DDRs anchor type IV collagen to cell surfaces. *In vitro* assays have identified an RGD tripeptide in type IV collagen that binds with high affinity to integrin, triggering downstream cell signaling (Pedchenko et al. 2004). Whether integrins recruit collagen IV to BMs *in vivo*, however, has not been established (discussed further in section 1.6).

1.2 Functions of basement membranes in polarity, differentiation, signaling, and tissue maintenance

BMs perform many functions throughout development and in adult tissues and organs. Laminin is deposited extracellularly very early in development. Mutations in laminin result in early embryonic lethality in *Drosophila*, mice, and *C. elegans*, with dramatic defects in tissue formation and adhesion, cell fate specification, cell migration, and polarity (Urbano et al. 2009; Huang et al. 2003; Li et al. 2003; Miner et al. 2004). Type IV collagen networks, however, appear later in development. BM integrity is heavily compromised in the absence of collagen, resulting in lethality during embryonic tissue movement and rearrangement. In collagen-deficient *C. elegans* embryos, muscle tissues

detach from the body wall or epidermis as the muscle BM is unable to resist the stresses of muscle contraction (Gupta et al. 1997). Mice lacking type IV collagen die by E10.5-11.5, following thinning and fracture of vascular and extra-embryonic BMs (Pöschl et al. 2004). Together, these observations support the idea that laminin initiates BM formation and mediates early cell differentiation and tissue formation, while type IV collagen stabilizes and protects the BM from mechanical stresses.

During early morphogenesis, BMs coordinate cell and tissue polarity (Figure 2). *In vitro* studies using embryonic stem cells have highlighted a requirement for laminin in polarizing the epiblast, the primordial outer embryonic layer (Li et al. 2003). During *C. elegans* pharyngeal (foregut) development, laminin signaling establishes the apical-basal polarity of pharyngeal cells (Rasmussen et al. 2012). Similarly, laminin directs polarity in mammalian cell culture. For example, a single Madin-Darby Canine Kidney epithelial cell will divide and organize into a ball-like cyst only when it is embedded in a laminin-rich matrix (McAteer et al. 1988)

BM can function as signaling platforms during development and in mature tissues by sequestering many growth factors and other ligands. BM proteoglycans perlecan, type XVIII collagen, and agrin tether growth factors such as vascular endothelial growth factor, transforming growth factor- β , and fibroblast growth factor through binding interactions with their heparan sulfate glycosaminoglycan

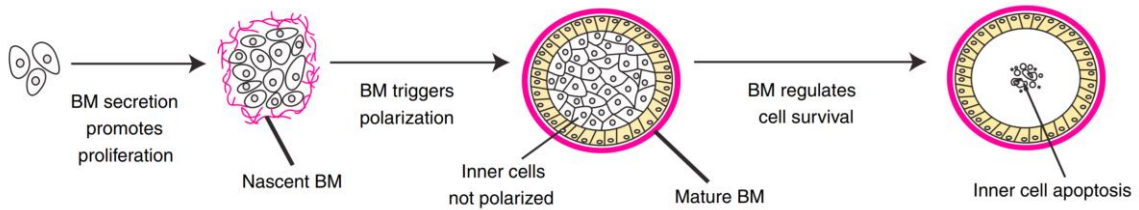


Figure 2: BM function in polarity and signaling.

BMs regulate many cell signaling events. BM molecules such as laminin, type IV collagen, and BM-associated growth factors induce cell proliferation. The interactions of BM molecules and cell surface receptors facilitate cell and tissue polarization. Cues from the BM regulate cell survival and cell death. Figure originally appeared in (Jayadev and Sherwood 2017) and is adapted with permission.

chains (Iozzo 2005). These growth factors regulate cell survival, stem cell divisions, migration, and proliferation by binding and signaling through cell surface receptors (Iozzo et al. 2009). BM laminin and type IV collagen can directly activate cell signaling pathways. Laminin promotes not only polarity, but also cell survival, migration, and differentiation by binding to the laminin receptors integrin and dystroglycan (Hohenester and Yurchenco 2013; Li et al. 2002). Several cell surface receptors interact with type IV collagen to regulate proliferation, migration, and polarity (Fidler et al. 2018; Khoshnoodi et al. 2008). These include type IV collagen-binding integrins and the discoidin domain receptor 1 (DDR1). BMs harbor matrix metalloproteases (MMPs), a large family of broad-spectrum proteases that function in BM degradation and remodeling (Kessenbrock et al. 2010; Page-McCaw et al. 2007). Importantly, by degrading BM scaffolds, MMPs can release cryptic fragments with signaling functions. For example, cleavage of collagen IV by MMP9 exposes a cryptic site involved in

angiogenesis (Xu et al. 2001), while cleavage of laminin $\alpha1\beta1\gamma1$ by MMP2 releases a laminin fragment that regulates the epithelial-to-mesenchymal transition in embryonic stem cells (Giannelli et al. 1997).

BMs provide essential barrier functions. The glomerular BM is a critical component of the kidney filtration barrier that prevents the leakage of plasma proteins into the urine (Miner 2012). The BM is sandwiched between the endothelial cells of the glomerular capillaries, and the podocytes that wrap around the glomerulus (Figure 3). The laminin and collagen IV networks of the glomerular BM are thought to maintain the selective permeability of the glomerular filter by controlling the porosity of the BM to plasma proteins, selecting for both size and charge (Suh and Miner 2013; Miner 2011). BM barrier function is also observed in the blood-brain barrier, the interface between the vascular system and the brain that controls the movement of solutes between the two tissues (Xu et al. 2018). The capillary endothelial BM and the parenchymal BM of brain astrocytes merge at the blood-brain barrier (Figure 3). Tight junctions that form between the endothelial cells prevent the paracellular transport of most molecules, especially small ions (Ballabh et al. 2004). BM laminin and type IV collagen are essential for the formation of these tight junctions and maintenance of transendothelial electrical resistance, indicating that the BM is a critical component of the blood-brain barrier (Gautam et al. 2016; Baeten and Akassoglou 2011).

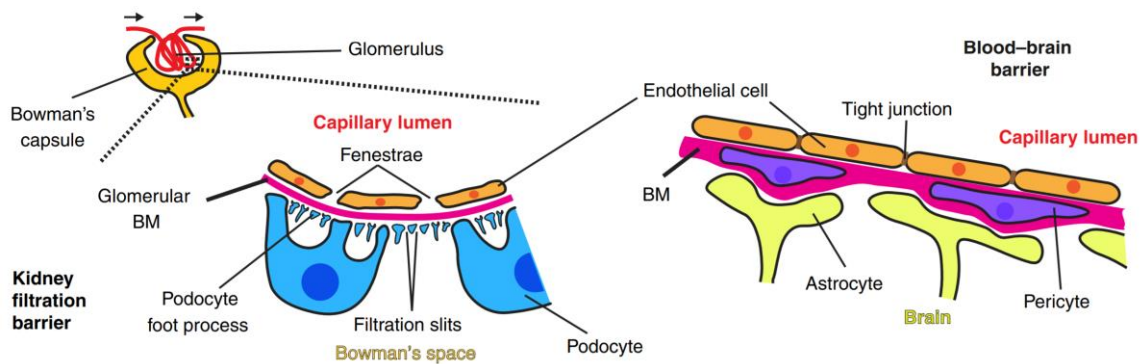


Figure 3: BMs form barriers between tissues.

(Left) The glomerular BM regulates the flow of molecules from the blood into the urine. **(Right)** At the blood–brain barrier, the BMs of the vasculature and the brain merge together and organize the endothelial cells that regulate the flow of solutes into the brain. Figure originally appeared in (Jayadev and Sherwood 2017) and is adapted with permission.

BMs separate epithelia from stromal connective tissues by facilitating stable cell-to-matrix adhesions through hemidesmosomes. BM laminin is a critical component of hemidesmosomes, interacting with both integrin on cell surfaces, and type VII collagen of stromal anchoring fibrils. This forms a stable adhesion between epithelia and connective tissues, thus protecting tissues from destabilizing shear forces (Borradori and Sonnenberg 1999; Walko et al. 2015).

1.3 Active and dynamic roles for basement membranes in shaping and connecting tissues

Recent studies are uncovering new roles for BMs as dynamic structures that help to sculpt tissues. One clear example is during *Drosophila* egg chamber elongation (Isabella and Horne-Badovinac 2016, 2015b). The egg chamber is made up of germ cells

surrounded by a follicular epithelium. At the time of elongation, the initially spherical egg chamber rotates within its surrounding BM, which remains static. As the egg chamber rotates, the follicular epithelium secretes and deposits laminin and collagen IV-containing BM fibrils perpendicular to the axis of elongation. These polarized BM fibrils constrict the egg chamber, restricting circumferential growth, causing the developing egg to grow elliptically. Further, a BM stiffness gradient along the anterior-posterior axis of the egg chamber, where the poles of the egg chamber are only half as stiff as the central regions, influences egg shape. Type IV collagen plays a direct role in establishing the gradient. Upregulation of collagen deposition from the follicular epithelium increased the stiffness of the central region of the egg chamber, resulting in hyper-elongated eggs. In contrast, depletion of collagen in follicle cells resulted in a homogeneously soft BM, leading to rounder egg chambers (Crest et al. 2017). Similar collagen “corsets” are thought to constrict and elongate the ducts of the developing salivary and mammary glands in mice (Hinck and Silberstein 2005; Harunaga et al. 2014).

The complex composition of BMs also shapes tissues. Type IV collagen networks apply constrictive forces on growing tissues. Loss of these constrictive forces by post-embryonic reduction of collagen in *Drosophila* results in the dilation of many tissues, including the wing disc (Figure 4; (Pastor-Pareja and Xu 2011)). In contrast, perlecan maintains the elasticity of BMs as tissues grow. Reduction of perlecan results in the

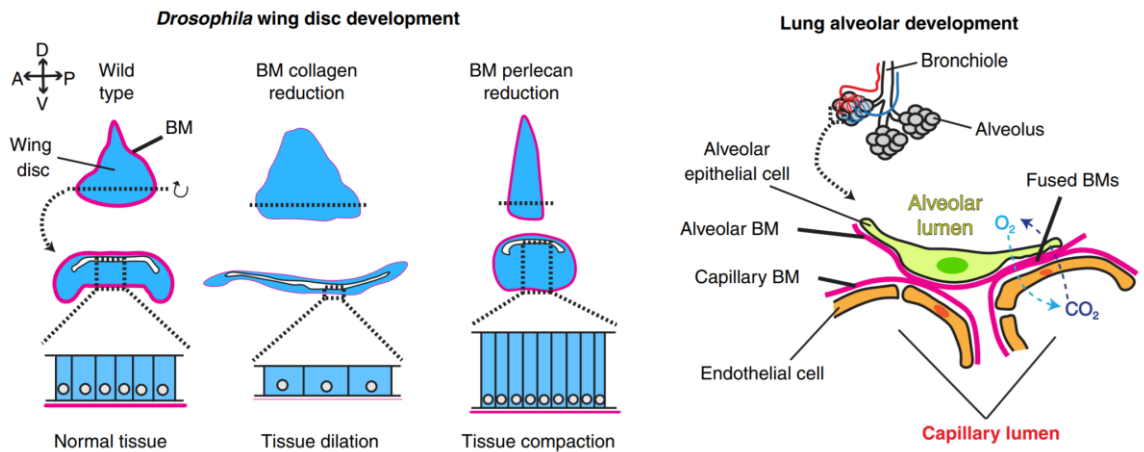


Figure 4: BMs shape and connect tissues and provide mechanical support.

(Left) BM collagen and perlecan act in opposition to shape the developing *Drosophila* wing disc. **(Right)** Fusion of the lung alveolar and capillary endothelial BMs brings the two tissues together to facilitate gas exchange. Figure originally appeared in (Jayadev and Sherwood 2017) and is adapted with permission.

aberrant compaction of the wing disc, suggesting an increase in BM tension (Figure 4).

Because perlecan does not affect the incorporation or levels of collagen in the BM, these observations suggest that perlecan directly counteracts the mechanical constriction provided by collagen in BMs to regulate tissue shaping.

BMs also shape tissues by connecting them together. In the kidney, BMs of the vascular endothelium and podocyte epithelium fuse together to form the glomerular BM. During lung alveolar development, fusion of the alveolar and capillary BMs into a single sheet brings the alveolus and capillaries into close contact, which likely facilitates efficient gas exchange (Figure 4). Studies in *C. elegans* have revealed a new BM adhesion system, the B-LINK, that connects the uterus to the vulva through attachments between

the uterine and vulval BMs (Morrissey et al. 2014). These attachments are mediated by the conserved extracellular matrix component hemicentin. The cytolinker plakin and adhesion receptor integrin are also components of the B-LINK complex. It is likely that the B-LINK adhesion system functions broadly to connect tissues through neighboring BMs (Keeley and Sherwood 2019). For example, hemicentin promotes attachment of the epidermal and somite BMs in zebrafish embryos and may function as part of an undescribed B-LINK complex (Feitosa et al. 2012; Carney et al. 2010).

1.4 *Basement membranes in disease*

Defects in basement membrane assembly or composition result in a multitude of human diseases. Many arise from mutations in one or more BM proteins and can affect a variety of tissue and organ systems. Mutations in laminin disrupt hemidesmosomes, leading to skin blistering diseases (Yurchenco and Patton 2009). Mutations in the $\alpha 3$, $\alpha 4$, and $\alpha 5$ chains of type IV collagen result in the kidney disease Alport's syndrome, which is primarily characterized by leakage of plasma proteins into the urine (proteinuria) due to disruptions in BM pore size (Mao et al. 2015; Khoshnoodi et al. 2008). BM protein mutations underlie many diseases of the muscle (Wiradjaja et al. 2010). Agrin mutations cause congenital myasthenic syndrome, where patients suffer from progressive muscle weakness and fatigue, due to defects at the neuromuscular junction. Mutations in

laminin $\alpha 2$ cause congenital muscular dystrophy type 1A, characterized by the early onset of muscle fiber degeneration .

Compositional and ultrastructural changes in BM are linked to human disorders. In Goodpasture's syndrome, autoantibodies form against the $\alpha 3$ chain of type IV collagen (Mao et al. 2015). The consequent disruption of BM collagen networks results in acute kidney failure and lung hemorrhage that can be fatal. In diabetes mellitus patients, the glomerular and tubular BMs of the kidney are abnormally thickened, causing reduced glomerular filtration and proteinuria (Marshall 2016). In addition, thickening of vascular BMs in the eye is commonly associated with diabetic retinopathy (Roy et al. 2010). Similarly, endothelial BM thickening has been observed in Alzheimer's disease (Zarow et al. 1997). As a result, β -amyloid peptides that are typically removed from the brain via the endothelial BM accumulate in the walls of cerebral blood vessels, which is associated with a decline in cognition (Morris et al. 2014). In multiple sclerosis, an inflammatory disease of the central nervous system, extensive BM deposition and concomitant leukocyte accumulation is observed in active white matter lesions (van Horssen et al. 2005). These aberrations are associated with astroglial scarring and axon damage as the disease progresses (van Horssen et al. 2007).

BM dysregulation is a hallmark of many cancers (Lu et al. 2012; Tanjore and Kalluri 2006). Overexpression of laminin is linked to cell hyperproliferation in breast, prostate, and colon tumors (Wiradjaja et al. 2010). Laminin and perlecan also stimulate

the development of new blood vessels to provide oxygen to proliferating cancer cells (Kalluri 2003). Recent proteomic analysis of the extracellular matrix signatures of metastatic tumors has revealed that several BM components—including laminin and type IV collagen—are secreted by both stromal and tumor cells in highly metastatic tumors, but are only secreted by the stroma in poorly metastatic tumors (Naba et al. 2014). These observations suggest that primary tumor cells actively alter the composition of BM, and that the resulting changes in BM ultrastructure or signaling or both may drive metastasis.

1.5 Gaps in our understanding of basement membrane assembly and type IV collagen incorporation into basement membranes

I have discussed key mechanical, signaling, and barrier functions of BM, and highlighted type IV collagen's essential role in all of these functions. Underscoring its importance to human health, mutations in collagen IV are associated with numerous genetic disorders that affect almost every major organ system (Fidler et al. 2018; Mao et al. 2015). Yet, the mechanisms directing type IV collagen to BMs of diverse tissues and organs *in vivo* remain elusive. Most of our current understanding of BM assembly stems from studies in the early embryos of *Drosophila*, mice, and *C. elegans*, and *in vitro* experiments on cultured embryoid bodies (aggregates of pluripotent stem cells) and Schwann cells (glial cells of peripheral nerves). Based on the embryonic studies, a

temporal hierarchy of BM assembly has been established: laminin assembles on cell surfaces and forms a scaffold on which the type IV collagen network is then assembled (Pöschl et al. 2004; Urbano et al. 2009; Matsubayashi et al. 2017; Huang et al. 2003).

Further, cell culture studies have identified the matrix receptor integrin, the transmembrane glycoprotein dystroglycan, and cell surface sulfated glycolipids in facilitating laminin anchorage to cell surfaces (Li et al. 2017, 2005). Whether laminin associates with cell surfaces through similar interactions *in vivo*, however, is unclear.

Moreover, how type IV collagen is incorporated into BMs, and whether it can be anchored to cell surfaces *in vivo* is poorly understood. RGD tripeptides in collagen have been implicated in binding to integrin and triggering downstream cell signaling in cell culture studies (Pedchenko et al. 2004; Khoshnoodi et al. 2008), but whether integrin tethers collagen to cell surfaces *in vivo* has not been experimentally determined.

Network-bridging matrix proteins, namely nidogen, agrin, and perlecan, are thought to facilitate the association of collagen IV networks with laminin networks on cell surfaces, as these matricellular proteins to bind to both networks or to one another (Yurchenco 2011; Yurchenco and Patton 2009). However, it is unclear whether these proteins bridge laminin and collagen IV networks *in vivo*. Loss of nidogen in mice affects collagen IV deposition into the embryonic lung BM, but kidney BMs appeared to be unaffected (Bader et al. 2005). In *C. elegans*, nidogen null mutant animals displayed wild-type incorporation of collagen into BMs. Taken together, it is possible that nidogen

may have tissue-specific functions in localizing collagen to BMs, or that it may function redundantly with other molecules in its cross-bridging function. Agrin and perlecan are both present in glomerular BMs. However, selective knockout of both agrin and perlecan in the kidney podocytes of mice did not affect the ultrastructure of the glomerular BM or kidney filtration function (Goldberg et al. 2009). Electron microscopy and biochemical assays on human skin samples suggests that perlecan is required to link the laminin and collagen IV networks of epidermal BM (Behrens et al. 2012). However, in *Drosophila* embryos and larvae, perlecan appears to be dispensable for BM collagen incorporation; instead, collagen IV is required to localize perlecan to BMs. (Pastor-Pareja and Xu 2011; Matsubayashi et al. 2017). These observations suggest that type IV collagen incorporation might in part be tissue-specific and that multiple (and complex) interactions with matrix proteins might mediate collagen deposition into BMs. A systematic analysis of nidogen, perlecan, and agrin function will be required to establish possible consistent functions for any of these proteins in mediating collagen IV recruitment to BMs *in vivo*.

One of the reasons for our lack of understanding of how collagen is incorporated into BMs is the challenge of examining type IV collagen and BMs *in vivo*. BMs of vertebrates are often located deep in tissues and optically inaccessible. Further, BM assembly cannot yet be visualized in these systems as their BM components have not been tagged with fluorescent proteins (Kelley et al. 2014). Furthermore, the expanded

BM matrix and receptor protein families in vertebrates complicates genetic analysis of their function. For example, vertebrates assemble three different type IV collagen molecules, 16 laminins, and at least 24 integrin heterodimers (Clay and Sherwood 2015). In addition, the essential embryonic functions of many of these BM components and the lethal phenotypes of BM null mutants have hampered our ability to study collagen incorporation into diverse BMs that surround post-embryonic tissues and organs (Li et al. 2017; Yurchenco and Patton 2009). Thus, how type IV collagen, an essential scaffolding and signaling BM component, is targeted to BMs *in vivo* remains a major gap in our understanding of BM biology.

1.6 Using *C. elegans* as a model to study collagen IV targeting to basement membranes in vivo

Caenorhabditis elegans is a free-living nematode that is a powerful model system to address the aforementioned challenges in our understanding of how type IV collagen is assembled into BMs *in vivo*. All major BM components and receptors are conserved in *C. elegans*, with single genes encoding most of these proteins. For example, worms assemble a single type IV collagen heterotrimer, three laminin molecules, and only two distinct integrins, thus facilitating genetic analysis of BM components (Kramer 2005; Clay and Sherwood 2015). Live, intact worms can be easily imaged, as *C. elegans* is less than 1mm long, has ~1000 cells, and is completely transparent (Corsi 2006; Brenner 1974). Further, most BM receptors and matrix proteins have been fluorescently tagged

in the worm, allowing visualization and quantification of BM dynamics *in vivo* (Hagedorn et al. 2009, 2013; McClatchey et al. 2016; Ihara et al. 2011). In addition, early embryonic lethality associated with genetic loss of BM proteins can be avoided through rapid and conditional RNAi-mediated reduction of BM protein levels (Conte et al. 2015), thus facilitating the study of diverse BMs surrounding post-embryonic tissues and organs *in vivo*.

Leveraging these strengths of the *C. elegans* system, I utilized live-cell imaging, visualization of endogenous localization, conditional knockdown, misexpression, and RNAi screening to investigate mechanisms of type IV collagen incorporation into BMs *in vivo* during larval development. I focused on two BMs in the worm: the thick BM ensheathing the pharyngeal tissue, a rigid, contractile feeding apparatus (Mango 2007); and the comparatively thinner BM surrounding the gonadal tissue, a flexible, tube-like organ containing the germline (Sherwood and Plastino 2018). I have investigated the roles of both cell surface receptors and BM matrix proteins in directing type IV collagen to the pharyngeal and gonadal BMs. In Chapter 2, I describe how α subunits of the matrix receptor integrin dictate distinct modes of collagen IV incorporation into the pharyngeal and gonadal BMs. In Chapter 3, I detail the roles of the matricellular proteins nidogen, agrin, perlecan, and SPARC in directing collagen to these BMs. In Chapter 4, I detail the initiation of a genome-scale RNAi screen to identify novel regulators of collagen IV synthesis, trafficking, secretion, and incorporation into BMs,

and discuss my preliminary findings of promising candidates. Finally, in Chapter 5, I address the implications of my discoveries.

2. α -integrins dictate distinct modes of type IV collagen recruitment to basement membranes

Chapter two is adapted from a manuscript of the same title currently in review at Journal of Cell Biology. The authors of this manuscript are Ranjay Jayadev, Qiuyi Chi, Daniel P. Keeley, Eric L. Hastie, and David R. Sherwood. I use first person plural pronouns where appropriate to acknowledge the valuable contributions of other authors (see Chapter 2.4 for details).

2.1 Introduction

Basement membrane (BM) is a thin, dense, sheet of extracellular matrix that underlies epithelia, endothelia, and surrounds most other tissues (Pozzi et al. 2017). BMs are comprised primarily of two independent self-assembling scaffolds of laminin and type IV collagen. The laminin and type IV collagen networks are thought to associate through several cross-bridging molecules, including nidogen, perlecan, and agrin (Yurchenco 2011). BMs are highly diverse, and this diversity arises from alternative splicing, post-translational modifications, and varying amounts of core BM components as well as numerous regulatory proteins that associate with BMs such as matricellular proteins, proteases, and growth factors (Glentis et al. 2014; Isabella and Horne-Badovinac 2015a). The diversity in BMs regulates key cell and tissue properties, including cell polarity, cell differentiation, cell survival, tissue shaping, filtration, and resistance to mechanical stresses (outlined in Chapter 1.2 and 1.3). How diverse BMs are

constructed on tissues is not well understood, particularly as many BM components are expressed and secreted from distant sources and selectively acquired from the extracellular fluid (Clay and Sherwood 2015; Glentis et al. 2014).

Type IV collagen is highly conserved among animals, and its emergence in unicellular ancestors was thought to be a requirement for the formation of BMs and appearance of complex tissues in animals (Fidler et al. 2018; Grau-Bové et al. 2017). Type IV collagen is a heterotrimer made up of two $\alpha 1$ and one $\alpha 2$ chains that wind around each other into a long and rigid 400nm triple helix. The stiff triple helical structure together with covalent cross-linking between type IV collagen molecules bestows BMs mechanical resistance to tensile forces (Fidler et al. 2018). In addition to providing structural integrity, distinct tissue levels, unique modes of deposition, and targeted remodeling of collagen helps shape organs (Crest et al. 2017; Gupta et al. 1997; Harunaga et al. 2014; Isabella and Horne-Badovinac 2016; Pöschl et al. 2004). Highlighting its importance to human health, mutations in type IV collagen are associated with at least ten distinct genetic disorders that disrupt brain, kidney, muscle, and vascular tissues (Fidler et al. 2018). In mice, *Drosophila*, and *C. elegans*, type IV collagen is often secreted by cells into the extracellular space and then incorporated into epithelial BMs at distant sites (Graham et al. 1997; Kedinger et al. 1998; Pastor-Pareja and Xu 2011) Work in *Drosophila* and mouse embryos have indicated type IV collagen recruitment to BMs requires the presence of laminin (Matsubayashi et al. 2017; Pöschl et

al. 2004; Urbano et al. 2009). Cell culture work has suggested that laminin deposition onto cell surfaces is mediated through interactions with integrin and dystroglycan receptors, and sulfated glycolipids (Li et al. 2005, 2017; Yurchenco 2011). The cell surface mechanisms that mediate laminin and collagen deposition *in vivo*, however, have remained elusive. Further, while most studies have examined initial BM formation in the embryo, little is known about BM construction on growing tissues, where most BMs are found (discussed in Chapter 1.5 and 1.6).

In this investigation I have examined type IV collagen addition into the growing BMs covering two organs during *C. elegans* larval development—the pharynx, a rigid pumping feeding organ; and the gonad, a flexible tube-like organ that houses the germline. Using RNAi-mediated knockdown and an mCherry-tagged collagen reporter, I show that collagen addition to BM was required to maintain both organs' structure, and that the pharyngeal BM contained significantly higher levels of collagen. Strikingly, I found that while laminin was necessary for type IV collagen addition into the gonadal BM, collagen addition was independent of laminin in the pharyngeal BM. Through RNAi screening and examination of endogenously tagged BM-binding receptors, I found that the putative laminin-binding integrin heterodimer α INA-1/ β PAT-3 mediated laminin and collagen addition to the gonadal BM; while the putative RGD-binding integrin α PAT-2/ β PAT-3 promoted collagen addition to the pharyngeal BM independent of laminin. However, both integrin heterodimers were expressed in the gonad and the

pharynx, suggesting that their selective activation was controlled by tissue-specific effectors. Consistent with this hypothesis, through domain swapping experiments I showed that the intracellular domain of the α integrin PAT-2 (normally active in pharynx to recruit collagen) attached to the extracellular domain of the α integrin INA-1 (normally active in gonad to recruit laminin) promoted laminin recruitment to the pharyngeal BM. Further, using an RNAi screen I identified RAP-3, an ortholog of the mammalian integrin-activating small GTPase Rap1, as a pharyngeal specific activator of PAT-2/PAT-3. Together, these results identify integrin receptors as key *in vivo* mediators of BM collagen incorporation during tissue growth and show that BM diversity and precise modulation of BM collagen levels can be driven in part by the tissue-specific activation of distinct integrins.

2.2 Results

2.2.1 The pharynx and gonad are basement membrane-encased growing organs supported by type IV collagen

In *C. elegans*, collagen IV is a heterotrimer formed from two α 1-like and one α 2-like chains, encoded by the *emb-9* and *let-2* genes respectively (Kramer 2005). Collagen is predominantly synthesized in body wall muscles, secreted into the extracellular space, and then recruited to the BM of other tissues (Graham et al. 1997; Morrissey et al. 2016). To understand how type IV collagen is targeted to the BM of growing organs, I examined the BMs of the pharynx and the gonad (Figure 5A). The *C. elegans* pharynx is

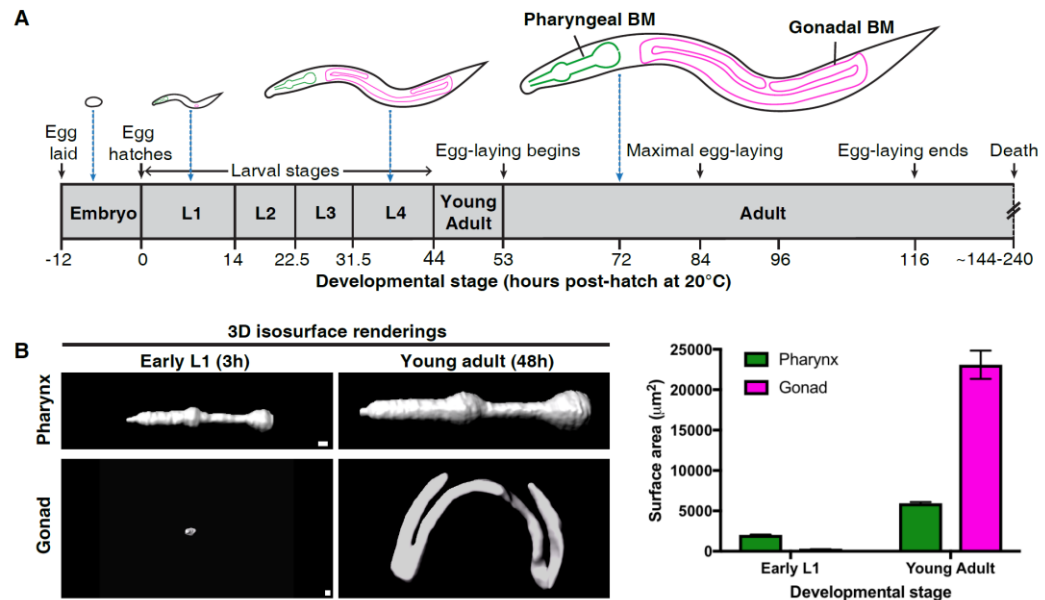


Figure 5: The *C. elegans* pharynx and gonad are growing basement membrane (BM)-encased organs.

(A) Illustrations of *C. elegans* at various stages of development (scaled to the length of the egg), with the pharyngeal and gonadal BMs outlined in green and magenta, respectively. (B) 3D isosurface renderings of pharyngeal and gonadal type IV collagen::mCh at the early L1 versus young adult stages on the left, and quantification of surface area on the right. Bar graphs show mean surface area and error bars represent standard error of the mean (n=10 all stages). Scale bars are 10 μm .

a rigid, contractile feeding apparatus largely composed of radially arranged muscle and marginal cells that form an epithelium (Mango 2007). The gonad is a flexible cylindrical reproductive organ, which is enwrapped predominantly by thin gonadal sheath cells (Sherwood and Plastino 2018). The pharyngeal epithelium and gonadal sheath cells are both surrounded by BMs that support each organ (Huang et al. 2003). Using a functional type IV collagen reporter (EMB-9::mCherry (Ihara et al. 2011), referred to as collagen::mCh) we examined surface area projections of the gonadal and pharyngeal

BMs and found that the pharyngeal BM grew approximately three-fold in surface area during larval development (L1 through young adult), while the gonadal surface area increased over 90-fold (Figure 5B). To determine if type IV collagen addition was required to maintain BM and tissue integrity during pharynx and gonad growth, I depleted EMB-9 ($\alpha 1$ -like chain) by RNAi beginning at the L1 larval stage and analyzed both organs at adulthood (72h, Figure 5A). I found that reduction of collagen frequently resulted in deformation of the anterior pharyngeal bulb (n=15/20 adult animals, Figure 6), and severe distortion and rupturing of gonadal tissue (n=20/20 adult animals, Figure 6). Similar results were observed upon knockdown of *let-2* (the $\alpha 2$ chain, n=20/20 animals examined). Linescan analysis of mean fluorescence intensity revealed a ~70% reduction in collagen::mCh levels in the pharyngeal BM. Further, gaps in collagen signal appeared at regions of pharyngeal bulb deformation (Figure 6). Collagen was reduced by ~60% in the gonad at the early L3 stage, prior to BM rupturing and the gonadal tissue becoming disorganized (Figure 6). Taken together, these results indicate that addition of type IV collagen to the BM is necessary to maintain tissue integrity during pharyngeal and gonadal growth.

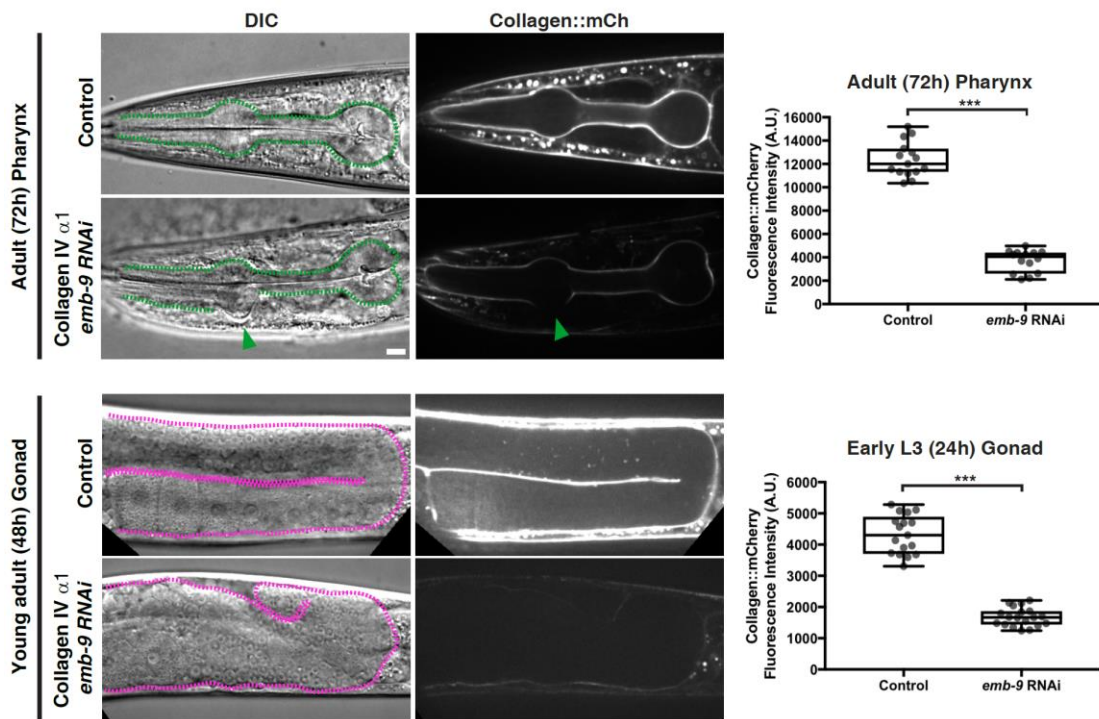


Figure 6: BM type IV collagen supports the growing pharynx and gonad.

DIC and collagen::mCh fluorescence images of adult pharynxes (top left) and gonads (bottom left) of control (L4440 empty vector) and *collagen IV α1* (*emb-9*) RNAi-treated 72h adult animals. Pharynxes in DIC images (top left) are outlined with green dotted lines. The green arrowhead indicates a deformation in the anterior pharyngeal bulb, corresponding to a region with undetectable collagen::mCh signal. Mean pharyngeal BM collagen::mCh fluorescence intensity in control (n=15) and *emb-9* RNAi treated (n=14) 72h adult animals are quantified on the top right. Dotted magenta lines outline gonads in DIC images (bottom left). The gonads of *emb-9* RNAi-treated animals are severely misshapen, correlating with near undetectable BM collagen::mCh signal. Mean gonadal BM collagen::mCh fluorescence intensity in control (n=17) and *emb-9* RNAi-treated (n=19) early L3 animals are quantified on the bottom right. *** $p < 0.0001$, unpaired two-tailed Student's *t* test. Box edges in boxplots depict the 25th and 75th percentile, the line in the box indicates the median value, and whiskers mark the minimum and maximum values. Scale bars are 10 μ m.

2.2.2 The pharyngeal basement membrane is collagen-rich, but laminin-poor, compared to the gonadal basement membrane

BMs of different tissues often vary in levels and composition of matrix components (Halfter et al. 2015; Randles et al. 2017). To determine if type IV collagen levels differ between the gonadal and pharyngeal BMs, I quantified collagen::mCh fluorescence intensity in both organs and found that collagen was present at two-fold higher levels in the pharyngeal BM versus the gonadal BM in 72h adults (Figure 7). As embryonic studies have suggested that collagen is recruited to BMs through association with laminin networks (Huang et al. 2003; Urbano et al. 2009; Pöschl et al. 2004; Matsubayashi et al. 2017), I next asked if higher levels of laminin might be required to recruit more collagen to the pharyngeal BM. Laminins are heterotrimers comprised of an α , β , and γ chain. *C. elegans* encodes two α subunits (*lam-3* and *epi-1*), one β subunit (*lam-1*), and one γ subunit (*lam-2*), that form two distinct laminin heterotrimers (Kramer 2005). To assess laminin levels in the BM, we used CRISPR/Cas9 genome editing to encode mNeonGreen at the *lam-2* genomic locus, generating worms expressing the LAM-2::mNeonGreen fusion protein (referred to as laminin::mNG). Surprisingly, I found that there were two-fold lower levels of laminin in the pharyngeal BM compared to the gonadal BM (Figure 7). Thus, there are higher levels of type IV collagen in the pharyngeal BM compared to the gonadal BM, but this collagen enrichment is not correlated with increased laminin.

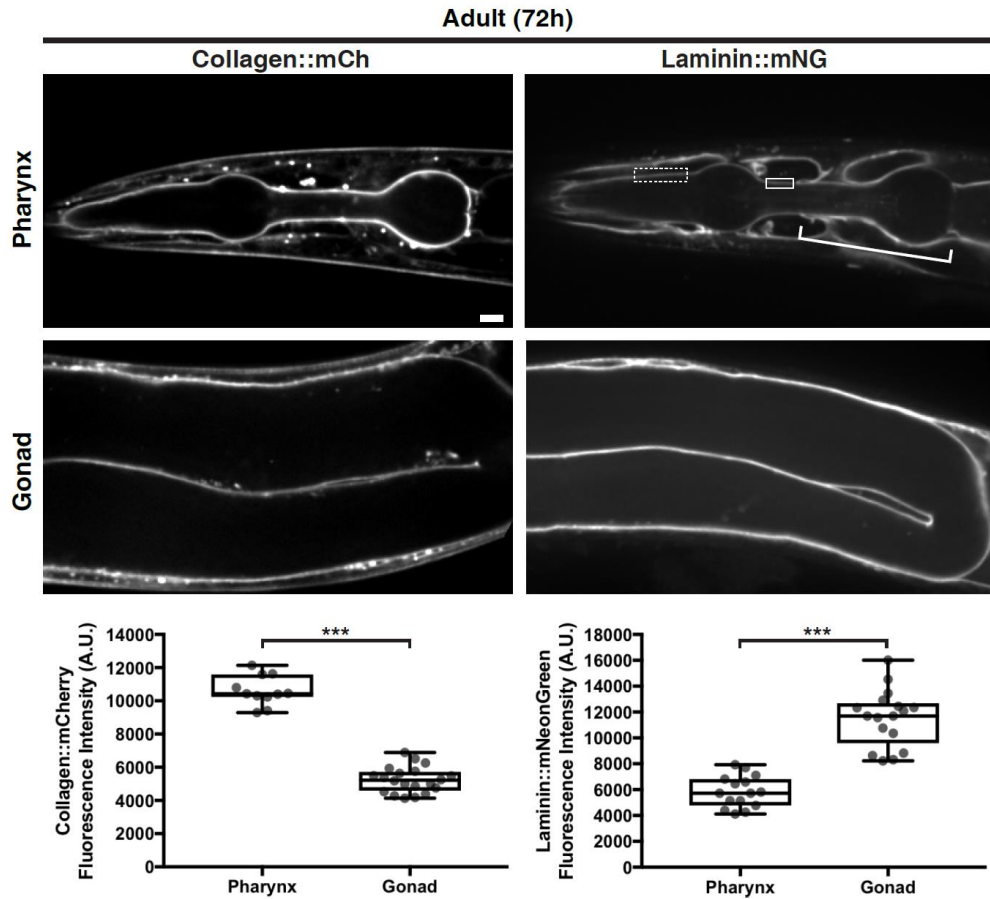


Figure 7: The pharyngeal BM is collagen-rich, while the gonadal BM is laminin-rich.

Fluorescence images of collagen::mCh and laminin::mNG in the pharynx and gonad of 72h adult animals. As laminin::mNG localizes strongly to the nerve ring BM that surrounds and contacts the pharyngeal BM at several regions (bracket), we confined our measurements of laminin signal to the dotted box where clear pharyngeal BM laminin is visible in this and all relevant figures, except figure 6C, where laminin signal in the solid box was also measured. Quantification of collagen::mCh and laminin::mNG levels in the pharyngeal (collagen::mCh n=11; laminin::mNG n=15) and gonadal BMs (collagen::mCh n=20; laminin::mNG n=17) are shown in boxplots at the bottom. *** $p < 0.0001$, unpaired two-tailed Student's t test. Box edges in boxplots depict the 25th and 75th percentile, the line in the box indicates the median value, and whiskers mark the minimum and maximum values. Scale bars are $10\mu\text{m}$.

2.2.3 Laminin is required for collagen recruitment to the gonadal but not pharyngeal basement membrane

My finding that the collagen enrichment in the pharyngeal BM relative to the gonadal BM is not correlated with similarly increased laminin levels suggested that the interaction between type IV collagen and laminin may differ in the BMs of these tissues. I next asked whether laminin was required to recruit collagen to these BMs. I used RNAi to deplete LAM-2 (the sole laminin γ subunit) beginning in the L1 larval stage and analyzed BM collagen levels during subsequent larval development and adulthood. By the early L3 larval stage (24h RNAi treatment), there was a ~50% reduction in gonadal BM laminin levels (Figure 8A), correlating with a similar reduction in type IV collagen levels (Figure 8B). Breaks in the BM were observed shortly after this time (~26h RNAi treatment, n=12/20 animals), followed by BM rupturing (Mid L4, Figure 8B, n=20/20 worms), and ultimately gonadal tissue disintegration (72h adult, Figure 8B, n=20/20 animals examined). In contrast, the pharyngeal BM collagen levels were unaffected (Figure 9B) despite a strong knockdown of laminin (~70% reduction in laminin levels by 96h adult, Figure 9A), and there were no defects in pharyngeal structure (n=14/14 animals). These observations suggest that type IV collagen recruitment to the growing BM is distinct in each tissue—laminin-dependent in the gonad but laminin-independent in the pharynx.

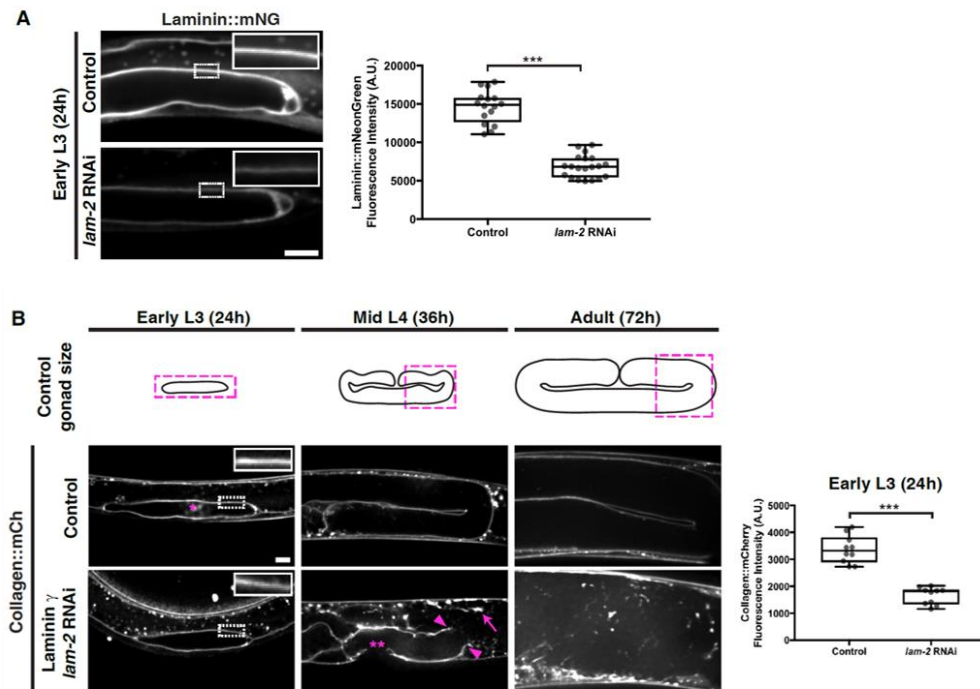


Figure 8: Collagen recruitment to the gonadal BM is dependent on laminin.

(A) Fluorescence images of gonadal BM laminin::mNG in control (L4440 empty vector) and *laminin γ* (*lam-2*) RNAi-treated animals (RNAi feeding initiated at the L1 stage and animals viewed at the early L3). Quantification of laminin::mNG fluorescence intensity is shown on the right (control n=16; *lam-2* RNAi n=20). (B) Fluorescence images of gonadal BM collagen::mCh shown at the early L3, mid-L4, and 72h adult stages in control and *lam-2* RNAi-treated animals (RNAi fed at the L1 stage onwards). Control gonad size at these stages are shown in schematics, and the magenta boxes denote regions of the gonad shown in the figure. Collagen::mCh signal in the dotted box regions are magnified in insets. The asterisk indicates non-BM collagen::mCh signal from coelomocytes. Gonadal BM collagen::mCh fluorescence intensity in control (n=10) and *lam-2* (n=10) RNAi-treated early L3 animals is quantified on the right. By the mid-L4 stage, rupturing of the gonadal BM (magenta arrowheads) and abnormal collagen aggregation (magenta arrow) was observed in *lam-2* RNAi treated animals (n=20/20). The double asterisks mark a break in the BM due to anchor cell invasion, a normal morphogenetic event during *C. elegans* vulval development. *** $p < 0.0001$, unpaired two-tailed Student's *t* test. Box edges in boxplots depict the 25th and 75th percentile, the line in the box indicates the median value, and whiskers mark the minimum and maximum values. Scale bars are 10 μ m.

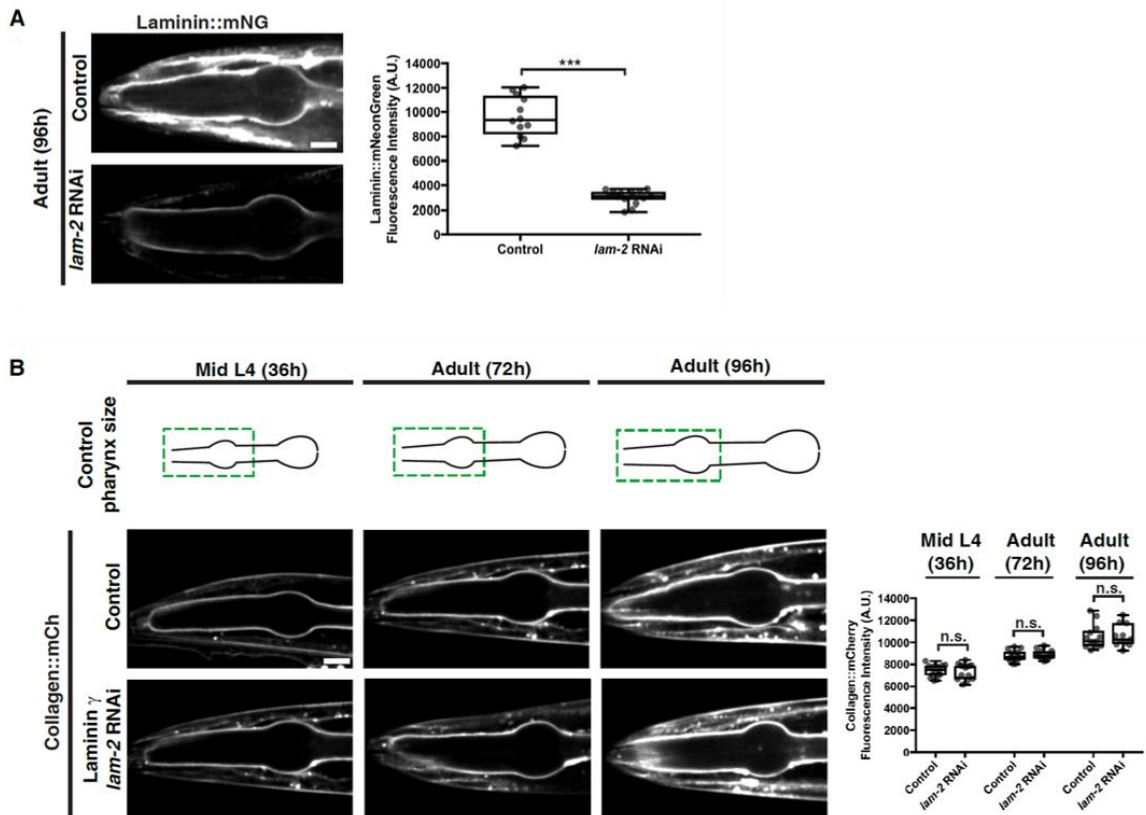


Figure 9: Collagen recruitment to the pharyngeal BM is independent of laminin.

(A) Fluorescence images of pharyngeal BM laminin::mNG in control and *laminin* γ (*lam-2*) RNAi-treated animals viewed in 96h adults. Quantification of laminin::mNG fluorescence intensity is shown on the right (control n=12; *lam-2* RNAi n=14). (B) Fluorescence images of pharyngeal BM collagen::mCh in control and *lam-2* RNAi-treated animals shown at the mid L4, 72h adult, and 96h adult stages. Control pharynx size at these stages are shown in schematics, and the green boxes denote regions of the pharynx shown in the figure. Pharyngeal BM collagen::mCh fluorescence intensity in control and *lam-2* RNAi-treated animals at all three stages are quantified on the right (mid L4 control n=14, *lam-2* RNAi n=14; 72h adult control n=14, *lam-2* RNAi n=12; 96h adult control n=13, *lam-2* RNAi n=11). *** $p < 0.0001$, unpaired two-tailed Student's t test; n.s., $p > 0.05$. Box edges in boxplots depict the 25th and 75th percentile, the line in the box indicates the median value, and whiskers mark the minimum and maximum values. Scale bars are 10 μ m.

2.2.4 INA-1/PAT-3 integrin mediates collagen recruitment to the gonadal basement membrane in a laminin-dependent manner

Work in cell culture has suggested that interactions with laminin-binding integrin and dystroglycan receptors as well as cell surface sulfated glycolipids (sulfatides) might seed laminin polymerization to initiate BM assembly, leading to subsequent collagen recruitment (Yurchenco and Patton 2009; Li et al. 2017). Because of possible redundancy between these mechanisms and within the large integrin gene family in vertebrates, however, there has not yet been clear genetic evidence for any of these mechanisms in regulating laminin and collagen recruitment to BMs *in vivo* (Yurchenco 2015). As *C. elegans* does not synthesize sulfated glycolipids (Bai et al. 2018), I hypothesized that tissue-specific roles for integrin and dystroglycan might explain the different modes of collagen recruitment to the pharyngeal and gonadal BMs.

To investigate the cell surface interactions that recruit type IV collagen to developing tissues, we initially focused on the gonadal BM. We first examined the dystroglycan receptor. *C. elegans* harbors a single vertebrate dystroglycan ortholog, *dgn-1* (Johnson et al. 2006). Endogenously tagged DGN-1::mNG (Naegeli et al. 2017) was expressed in the gonad and localized to the gonad-BM interface (Figure 10A). Knockdown of *dgn-1* by RNAi eliminated detectable DGN-1::mNG but did not affect either laminin or collagen levels in adult animals (Figure 10B). I thus next investigated the integrin receptor system. *C. elegans* assembles two integrin heterodimers, composed of the α subunits PAT-2 (most similar to RGD-binding integrins) or INA-1 (most similar

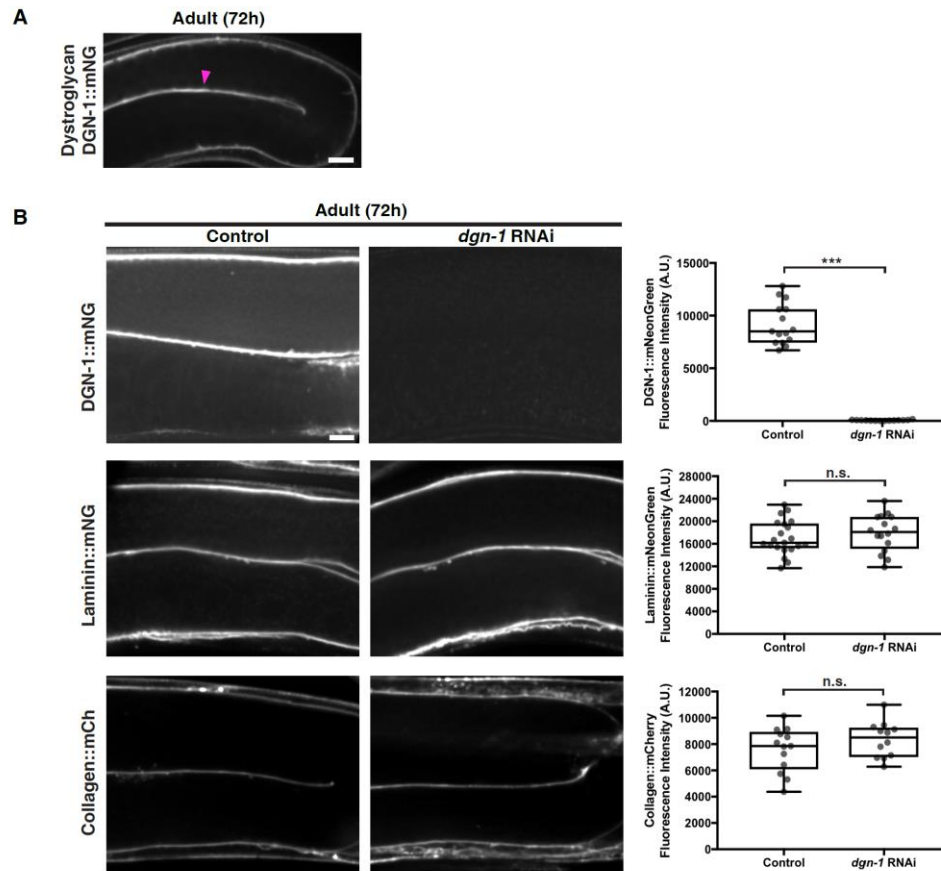


Figure 10: Dystroglycan is not required for laminin or collagen recruitment to the gonadal BM.

(A) Fluorescence image of DGN-1::mNG localization in a 72h adult gonad. The magenta arrowhead denotes enrichment of fluorescence signal at the gonadal sheath-BM interface. (B) Fluorescence images of DGN-1::mNG in the gonad in control and *dgn-1* RNAi-treated 72h adult animals is shown in the top panel, with quantification of DGN-1::mNG fluorescence intensity on the right (control n=15; *dgn-1* RNAi n=14). The middle panel shows fluorescence images of gonadal BM laminin::mNG in control and *dgn-1* RNAi-treated 72h adult animals, with quantification of laminin::mNG fluorescence intensity on the right (control n=21; *dgn-1* RNAi n=16). The bottom panel shows fluorescence images of gonadal BM collagen::mCh in control and *dgn-1* RNAi-treated 72h adult animals, with quantification of laminin::mNG fluorescence intensity on the right (control n=13; *dgn-1* RNAi n=12). *** $p < 0.0001$, unpaired two-tailed Student's t test; n.s., $p > 0.05$. Box edges in boxplots depict the 25th and 75th percentile, the line in the box indicates the median value, and whiskers mark the minimum and maximum values. Scale bars are 10 μ m.

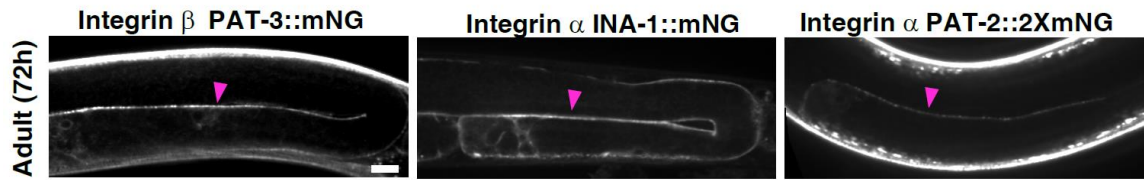


Figure 11: The integrin α subunits INA-1 and PAT-2 and the integrin β subunit PAT-3 are expressed in the gonadal sheath.

Fluorescence images of the integrin β subunit PAT-3::mNG and the integrin α subunits INA-1::mNG and PAT-2::2xmNG in the gonad. Magenta arrowheads indicate enrichment of fluorescence signal at the gonadal sheath-BM interface. Scale bars are 10 μ m.

to laminin-binding integrins) dimerized to the sole β subunit PAT-3 (Kramer 2005).

Endogenously tagged INA-1::mNG, PAT-2::2XmNG, and PAT-3::mNG were expressed in the gonadal sheath cells and localized to the cell-BM interface (Figure 11). L1 RNAi mediated knockdown of *ina-1* and *pat-3* each resulted in a ~50% reduction in collagen::mCh levels in adult animals (Figure 12), suggesting that the INA-1/PAT-3 integrin heterodimer is required for type IV collagen recruitment to the gonadal BM.

Importantly, RNAi against *ina-1* and *pat-3* did not appear to alter collagen secretion from the muscle cells (Figure 13), suggesting a direct function for INA-1/PAT-3 in the gonad.

As gonadal BM collagen localization is dependent on laminin, I analyzed laminin::mNG levels upon *ina-1* and *pat-3* knockdown and found a similar ~50% reduction (Figure 12) in each condition. Surprisingly, depletion of the other integrin α subunit PAT-2 by RNAi yielded an increase in BM collagen and laminin levels (Figure 12). I speculated that this could be due to more INA-1/PAT-3 heterodimers forming upon reduction of

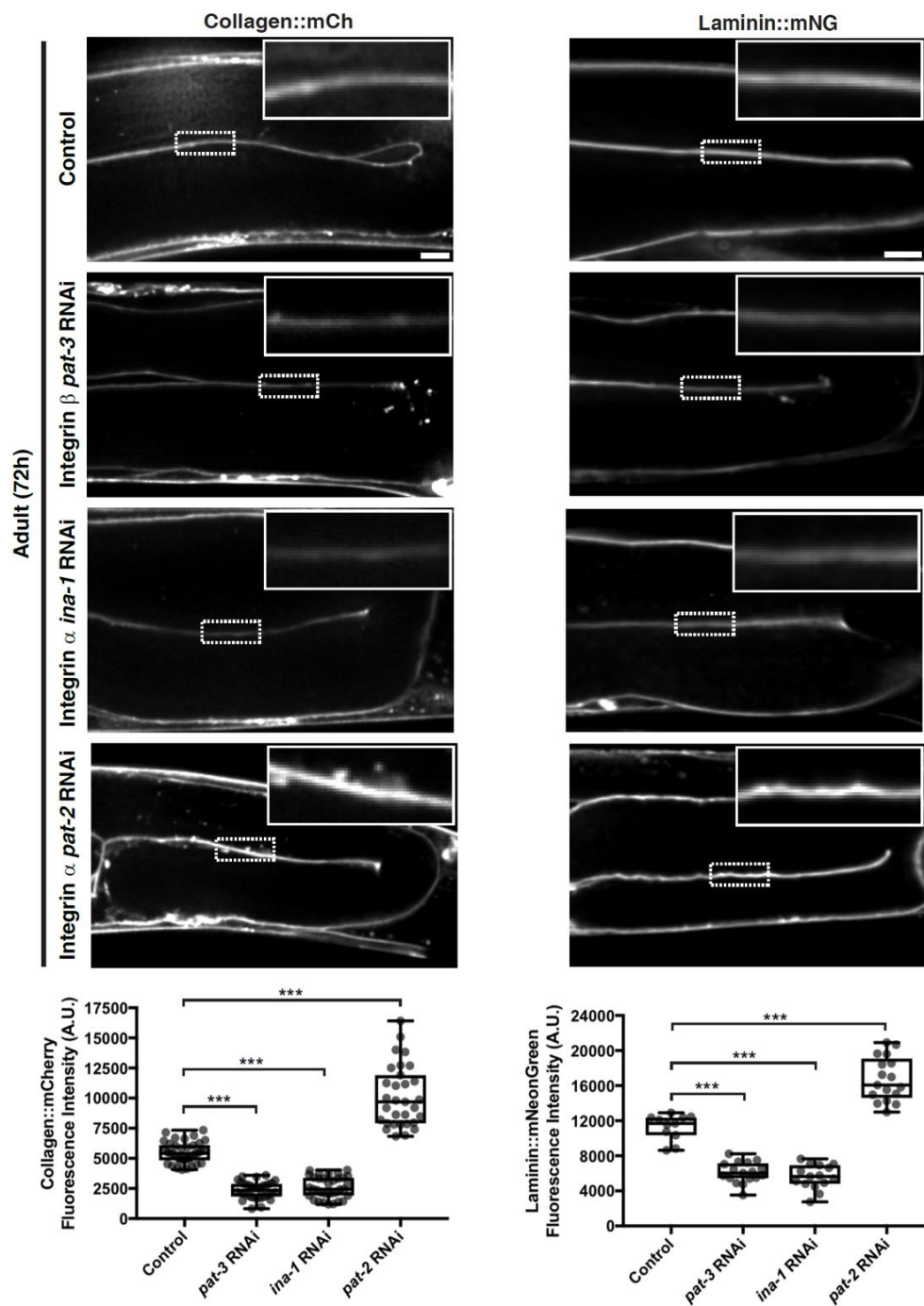


Figure 12: The INA-1/PAT-3 integrin heterodimer is required for laminin-dependent collagen recruitment to the gonadal BM.

Fluorescence images of gonadal BM collagen::mCh (left) and laminin::mNG (right) in control versus *pat-3*, *ina-1*, and *pat-2* RNAi-treated 72h adult animals. Regions of the BM in the dotted boxes are magnified in insets. Quantification of collagen::mCh (control n=38; *pat-3* RNAi n=34; *ina-1* RNAi n=34; *pat-2* RNAi n=31) and laminin::mNG (control n=11; *pat-3* RNAi n=17; *ina-1* RNAi n=15; *pat-2* RNAi n=17) fluorescence intensity for all treatments is shown at the bottom. *** $p < 0.0001$, one-way analysis of variance (ANOVA) followed by post-hoc Dunnett's test. Box edges in boxplots depict the 25th and 75th percentile, the line in the box indicates the median value, and whiskers mark the minimum and maximum values. Scale bars are 10 μ m.

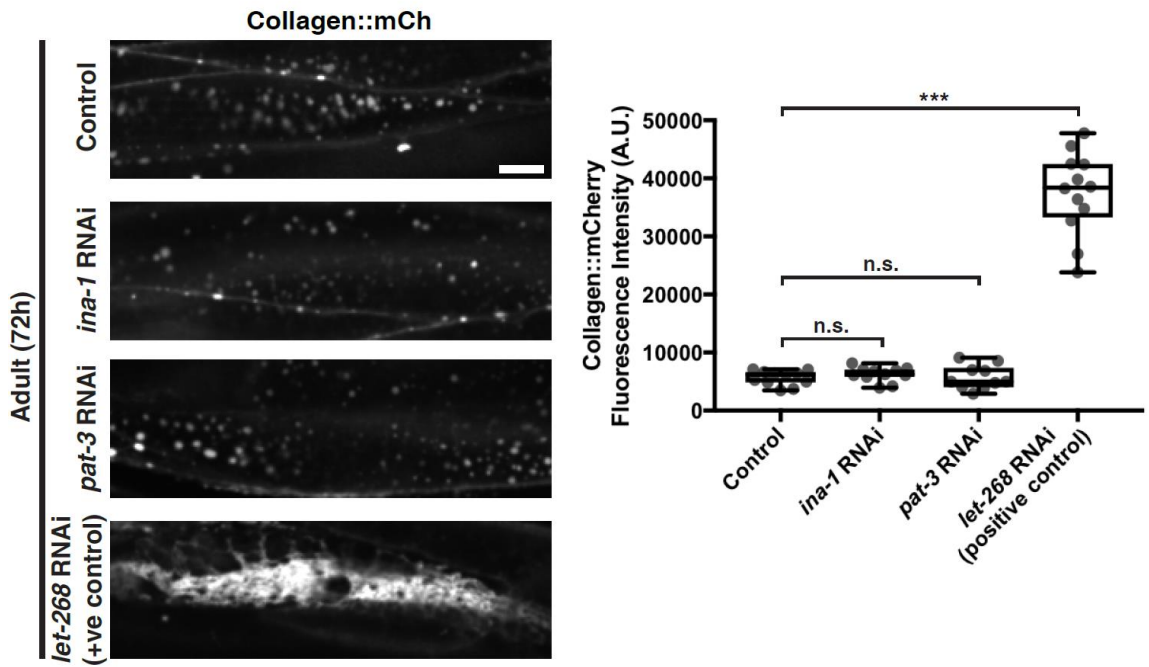


Figure 13: Loss of integrin does not perturb collagen secretion.

Fluorescence images of body wall muscle collagen::mCh in control, *ina-1*, *pat-3*, and *let-268* RNAi-treated 72h adult animals, with quantification of collagen::mCh fluorescence intensity on the right (control n=11; *ina-1* RNAi n=11; *pat-3* RNAi n=10; *let-268* RNAi n=12). *let-268* encodes a procollagen lysyl hydroxylase that is essential for collagen IV secretion (Norman and Moerman 2000). *** $p < 0.0001$, one-way ANOVA followed by post-hoc Dunnett's test; *n.s.*, $p > 0.05$. Box edges in boxplots depict the 25th and 75th percentile, the line in the box indicates the median value, and whiskers mark the minimum and maximum values. Scale bars are 10 μ m.

PAT-2. Consistent with this idea, RNAi against *pat-2* by RNAi more than doubled INA-1::mNG levels at cell surfaces contacting the gonadal BM (Figure 14).

To determine if any other matrix receptors contribute to collagen recruitment to the gonadal BM, I performed RNAi against worm orthologs of glypican (*gpn-1* and *lon-2*), LAR-RPTP (*ptp-3*), teneurin (*ten-1*), and discoidin domain receptors (*ddr-1* and *ddr-2*) (Kramer, 2005). Knockdown of these receptors did not affect gonadal collagen levels (Figure 15). Taken together, my findings suggest that the putative laminin-binding INA-1/PAT-3 integrin heterodimer is the predominant cell surface receptor that mediates collagen IV recruitment to the gonadal BM through a laminin-dependent mechanism.

2.2.5 The PAT-2/PAT-3 integrin heterodimer promotes collagen recruitment to the pharyngeal basement membrane independent of laminin

I next sought to determine the cell surface receptor(s) that mediates collagen recruitment to the pharyngeal BM. DGN-1::mNG expression was not detectable in the pharynx (Figure 16A). In contrast, all three integrin subunits were present in the pharyngeal epithelium and localized to the pharynx-BM interface (Figure 16B). RNAi against *ina-1* did not affect pharyngeal BM collagen or laminin levels (96h RNAi treatment, Figure 17). However, RNAi targeting *pat-2* and *pat-3* each reduced pharyngeal BM collagen levels by over 40% (Figure 17). Notably, RNAi against *pat-2* or *pat-3* did not affect pharyngeal BM laminin levels (Figure 17). These results suggest the PAT-2/PAT-3 integrin promotes pharyngeal BM collagen recruitment independent of

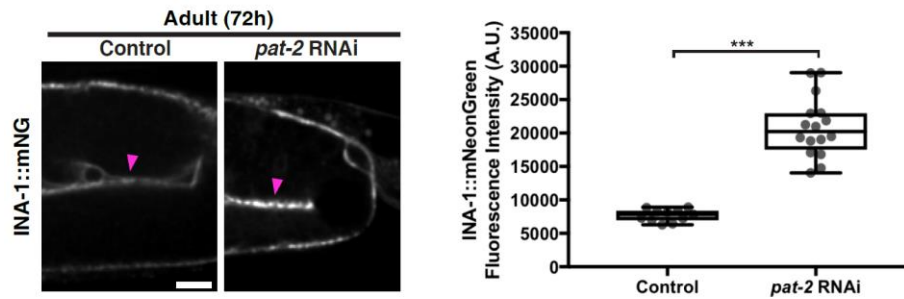


Figure 14: Reduction of *pat-2* results in increased INA-1 levels at the gonadal sheath surface.

Fluorescence images of gonadal INA-1::mNG in control and *pat-2* RNAi-treated 72h adult animals, with quantification of INA-1::mNG fluorescence intensity on the right (control n=11; *ina-1* RNAi n=16). The magenta arrowheads denote INA-1::mNG enrichment at the gonadal sheath-BM interface. *** $p < 0.0001$, unpaired two-tailed Student's *t* test. Box edges in boxplots depict the 25th and 75th percentile, the line in the box indicates the median value, and whiskers mark the minimum and maximum values. Scale bars are 10 μ m.

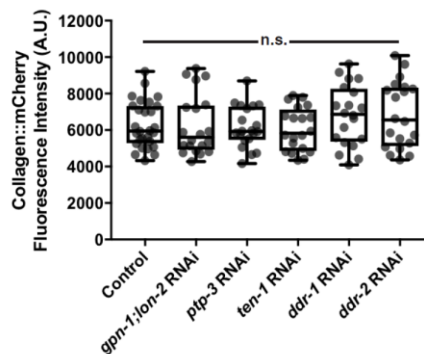


Figure 15: Knockdown of targeted matrix receptors does not affect collagen recruitment to the gonadal BM.

Quantification of gonadal BM collagen::mCh fluorescence intensity in 72h adult animals upon knockdown of matrix receptors (control n=28 and n=20 each for all RNAi treatments). n.s., $p > 0.05$, one-way ANOVA. Box edges in boxplots depict the 25th and 75th percentile, the line in the box indicates the median value, and whiskers mark the minimum and maximum values.

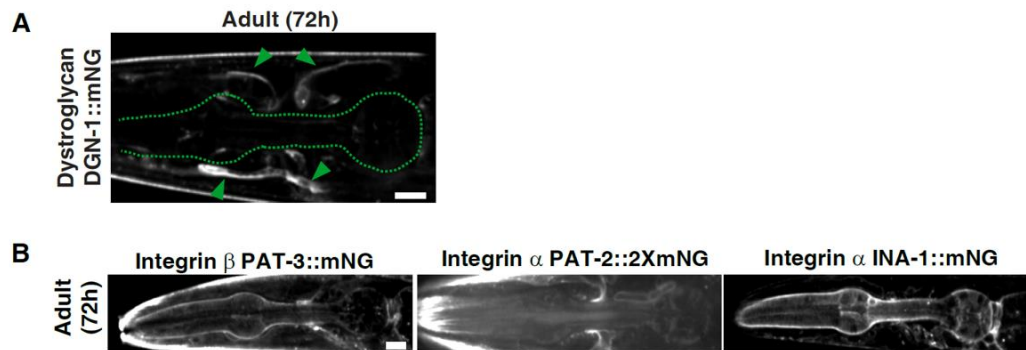


Figure 16: All three integrin subunits—INA-1, PAT-2, and PAT-3—but not dystroglycan are expressed in the pharynx.

(A) Fluorescence image of DGN-1::mNG localization in the head of a 72h adult animal. The pharynx is outlined in green. Green arrowheads indicate enrichment of DGN-1::mNG at the nerve ring-nerve BM interface. **(B)** Fluorescence images of the integrin β subunit PAT-3::mNG and the integrin α subunits PAT-2::2xmNG and INA-1::mNG in the pharynx. Scale bars are 10 μ m.

laminin. To determine whether PAT-2 is sufficient to recruit collagen to the pharyngeal BM, I over-expressed PAT-2::mNG specifically in pharyngeal muscle cells by using the *myo-2* promoter (Figure 18). Mosaic analysis of adult animals revealed that pharyngeal BM collagen::mCh levels were increased by ~30% in regions where PAT-2 was over-expressed (Figure 18). Finally, RNAi-mediated reduction of other major matrix receptors did not affect collagen levels in the pharyngeal BM (Figure 19). Together, these observations indicate that the putative RGD-binding PAT-2/PAT-3 integrin heterodimer is the predominant cell surface receptor that is required and sufficient to mediate type IV collagen recruitment to the pharyngeal BM independent of laminin. Further, these results suggest that the recruitment of laminin in the growing pharyngeal

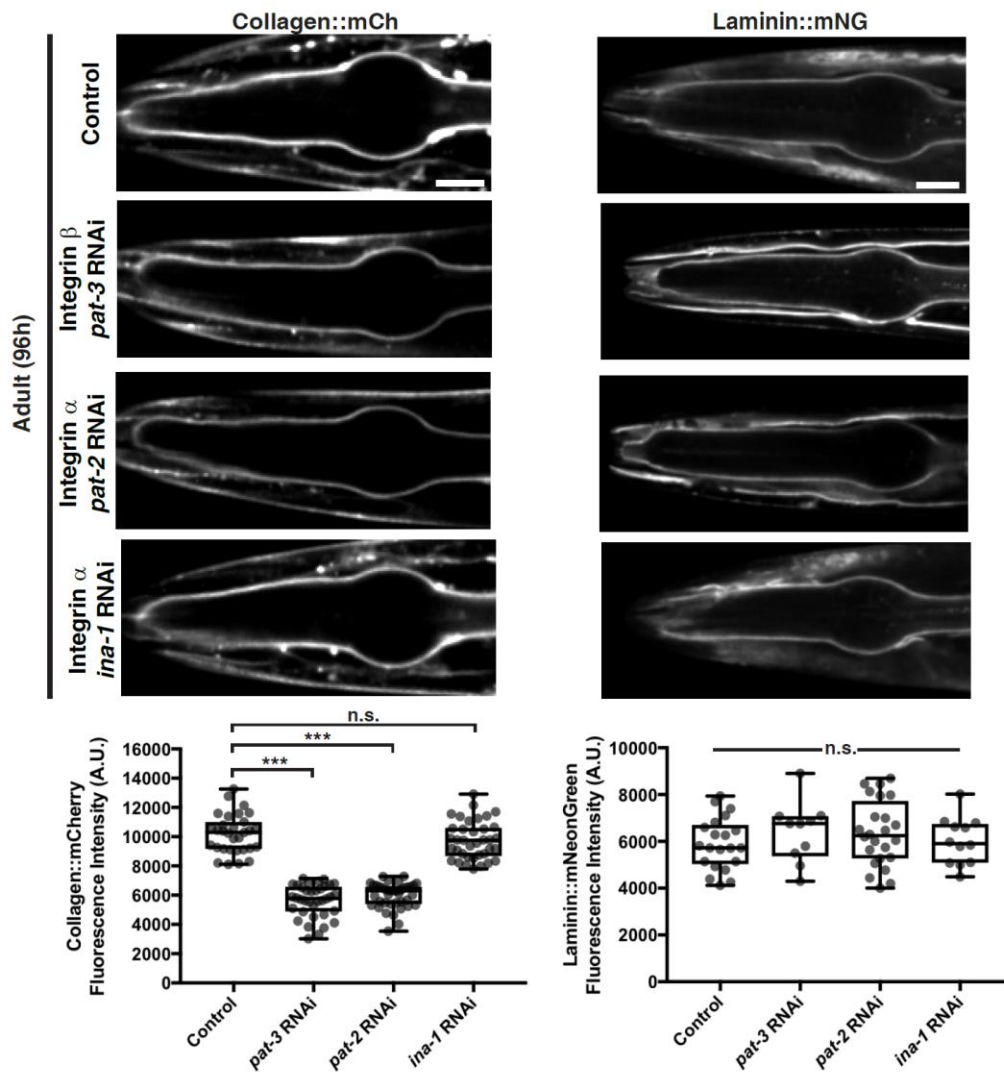


Figure 17: The PAT-2/PAT-3 integrin heterodimer is required for laminin-independent collagen recruitment to the pharyngeal BM.

Fluorescence images of pharyngeal BM collagen::mCh (left) and laminin::mNG (right) in control versus *pat-3*, *pat-2*, and *ina-1* RNAi-treated 96h adult animals. Quantification of collagen::mCh (control n=31; *pat-3* RNAi n=36; *pat-2* RNAi n=39; *ina-1* RNAi n=37) and laminin::mNG (control n=21; *pat-3* RNAi n=10; *pat-2* RNAi n=24; *ina-1* RNAi n=12) fluorescence intensity for all treatments is shown at the bottom. *** $p < 0.0001$, one-way ANOVA followed by post-hoc Dunnett's test. n.s., $p > 0.05$, one-way ANOVA. Box edges in boxplots depict the 25th and 75th percentile, the line in the box indicates the median value, and whiskers mark the minimum and maximum values. Scale bars are 10 μ m.

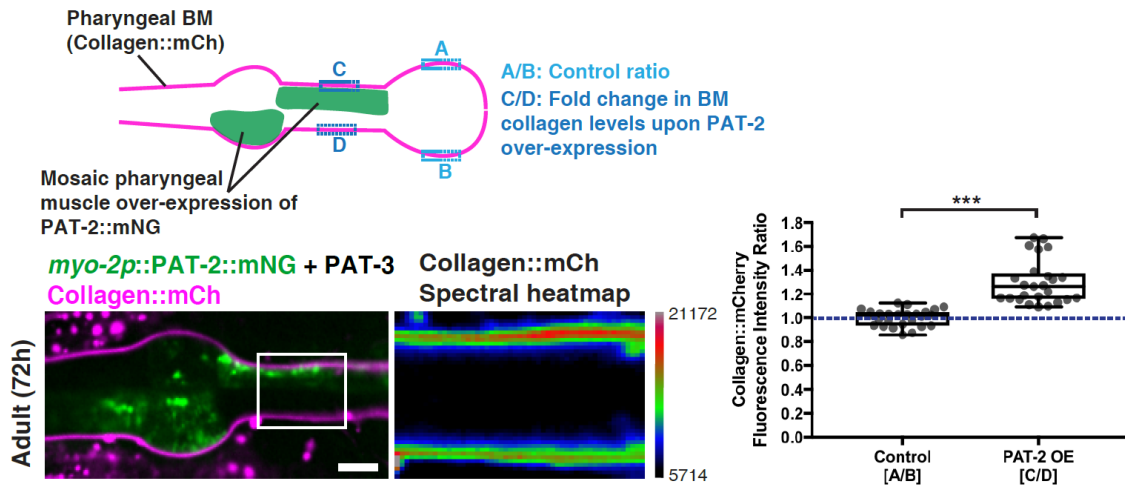


Figure 18: PAT-2 is sufficient for collagen recruitment to the pharyngeal BM.

A schematic outlining mosaic over-expression of PAT-2::mNG in the pharyngeal muscle cells and method for quantification of collagen levels is shown on top. A merged fluorescence image of *myo-2p::PAT-2::mNG* (green) and collagen::mCh (magenta) in a 72h adult pharynx is shown on the bottom left. A spectral heatmap of collagen::mCh fluorescence intensity in the boxed region is shown on the bottom right. Quantification of the fold change in pharyngeal BM collagen::mCh fluorescence intensity upon PAT-2 over-expression is shown on the right (n=25). *** $p < 0.0001$, paired two-tailed Student's *t*-test. Box edges in boxplots depict the 25th and 75th percentile, the line in the box indicates the median value, and whiskers mark the minimum and maximum values. Scale bars are 10 μ m.

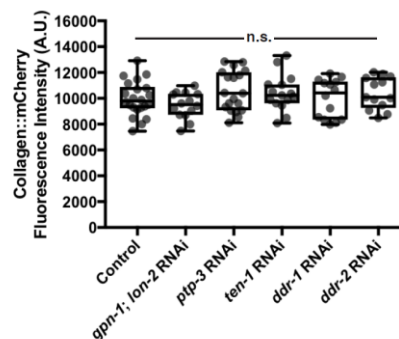


Figure 19: Knockdown of targeted matrix receptors does not affect collagen recruitment to the pharyngeal BM.

Quantification of pharyngeal BM collagen::mCh fluorescence intensity in 96h adult animals upon knockdown of matrix receptors (control n=22, *gpn-1*, *lon-2* RNAi n=14; *ptp-3* RNAi n=19; *ten-1* RNAi n=15; *ddr-1* RNAi n=14; *ddr-2* RNAi n=15). n.s., $p>0.05$, one-way ANOVA. Box edges in boxplots depict the 25th and 75th percentile, the line in the box indicates the median value, and whiskers mark the minimum and maximum values.

BM is not dependent on integrins (either INA-1/PAT-3 or PAT-2/PAT-3) but is mediated by an unknown mechanism.

2.2.6 The PAT-2 intracellular domain dictates basement membrane recruiting activity of integrins in the pharynx

All integrin subunits were expressed in both the gonadal and pharyngeal tissues. Thus, we next sought to determine the mechanism controlling the tissue-specific activity of the two integrin heterodimers in matrix recruitment. Recent studies have suggested that the diverse intracellular C-terminal membrane-distal regions (CTMDs) of vertebrate α integrins may provide specificity for integrin inside-out activation—a form of integrin activation where intracellular regulators bind the cytoplasmic tails of integrin heterodimers and trigger conformational changes that allow high affinity binding of the integrin extracellular domain with matrix ligands (Thinn et al. 2018). As the sole difference between INA-1/PAT-3 and PAT-2/PAT-3 integrin heterodimers is the α subunit, I speculated that their tissue-specific activity in collagen recruitment could be regulated by their distinct α -integrin intracellular domains mediating inside-out

activation. Indeed, INA-1 and PAT-2 diverge significantly in their CTMD regions (Figure 20A).

Building off of these studies, and my findings that INA-1/PAT-3 integrin is expressed in the pharynx but does not recruit laminin to the pharyngeal BM, I hypothesized that the pharynx-active intracellular domain of PAT-2 fused to the laminin-binding extracellular domain of INA-1 might be able to recruit laminin in this tissue. I engineered animals that express this chimeric α integrin subunit in the pharynx (myo-2p::INA-1[EX]::PAT-2[CTMD]::mNG, Figure 20B). Over-expression of this chimeric integrin resulted in a ~50% increase in laminin levels in regions of the BM contacting chimera-expressing pharyngeal cells (Figure 20C). Together, my findings suggest that the cytoplasmic domain of PAT-2 facilitates the PAT-2/PAT-3-mediated recruitment of collagen to the pharyngeal BM, and when attached to the extracellular domain of INA-1, triggers laminin recruitment instead.

2.2.7 RAP-3 is a pharyngeal-specific activator of PAT-2/PAT-3 integrin

My results suggested that there might be tissue-specific factors that activate PAT-2/PAT-3 in the pharynx via the PAT-2 intracellular domain to mediate BM matrix recruitment. Proteomic, localization, and genetic screening approaches have identified numerous proteins that localize with integrins or regulate integrin activity (Horton et al. 2016). To identify potential tissue-specific regulators of PAT-2/PAT-3 integrin-mediated

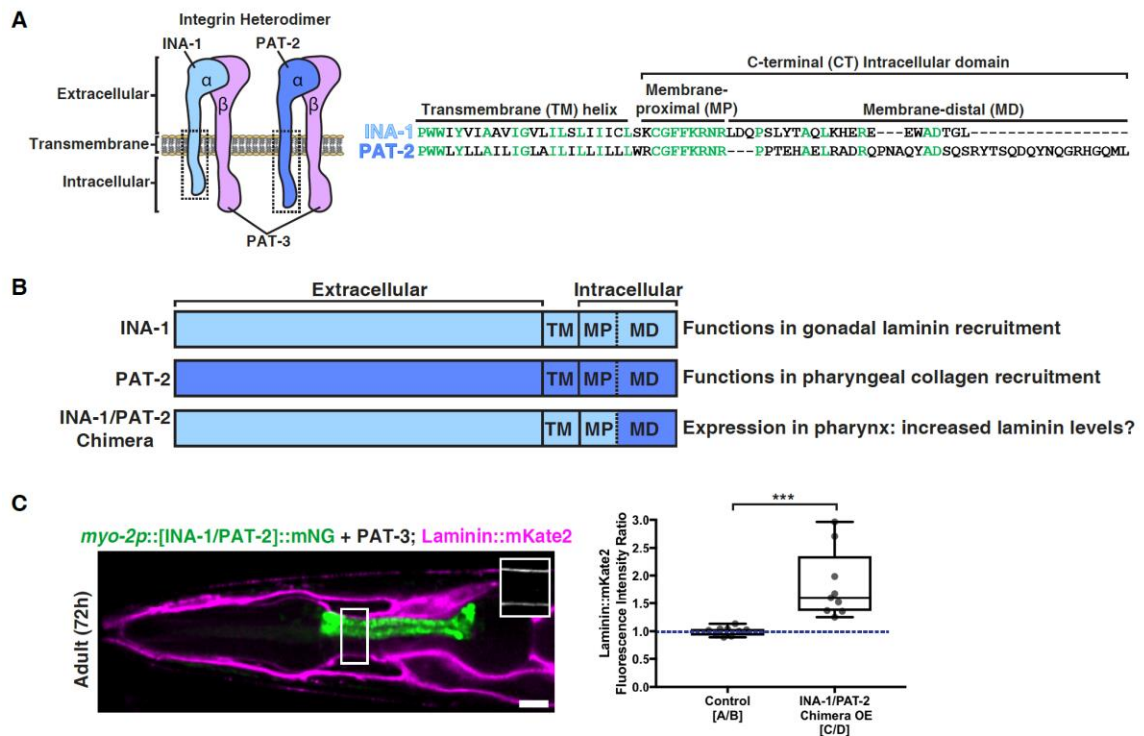


Figure 20: The intracellular domain of PAT-2 controls the activity of PAT-2/PAT-3 in the pharynx to promote collagen recruitment.

(A) A schematic of the two integrin heterodimers expressed in the worm, highlighting the extracellular, transmembrane, and C-terminal intracellular regions of these proteins. Amino acid alignments of the boxed transmembrane and intracellular regions of INA-1 and PAT-2 are shown on the right. Highly conserved residues are shown in green. (B) Schematics of chimeric integrin α subunits. Determined functions of INA-1 and PAT-2, and the predicted outcomes of expression of the relevant chimeric integrin in the pharynx or gonad are listed. (C) A merged fluorescence image of myo-2p::[INA-1/PAT-2]::mNG (green) and laminin::mKate2 (magenta) in a 72h adult pharynx is shown. Laminin::mKate2 signal in the boxed region is magnified in the inset. Quantification of the fold change in pharyngeal BM laminin::mKate2 fluorescence intensity upon over-expression of the INA-1/PAT-2 chimera is shown on the right (n=9). *** $p < 0.0001$, paired two-tailed Student's *t*-test. Box edges in boxplots depict the 25th and 75th percentile, the line in the box indicates the median value, and whiskers mark the minimum and maximum values. Scale bars are 10 μ m.

collagen IV recruitment to BM, I performed a targeted RNAi screen (Table 1) of *C. elegans* orthologs of 33 known integrin-associated or regulatory proteins (Horton et al. 2015; Bouvard et al. 2013; Lilja et al. 2017). I searched for proteins whose loss reduced type IV collagen in the pharyngeal BM but did not affect gonadal collagen levels. RNAi against one gene, *rap-3*, led to a ~40% reduction of pharyngeal type IV collagen levels without affecting gonadal BM collagen, suggesting it could be a specific activator of PAT-2/PAT-3 in the pharynx (Figure 21A and Figure 21B).

The *rap-3* gene encodes a Rap-like protein most similar to the mammalian Rap1 isoforms Rap1A and Rap1B (Reiner and Lundquist 2018). Rap1 is a member of the Ras family of small GTPases, and Rap1 has been implicated as an activator of integrins in numerous contexts, especially in blood and endothelial cells (Lagarrigue et al. 2016; Carmona et al. 2009; Boettner and Van Aelst 2009). To determine if the RAP-3 protein might be a tissue-specific regulator of PAT-2/PAT-3 integrin activity, we first generated RAP-3::mNG expressing animals using CRISPR/Cas9 genome editing. Consistent with a pharynx-specific function, I found that RAP-3::mNG was expressed in the pharynx of larval and early adult animals but was not detectable in gonadal tissue (Figure 22).

I hypothesized that if RAP-3 specifically activates PAT-2/PAT-3 to recruit type IV collagen, then it would not be involved in laminin recruitment. Supporting this notion, I found that pharyngeal BM laminin levels were unaffected by RNAi targeting *rap-3* (Figure 23). Further, pharyngeal-specific over-expression of a constitutively active form

Table 1: Targeted screen of vertebrate integrin-associated proteins with *C. elegans* orthologs

Vertebrate integrin-associated protein	<i>C. elegans</i> ortholog
ACTN4/1	<i>atn-1</i>
ILK	<i>pat-4</i>
PDLIM5/7/1	<i>alp-1</i>
VCL	<i>deb-1</i>
CNN2	<i>cpn-2</i>
GIT2	<i>cnt-1</i>
	<i>git-1</i>
ZYX	<i>zyx-1</i>
PALLD	<i>ketn-1</i>
	<i>unc-89</i>
PARVA	<i>pat-6</i>
TES	<i>tes-1</i>
TLN1	<i>tln-1</i>
ANXA1	<i>nex-1</i>
	<i>nex-3</i>
SORBS1/3	<i>sorb-1</i>
TNS3	<i>tns-1</i>
PINCH	<i>unc-97</i>
PTK2	<i>kin-32</i>
RSU1	<i>rsu-1</i>
CSK	<i>csk-1</i>
FHL2/3	<i>lim-9</i>
PXN/TGFB111	<i>pxl-1</i>
ARHGEF7	<i>pix-1</i>
IQGAP1	<i>pes-7</i>
FERMT2	<i>unc-112</i>
SHANK	<i>shn-1</i>
SHRPN	Y57A10A.31
FLNC	<i>fln-1</i>
	<i>fln-2</i>
RAP	<i>rap-1</i>
	<i>rap-2</i>
	<i>rap-3</i>

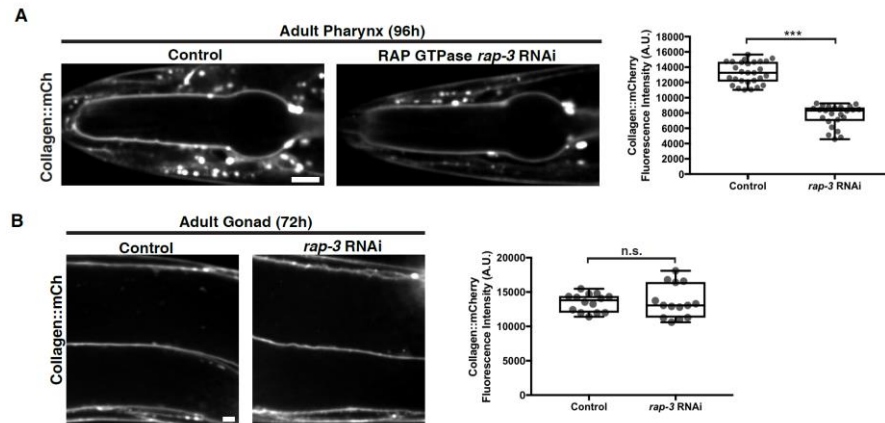


Figure 21: Loss of *rap-3* affects pharyngeal but not gonadal BM collagen levels.

(A) Fluorescence images of pharyngeal BM collagen::mCh in control and *rap-3* RNAi-treated 96h adult animals, with quantification of collagen::mCh fluorescence intensity on the right (control n=28; *rap-3* RNAi n=24). (B) Fluorescence images of gonadal BM collagen::mCh in control and *rap-3* RNAi-treated 72h adult animals, with quantification of collagen::mCh fluorescence intensity on the right (control n=14; *rap-3* RNAi n=14). *** $p < 0.0001$, unpaired two-tailed Student's *t* test; n.s., $p > 0.05$. Box edges in boxplots depict the 25th and 75th percentile, the line in the box indicates the median value, and whiskers mark the minimum and maximum values. Scale bars are 10 μ m.

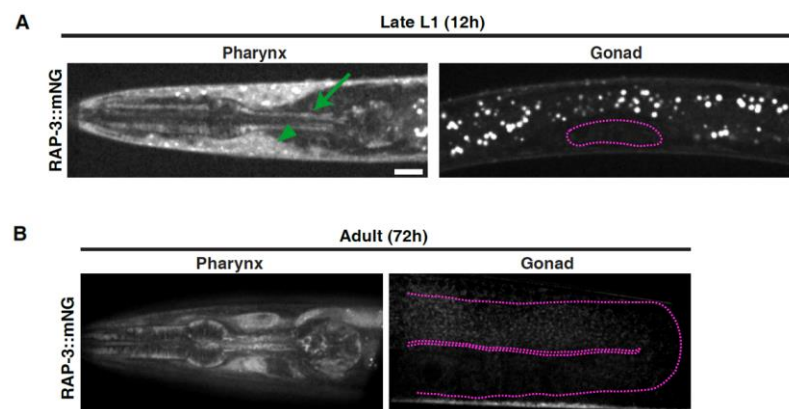


Figure 22: RAP-3 is expressed in the larval and adult pharynx, but not the gonad.

(A) Fluorescence images of RAP-3::mNG localization in the pharynx (left) and gonad (right) of a late L1 animal. The green arrow indicates pharyngeal muscle localization of RAP-3::mNG, while the green arrowhead denotes RAP-3::mNG signal in the body wall muscle. The gonad is outlined in magenta. (B) Fluorescence images of RAP-3::mNG localization in the pharynx and its absence in the gonad (outlined in magenta) of a 72h adult animal. Scale bars are 10 μ m.

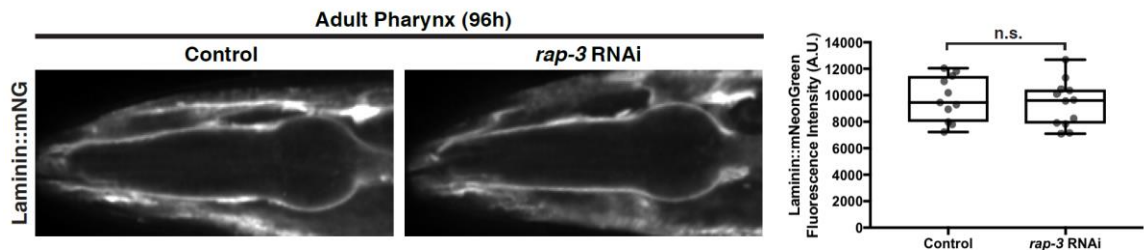


Figure 23: Loss of *rap-3* does not affect pharyngeal BM laminin levels.

Fluorescence images of pharyngeal BM laminin::mNG in control and *rap-3* RNAi-treated 96h adult animals, with quantification of laminin::mNG fluorescence intensity on the right (control n=11; *rap-3* RNAi n=12). *** $p < 0.0001$, unpaired two-tailed Student's *t* test; n.s., $p > 0.05$.

of RAP-3 (RAP-3^{G12V} (Jeon et al. 2007)) resulted in a ~50% increase in collagen levels in regions of the pharyngeal BM in contact with RAP-3^{G12V} over-expressing cells (Figure 24). To test whether RAP-3 and PAT-2 might function in the same genetic pathway to mediate type IV collagen recruitment, we first generated a *rap-3* null mutation, *rap-3(qy67)*, using CRISPR/Cas9 genome editing. However, I was unable to view homozygous *rap-3(qy67)* mutant larval animals due to embryonic lethality. To circumvent embryonic lethality, we knocked both *pat-2* and *rap-3* down simultaneously by RNAi. The combined RNAi against *rap-3* and *pat-2* did not worsen the reduction in pharyngeal BM collagen levels caused by individual *pat-2* or *rap-3* knockdown,

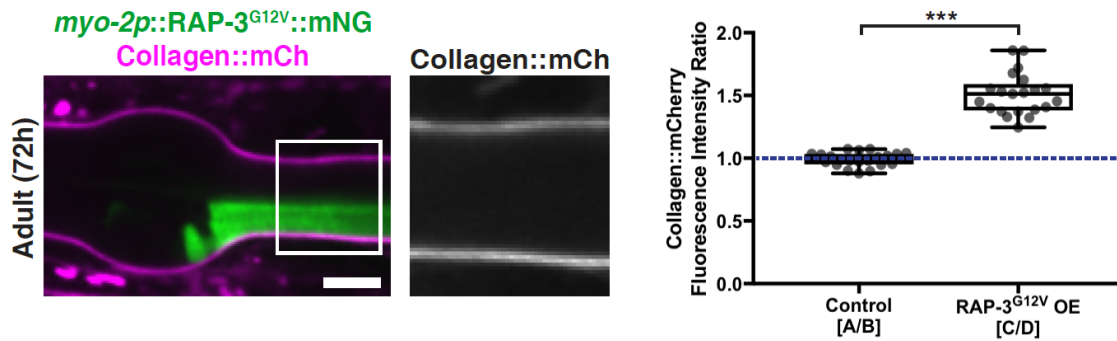


Figure 24: Expression of constitutively active RAP-3 in results in an increase in pharyngeal BM collagen levels.

Merged fluorescence image of *myo-2p::RAP-3^{G12V}::mNG* (green) and *collagen::mCh* (magenta) in a 72h adult pharynx. Pharyngeal BM *collagen::mCh* signal in the boxed region is magnified on the right. Quantification of fold increase in *collagen::mCh* fluorescence intensity upon *RAP-3^{G12V}* over-expression is shown on the right (n=21). *** $p < 0.0001$, paired two-tailed Student's *t*-test. Box edges in boxplots depict the 25th and 75th percentile, the line in the box indicates the median value, and whiskers mark the minimum and maximum values. Scale bars are 10 μ m.

consistent with these genes functioning within the same pathway (Figure 25). I also found that knockdown of *rap-3* did not alter PAT-2 or PAT-3 localization or levels (Figure 26), suggesting that it does not activate PAT-2/PAT-3 by regulating integrin trafficking. Together, our observations support the idea that RAP-3 is a pharyngeal-specific activator of the PAT-2/PAT-3 integrin, triggering its ability to recruit type IV collagen to the pharyngeal BM.

Finally, I wanted to test if ectopic expression of RAP-3 in the gonad was sufficient to activate PAT-2/PAT-3 integrin in this tissue to facilitate collagen recruitment. We used the *inx-8* promoter to drive *RAP-3::mNG* expression in the gonadal sheath cells that contact BM (Starich et al. 2014) (Figure 27A). Strikingly, I

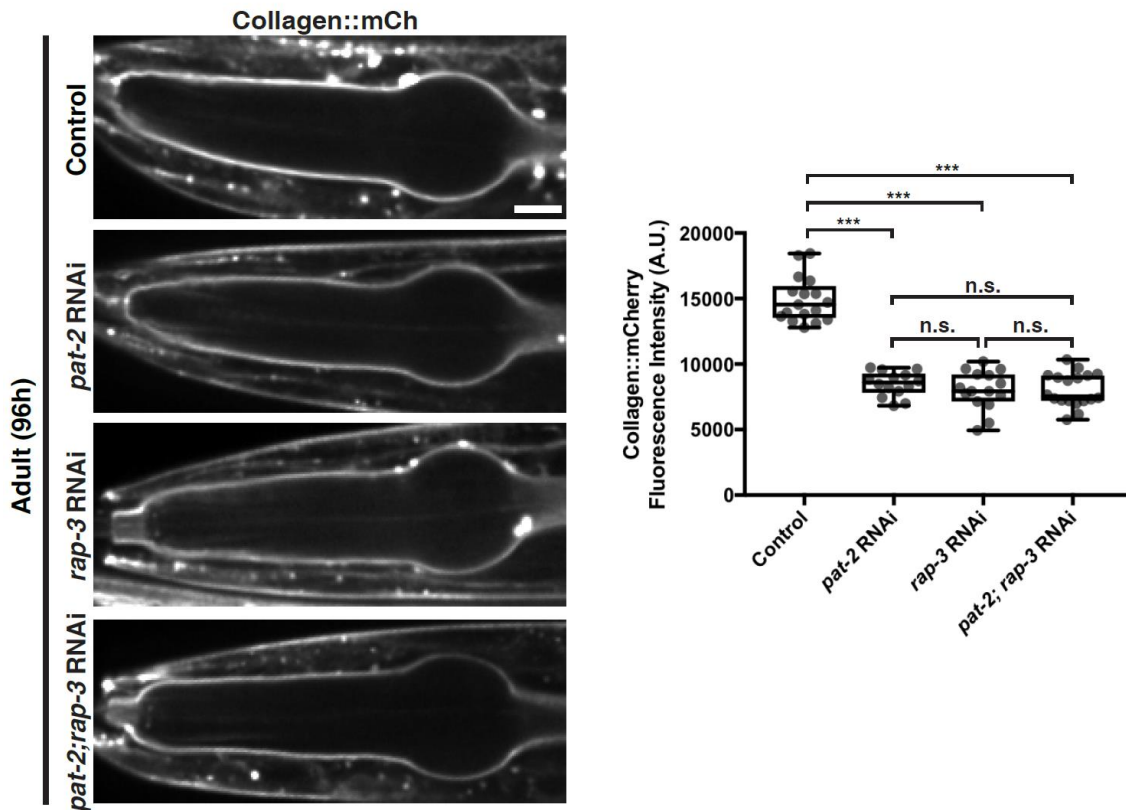


Figure 25: RAP-3 and PAT-2/PAT-3 integrin function together to promote pharyngeal BM collagen recruitment.

Fluorescence images of pharyngeal BM collagen::mCh in control, *pat-2*, *rap-3*, and *pat-2; rap-3* RNAi-treated 96h adult animals. Collagen::mCh fluorescence intensity is quantified on the right (control n=17; *pat-2* RNAi n=14; *rap-3* RNAi n=15; *pat-2; rap-3* RNAi n=18). *** $p < 0.0001$, one-way ANOVA followed by post-hoc Tukey's test; n.s., $p > 0.05$. Box edges in boxplots depict the 25th and 75th percentile, the line in the box indicates the median value, and whiskers mark the minimum and maximum values. Scale bars are 10 μ m.

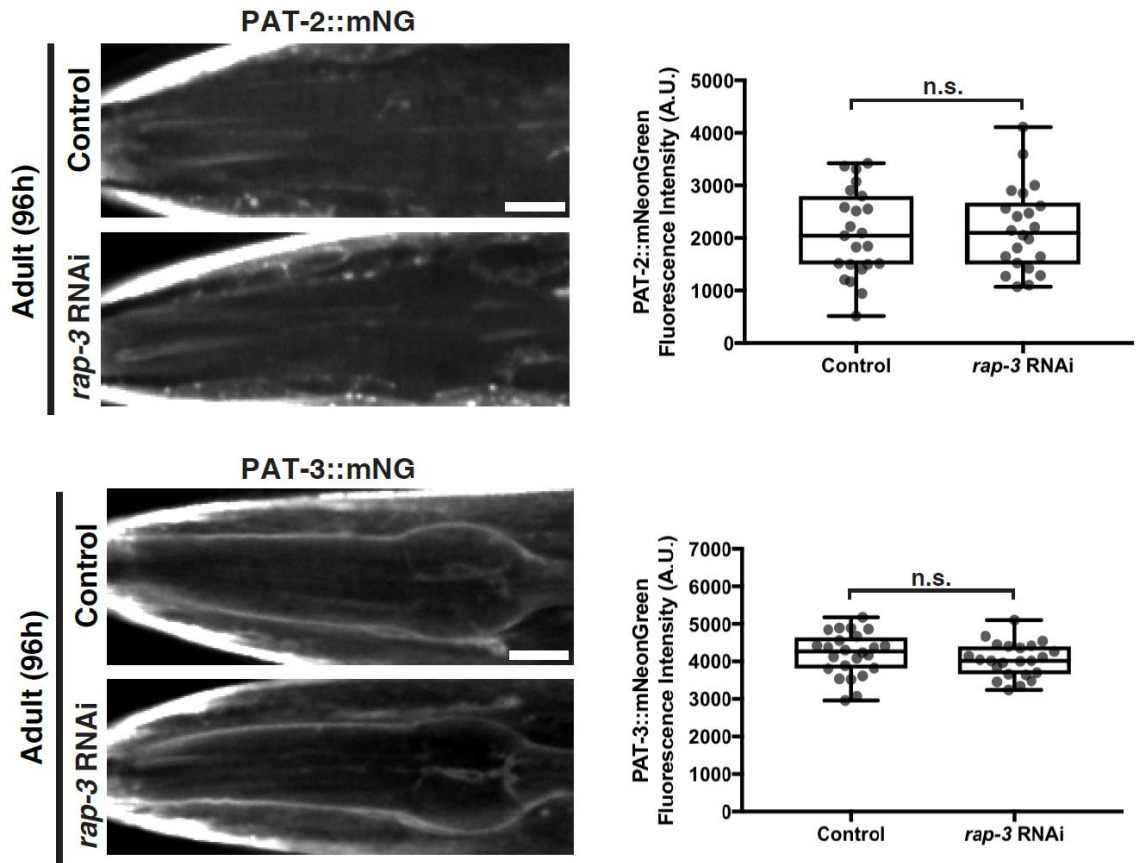


Figure 26: RAP-3 does not regulate PAT-2 or PAT-3 levels.

The top panel shows fluorescence images of pharyngeal PAT-2::mNG in control and *rap-3* RNAi-treated 96h adult animals, with quantification of PAT-2::mNG fluorescence intensity on the right (control n=23, *rap-3* RNAi n=22). The bottom panel shows fluorescence images of pharyngeal PAT-3::mNG in control and *rap-3* RNAi-treated 96h adult animals, with quantification of PAT-3::mNG fluorescence intensity on the right (control n=24, *rap-3* RNAi n=23). n.s., $p > 0.05$, unpaired two-tailed Student's *t* test. Box edges in boxplots depict the 25th and 75th percentile, the line in the box indicates the median value, and whiskers mark the minimum and maximum values. Scale bars are 10µm.

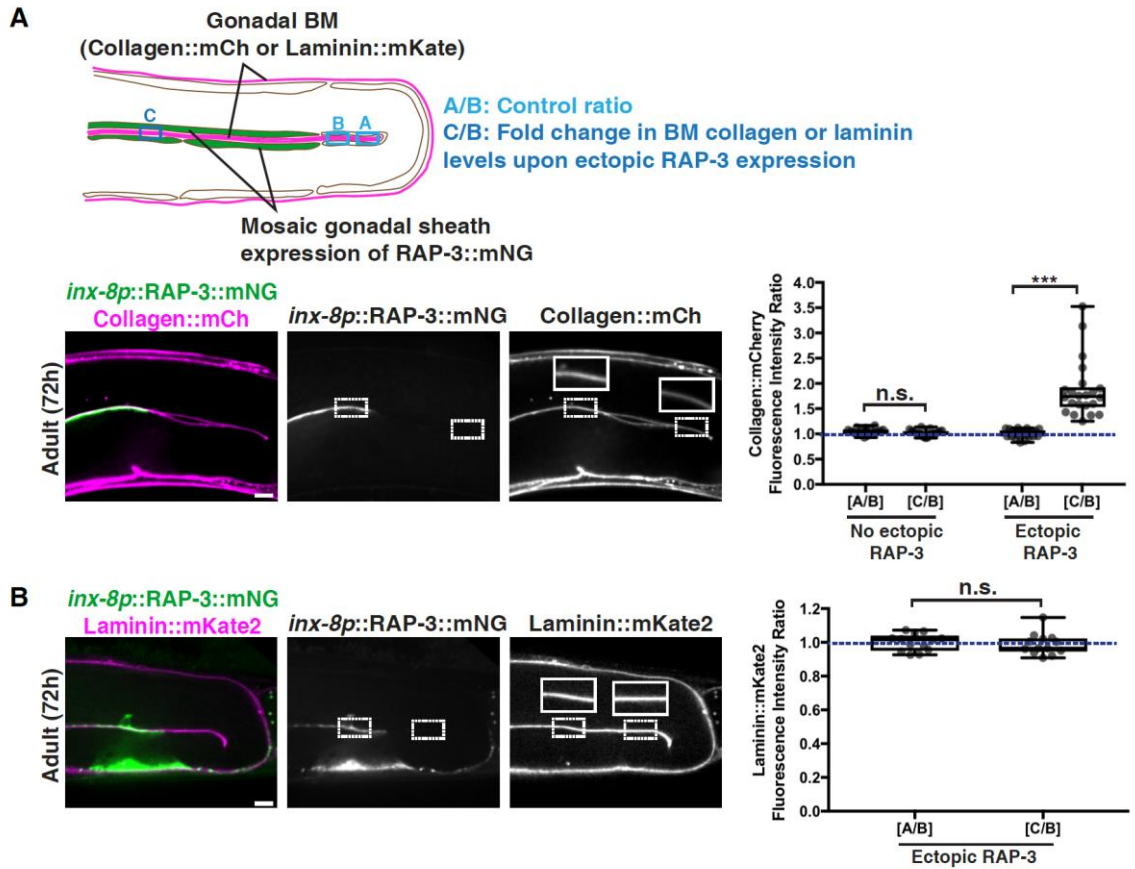


Figure 27: Ectopic gonadal expression of RAP-3 increases BM collagen but not laminin levels.

(A) A schematic outlining mosaic expression of RAP-3::mNG in the gonadal sheath cells and method for quantification of collagen and laminin levels is shown on top. A merged fluorescence image of *inx-8p::RAP-3::mNG* (green) and *collagen::mCh* (magenta) in a 72h adult gonad is shown on the bottom left, and split RAP-3::mNG and *collagen::mCh* channel images on the bottom right. The dotted box on the left indicates a region of RAP-3 expression and the dotted box on the right denotes absence of RAP-3 expression. *Collagen::mCh* signal in the dotted box regions are magnified in insets. Quantification of fold increase in gonadal BM *collagen::mCh* fluorescence intensity upon ectopic RAP-3 expression is shown on the right (n=22).

(B) A merged fluorescence image of *inx-8p::RAP-3::mNG* (green) and *laminin::mKate2* (magenta) in a 72h adult gonad is shown on the left, and split RAP-3::mNG and *laminin::mKate2* channel images on the right. The dotted box on the left indicates a region of RAP-3 expression and the dotted box on the right denotes absence of RAP-3 expression. *Laminin::mKate2* signal in the dotted box regions are magnified in insets.

Quantification of fold increase in gonadal BM laminin::mKate2 fluorescence intensity upon ectopic RAP-3 expression is shown on the right (n=13). .* $p < 0.0001$, paired two-tailed Student's t -test; n.s., $p > 0.05$. Box edges in boxplots depict the 25th and 75th percentile, the line in the box indicates the median value, and whiskers mark the minimum and maximum values. Scale bars are 10 μ m.**

found that ectopic RAP-3 expression in the gonadal sheath cells increased collagen levels by ~80% in regions of the BM contacting RAP-3 expressing cells (Figure 27A). I predicted that if RAP-3 was triggering collagen recruitment by activating PAT-2/PAT-3 integrin in the gonad, then laminin levels would not be altered. Consistent with this, I found that gonadal expression of RAP-3 did not affect BM laminin levels (Figure 27B). Together these observations strongly suggest that RAP-3 is a tissue-specific activator of PAT-2/PAT-3 integrin, which directs the laminin-independent addition of type IV collagen into the BM.

2.3 Discussion

Type IV collagen is critical for BM function and numerous human diseases are associated with its misregulated accumulation or loss (Fidler et al. 2018). Previous work has suggested that a meshwork of laminin forms a cell-bound template that recruits the type IV collagen network through cross-bridging components (Pozzi et al. 2017; Glentis et al. 2014). How laminin is targeted to cell surfaces and whether there are other mechanisms to direct collagen to BMs *in vivo* has remained unclear. Through live-cell imaging of endogenous localization, conditional knockdown, misexpression, and RNAi

screening, I have discovered distinct mechanisms for type IV collagen recruitment to the growing BMs of the *C. elegans* pharyngeal and gonadal tissues. I found that the two *C. elegans* integrin α subunits INA-1 (laminin-binding) and PAT-2 (RGD-binding) are expressed with the sole β subunit PAT-3 in both organs. My results suggest each tissue promotes selective activation of a specific integrin heterodimer to recruit collagen from the extracellular fluid: α INA-1/ β PAT-3 activation in the gonad recruits laminin, which directs moderate levels of collagen to the BM; while α PAT-2/ β PAT-3 activation in the pharynx recruits high levels of collagen independent of laminin. Supporting this model, I identified a putative pharyngeal-specific PAT-2/PAT-3 activator, the small GTPase RAP-3, an ortholog of mammalian Rap1, that mediates inside-out activation of mammalian integrins (Boettner and Van Aelst 2009). Collectively, these data reveal how tissues dictate collagen incorporation into BM through selective integrin activation and provide insight into how cells can use distinct mechanisms to target collagen to BMs, thereby precisely controlling collagen levels and constructing diverse BMs (Figure 28).

Due to the challenge of imaging of BMs *in situ*, the lethal phenotypes of null mutations of many BM components, and the expanded gene families of BM receptors and matrix components in vertebrates, it has been difficult to establish the mechanisms that mediate type IV collagen recruitment to BM *in vivo* (Yurchenco and Patton 2009; Li et al. 2017). Studies *in vitro* suggest several mechanisms might recruit laminin to cell surfaces, which in turn mediates type IV collagen incorporation. For example, work on

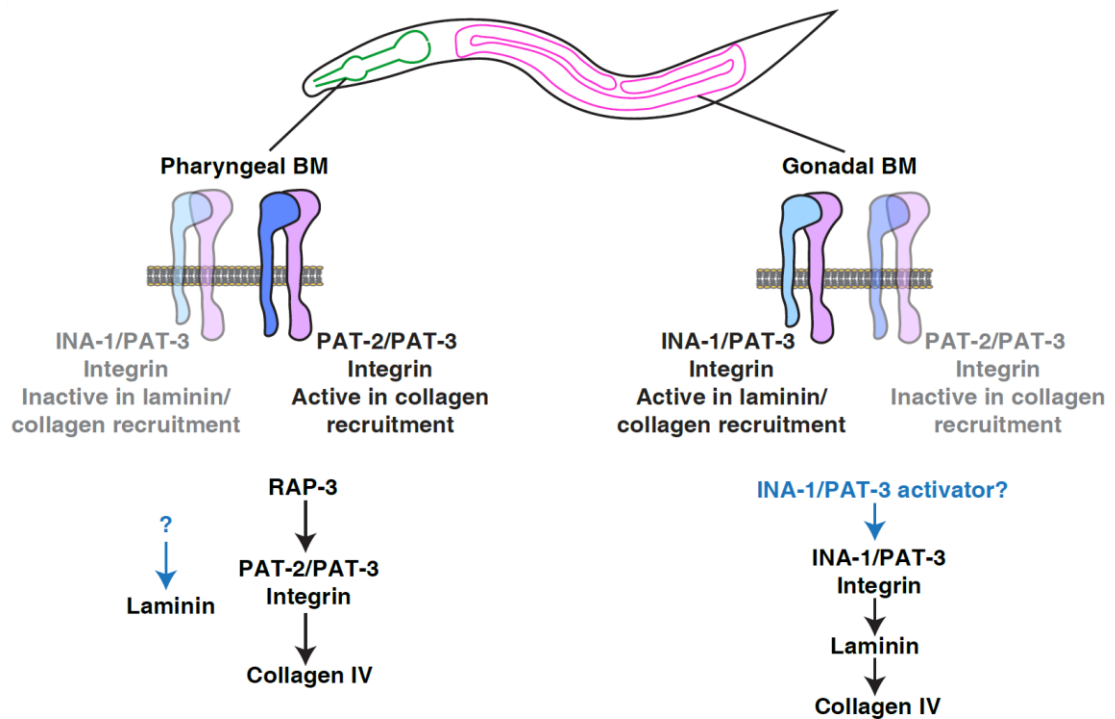


Figure 28: Model for distinct modes of collagen recruitment to the pharyngeal and gonadal BMs.

embryoid bodies—aggregates of pluripotent stem cells—indicates that integrin $\beta 1$ and dystroglycan matrix receptors function redundantly to promote the anchorage of laminin to the surfaces of cells (Li et al. 2017). Findings in cultured rat Schwann cells further suggests that sulfated glycolipids mediate laminin deposition (Li et al. 2005). Here, I exploited the small BM receptor and matrix families of *C. elegans* (Clay and Sherwood 2015), as well as their conditional knockdown by RNAi, to investigate how the sole *C. elegans* type IV collagen molecule is recruited to the BMs of growing gonadal and pharyngeal organs during larval development. I demonstrate that the two *C.*

C. elegans integrin heterodimers play key roles in BM recruitment: α INA-1/ β PAT-3 promotes laminin-dependent type IV collagen recruitment to the gonadal BM, while α PAT-2/ β PAT-3 directs collagen IV to the pharyngeal BM independent of laminin. RNAi against these integrins did not reduce type IV collagen incorporation into the BMs as severely as knockdown of type IV collagen itself, suggesting that another cell surface system(s) may function with integrin. However, *C. elegans* does not synthesize sulfated glycolipids (Bai et al. 2018), and neither knockdown of dystroglycan nor the matrix receptors glypican, discoidin domain receptors, LAR-RPTP, or teneurin reduced type IV collagen recruitment. Thus, integrins are likely the chief mediators of type IV collagen recruitment to the gonadal and pharyngeal BMs.

Laminin is required for the recruitment of type IV collagen to the BM of *Drosophila* and mouse embryos (Matsubayashi et al. 2017; Urbano et al. 2009; Pöschl et al. 2004). In addition, in embryoid bodies, the inhibition of laminin polymerization prevents the assembly of collagen IV on cell surfaces (Li et al. 2002). Further, in cultured Schwann cells, exogenously added collagen assembles into the BM-like matrix only in the presence of laminin (Tsiper and Yurchenco 2002). Similarly, I found that collagen IV targeting to the gonadal BM was dependent on laminin. Comparatively little is known about laminin-independent collagen recruitment. BM collagen addition independent of laminin has recently been observed during wound repair in the *Drosophila* larval epidermal BM (Ramos-Lewis et al. 2018), but the receptor(s) facilitating this mode of

collagen targeting has not been identified. In my study, I found that the PAT-2/PAT-3 integrin is both required and sufficient for laminin-independent collagen IV recruitment to the pharyngeal BM. Sequence analysis suggests that PAT-2/PAT-3 is an RGD-binding integrin (Brown 2000). As multiple RGD sequences are present in both $\alpha 1$ and $\alpha 2$ chains of *C. elegans* collagen IV, it is possible that PAT-2/PAT-3 directly binds collagen, thus precluding the need for a laminin template. Supporting this notion, I found that mosaic over-expression of PAT-2/PAT-3 in the pharyngeal tissue caused an increase in BM collagen levels only in regions of the BM contacting overexpressed PAT-2/PAT-3. Countering this idea, it has been suggested that the RGD sequences in collagen may not be accessible to integrins (Khoshnoodi et al. 2008). Hence, an alternative possibility is that PAT-2/PAT-3 binds either to a cell surface or BM molecule that directly interacts with collagen.

Both the integrin α subunits INA-1 and PAT-2 and the β subunit PAT-3 are expressed in the gonad and the pharynx. Thus, tissue-specific integrin expression cannot account for the tissue-specific activity of gonadal INA-1/PAT-3 and pharyngeal PAT-2/PAT-3 in collagen recruitment. I considered the possibility that tissue-specific synthesis of laminin or type IV collagen might selectively activate gonadal INA-1/PAT-3 or pharyngeal PAT-2/PAT-3 heterodimers respectively as they are trafficked to cell surfaces (analogous to outside-in activation of integrin). However, this is unlikely as laminin is produced by both tissues (Huang et al. 2003) and collagen is not synthesized

in the pharyngeal epithelium (Graham et al. 1997). Since the sole difference between the α INA-1/ β PAT-3 and the α PAT-2/ β PAT-3 integrins is the α subunit, I propose instead that tissue-specific factors activate α INA-1 or α PAT-2 to promote their tissue specific matrix-recruiting activity. One possible mode of activation is through the diverse cytoplasmic tail region of the α subunits. Studies in mammalian cell lines have shown that the cytoplasmic tails α of integrin subunits are required for the inside-out activation of integrin receptors and may bestow specificity to integrin activation (Thinn et al. 2018; Liu et al. 2015). Supporting this idea, I found that expressing the PAT-2 integrin α cytoplasmic tail fused to the INA-1 extracellular domain in the pharynx activated its ability to recruit laminin, even though INA-1 does not normally function in pharyngeal BM laminin recruitment during larval development. One puzzling question is the functional significance of the α subunit expressed in each tissue and localized to the cell-BM interface, but not involved in BM recruitment. In the gonad, my evidence suggests that the α subunit PAT-2 acts in part to sequester the β subunit PAT-3, thus limiting the amount of active INA-1/PAT-3 heterodimer and thereby limiting laminin addition to the BM. It is also possible that α subunits not involved with BM recruitment might help localize proteases involved in matrix remodeling (Desgrosellier and Cheresch 2010) or might be associated with intracellular effectors that allow it to be activated and signal in response to changing matrix and physiological conditions (Wolfenson et al. 2013).

In lymphocytes, co-expressed integrins $\alpha\text{L}\beta\text{2}$ and $\alpha\text{M}\beta\text{2}$, which share a common β subunit, are differentially activated through their divergent α cytoplasmic tails, triggering distinct adhesion responses to chemokine stimulation (Weber et al. 1999). Notably, the mammalian small GTPase Rap1 facilitates the activation of the $\alpha\text{L}\beta\text{2}$ integrin through the lymphoid-enriched Rap1 effector molecule RapL, which binds to the αL subunit (Katagiri et al. 2004; Zhang and Wang 2012). In my study, through a targeted RNAi screen of integrin-associated proteins, I identified *rap-3*, a *C. elegans* ortholog of mammalian Rap1, as a pharyngeal-expressed activator of the PAT-2/PAT-3 integrin's collagen IV recruiting function. *C. elegans* encodes two Rap1 orthologs, *rap-1* and *rap-3* (Reiner and Lundquist 2018), with *rap-3* appearing to be more divergent (Rasmussen et al. 2018). I provide strong evidence that the RAP-3 is a specific activator of PAT-2/PAT-3 integrin. First, similar to loss of PAT-2/PAT-3, loss of RAP-3 resulted in reduction of pharyngeal BM collagen but not laminin levels. Second, over-expression of a constitutively active mutant of RAP-3 in the pharyngeal epithelium increased collagen levels in regions of the pharyngeal BM contacting over-expressing cells, phenocopying my observations with pharyngeal PAT-2 over-expression. Third, my genetic analysis suggested that RAP-3 and PAT-2 act in the same pathway to promote collagen recruitment. Finally, ectopic expression of RAP-3 in the gonad increased type IV collagen levels in the gonadal BM, but not laminin levels, indicative of ectopic PAT-2/PAT-3 activation. The effector(s) of RAP-3 that promotes PAT-2/PAT-3 activity in

collagen recruitment to the BM is not known, but my data suggest it is likely expressed in both gonadal and pharyngeal tissues, as RAP-3 can activate PAT-2/PAT-3 in either tissue. Collectively, these observations support a model where the tissue-specific expression of RAP-3 in the pharynx promotes activation of PAT-2/PAT-3 to facilitate laminin-independent collagen recruitment to the BM, and suggest that a distinct tissue-specific factor(s) might mediate INA-1/PAT-3 activation in the gonad to promote laminin-dependent BM collagen recruitment (Figure 28).

The triple helical nature of collagen combined with its intermolecular covalent cross-links provides BMs their tensile strength, and genetic elimination of type IV collagen results in embryonic lethality in mice and *C. elegans* when tissues first experience mechanical loads (Pöschl et al. 2004; Gupta et al. 1997). Type IV collagen also tethers numerous matrix proteins and growth factors (Fidler et al. 2018). As a result of its complex and essential roles, precise levels of BM collagen are required for many cell and tissue functions. For example, the BMP/TGF β ligand Dpp binds type IV collagen in *Drosophila* BMs, and collagen levels influence Dpp mediated signaling during dorsal ventral patterning in the embryo, germ stem cell production in the ovary, renal tubule morphogenesis, and wing disc growth (Ma et al. 2017; Bunt et al. 2010; Wang et al. 2008). Further, specific levels and gradients of type IV collagen mediate tissue constriction and shaping in the *Drosophila* egg chamber and wing disc and the *C. elegans* gonad (Crest et al. 2017; Kubota et al. 2012; Morrissey and Sherwood 2015). Distinct integrin receptors

that mediate different modes of type IV collagen recruitment may provide tissues robust mechanisms to control BM collagen levels. In particular, as PAT-2/PAT3 activity is controlled by the small GTPase RAP-3, its activity, and thus levels of type IV collagen, can be finely tuned through GTPase activating proteins (GAPs) and guanine nucleotide exchange factors (GEFs). This could be a dynamic mechanism for tissues to increase, decrease, and even translate signaling pathways into collagen gradients (Crest et al. 2017; Jayadev and Sherwood 2017). Therapeutically targeting specific activators of collagen-recruiting integrins may also be a promising means to modulate collagen levels during aging, in fibrotic diseases, and with type IV collagen genetic disorders where type IV collagen levels in BMs are altered, leading to tissue decline (Karsdal et al. 2016; Uspenskaia et al. 2004; Mao et al. 2015; Fidler et al. 2018).

2.4 Acknowledgements

The work completed in this chapter is primarily mine, but I would like to acknowledge the important contributions of co-authors. Qiuyi Chi built several molecular biology constructs used in this study, including those detailed in Appendix A.1.2.1, A.1.2.2, A.1.2.5, A.1.2.6, and A.1.4. Daniel P. Keeley constructed the isosurface renderings for the gonadal BMs in Figure 5. Both Eric L. Hastie and Daniel P. Keeley injected several constructs detailed in A.1.2.1. Some strains were provided by the CGC, which is funded by the NIH Office of Research Infrastructure Programs (P40 OD010440).

I thank Laura Kelley for helpful discussions on the chimeric integrin experiments. I thank all members of the Sherwood Laboratory, Brent Hoffman, Bernard Mathey-Prevot, David Reiner, Arnoud Sonnenberg, and Thomas Hannich for helpful intellectual discussions throughout the course of this project. Finally, I would like to acknowledge my advisor David Sherwood, whose mentorship was integral to the completion of this work.

3. Roles of the matricellular proteins nidogen, agrin, perlecan, and SPARC in type IV collagen recruitment to basement membranes

This work was completed in collaboration with Varun Jain, an undergraduate student whose research activities I supervised. In addition, some of the data on SPARC function was adapted from an article published in PLOS Genetics entitled “SPARC promotes cell invasion in vivo by decreasing type IV collagen levels in the basement membrane” (Morrissey et al. 2016). The authors of this article are Meghan A. Morrissey, Ranjay Jayadev, Ginger R. Miley, Catherine A. Blebea, Qiuyi Chi, Shinji Ihara, and David R. Sherwood.

3.1 Introduction

In chapter 1, I outlined the structure and function of basement membranes (BMs), thin and dense cell-associated extracellular matrices that surround most tissues and organs (Kalluri 2003). I discussed current gaps in our understanding of BM biology, highlighting the key unresolved question of how type IV collagen, a critical BM scaffolding and signaling component, is incorporated into BMs *in vivo*. I also introduced the nematode *C. elegans* as an excellent model system to investigate this question. In chapter 2, I focused on the cell surface interactions that facilitate the assembly of the type IV collagen network in BMs. I discovered that the α subunits of the matrix receptor integrin control the recruitment of collagen to the *C. elegans* pharyngeal and gonadal

BMs through distinct modes. In this chapter, I investigated the roles of extracellular proteins in the BM in directing type IV collagen to BMs *in vivo*.

The prevailing model of BM assembly, based largely on cell culture work and early embryonic studies, suggests that a polymeric lattice of laminin first assembles on cell surfaces, and that the type IV collagen network then associates with the laminin template through interactions with cross-bridging molecules (Yurchenco 2011; Yurchenco and Patton 2009). The proteoglycans agrin and perlecan, and the glycoprotein nidogen, are thought to function as network-bridging molecules, owing to their ability to bind to one another, or to both networks (Yurchenco 2011). However, due to the tissue-specific expression of these proteins, as well as their potential functional redundancy, it is unclear how they target type IV collagen to BMs *in vivo* (see Chapter 1.5).

SPARC is a type IV collagen-binding matricellular glycoprotein (Chioran et al. 2017). SPARC is thought to function as an extracellular chaperone, binding to and transporting type IV collagen from sites of synthesis and secretion, to sites of incorporation in BMs. Several studies in *Drosophila* have highlighted this chaperone-like activity of SPARC is required for type IV collagen assembly into BMs (Pastor-Pareja and Xu 2011; Isabella and Horne-Badovinac 2015b; Martinek et al. 2008; Shahab et al. 2015). SPARC may perform a similar role in vertebrates. Loss of SPARC in mice results in disorganization and compromised integrity of the lens BM (Yan et al. 2003). In *C.*

elegans, SPARC is required for embryonic viability and fertility, but its precise functions in BMs have not yet been investigated (Fitzgerald and Schwarzbauer 1998).

In this study, I used live-cell imaging, genetic analysis, and RNAi knockdown to investigate the role of the BM proteins agrin, nidogen, perlecan, and SPARC in localizing collagen to the pharyngeal and gonadal BMs in *C. elegans*. I discovered that the network bridging molecules agrin, nidogen, and perlecan are required to recruit type IV collagen to both the anterior and posterior pharyngeal BM. However, none of these proteins were necessary for type IV collagen localization to gonadal BM. SPARC was essential for collagen recruitment to the pharyngeal BM, but was not required to target collagen to the gonadal BM. Collectively, our observations reveal aspects of tissue-specific regulation of type IV collagen incorporation into BMs.

3.2 Results

3.2.1 Agrin, perlecan, and nidogen are individually required for the recruitment of collagen to the posterior pharyngeal basement membrane

In addition to cell surface molecules that could directly recruit collagen (discussed in Chapter 2), proteins within the BM could also affect the localization of collagen. To explore this possibility, I first focused on the network bridging matricellular proteins agrin, nidogen, and perlecan. These molecules are thought to facilitate the connection of laminin and collagen networks in the BM, as they have high affinities for both collagen IV and laminin (Yurchenco 2011; Yurchenco and Patton 2009).

Moreover, previous studies have suggested that these proteins may have tissue-specific functions. Perlecan is highly abundant in human skin BMs, and electron microscopy studies have shown that perlecan connects the laminin and collagen networks together in these BMs (Behrens et al. 2012; Breitzkreutz et al. 2013). In contrast, renal BMs appear to be agrin-rich, although the network-bridging function of agrin in these BMs has not been established (Miner 2012, 2011; Goldberg et al. 2009). Other cell culture studies have suggested that nidogen, agrin, and perlecan could have redundant functions (Clay and Sherwood 2015; Hohenester and Yurchenco 2013). However, the exact role of each of these molecules in recruiting type IV collagen to the BM *in vivo* remains unclear.

I first visualized the localization pattern of perlecan in endogenously tagged UNC-52::mNG animals. UNC-52::mNG was prevalently seen surrounding both the pharynx and the gonad (Figure 29A). To determine if perlecan is required for the localization of type IV collagen to pharyngeal or gonadal BMs, I used RNAi targeting *unc-52* to reduce perlecan levels beginning at the L1 larval stage. Collagen::mCh levels at the anterior pharyngeal BM were ~11% lower in RNAi treated 72h adult animals as compared to control worms. Additionally, collagen::mCherry levels at the posterior pharyngeal BM was ~15% lower in RNAi- treated worms. However, collagen::mCh levels in the gonadal BMs of these animals did not appear to be affected (Figure 29B and Figure 29C). Taken together, my observations suggest that perlecan is required for

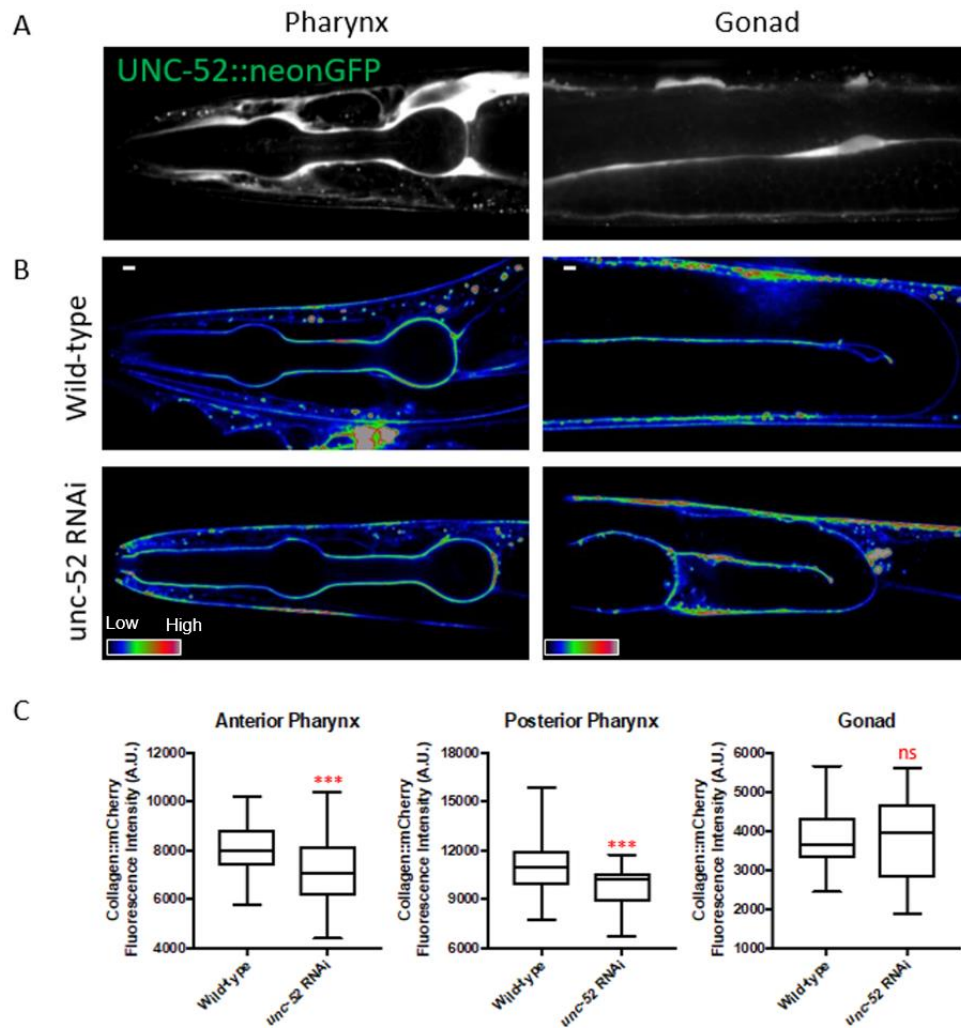


Figure 29: Perlecan is required for collagen requirement to the anterior and posterior pharyngeal basement membrane (BM), but not the gonadal BM.

(A) Perlecan is detected around both the pharyngeal and gonadal tissues. (B) Spectral representation of fluorescence intensity of collagen::mCherry at the pharyngeal (left) and gonadal (right) BMs in control animals (top) and animals treated with RNAi targeting *unc-52* (bottom). (C) Quantification of collagen::mCherry fluorescence intensity at the anterior and posterior pharyngeal BMs (left) and the gonadal BM ($n \geq 33$ for each treatment). *** $p < 0.001$, unpaired two-tailed Student's *t*-test; n.s., $p > 0.05$. Box edges in boxplots depict the 25th and 75th percentile, the line in the box indicates the median value, and whiskers mark the minimum and maximum values. Scale bars are 5 μ m.

collagen localization to the anterior and posterior pharyngeal BM, but not the gonadal BM.

I next examined the localization of nidogen in endogenously tagged NID-1::mNG animals (Figure 30A). NID-1::mNG was observed prominently surrounding both the pharynx and the gonad. To investigate whether nidogen recruits type IV collagen to the pharyngeal and gonadal BMs, I examined collagen::mCherry levels in a viable molecular null for nidogen (*nid-1 (cg119)*). Loss of nidogen resulted in a decrease of 15% in type IV collagen levels in the posterior pharyngeal BM. Interestingly, there was no corresponding reduction in the type IV collagen levels at the anterior pharyngeal BM or the gonadal BM (Figure 30B and Figure 30C). These observations suggest that nidogen is required to recruit collagen specifically to the pharyngeal but not gonadal BM.

Finally, I examined the localization of agrin in endogenously tagged AGR-1::mNG worms. Agrin is localized prominently to the pharyngeal BM and appeared to be more densely localized to the anterior of the pharynx. However, I did not detect agrin in the gonadal BM (Figure 31A). These observations raised the possibility that agrin could function in a tissue-specific manner to recruit collagen to the BM. To test this, I examined collagen::mCherry levels in animals harboring a viable putative null mutation for agrin (*agr-1(oxTi4)*). Loss of agrin caused a decrease of 15% of type IV collagen levels in the posterior pharynx, but collagen levels in the anterior pharyngeal

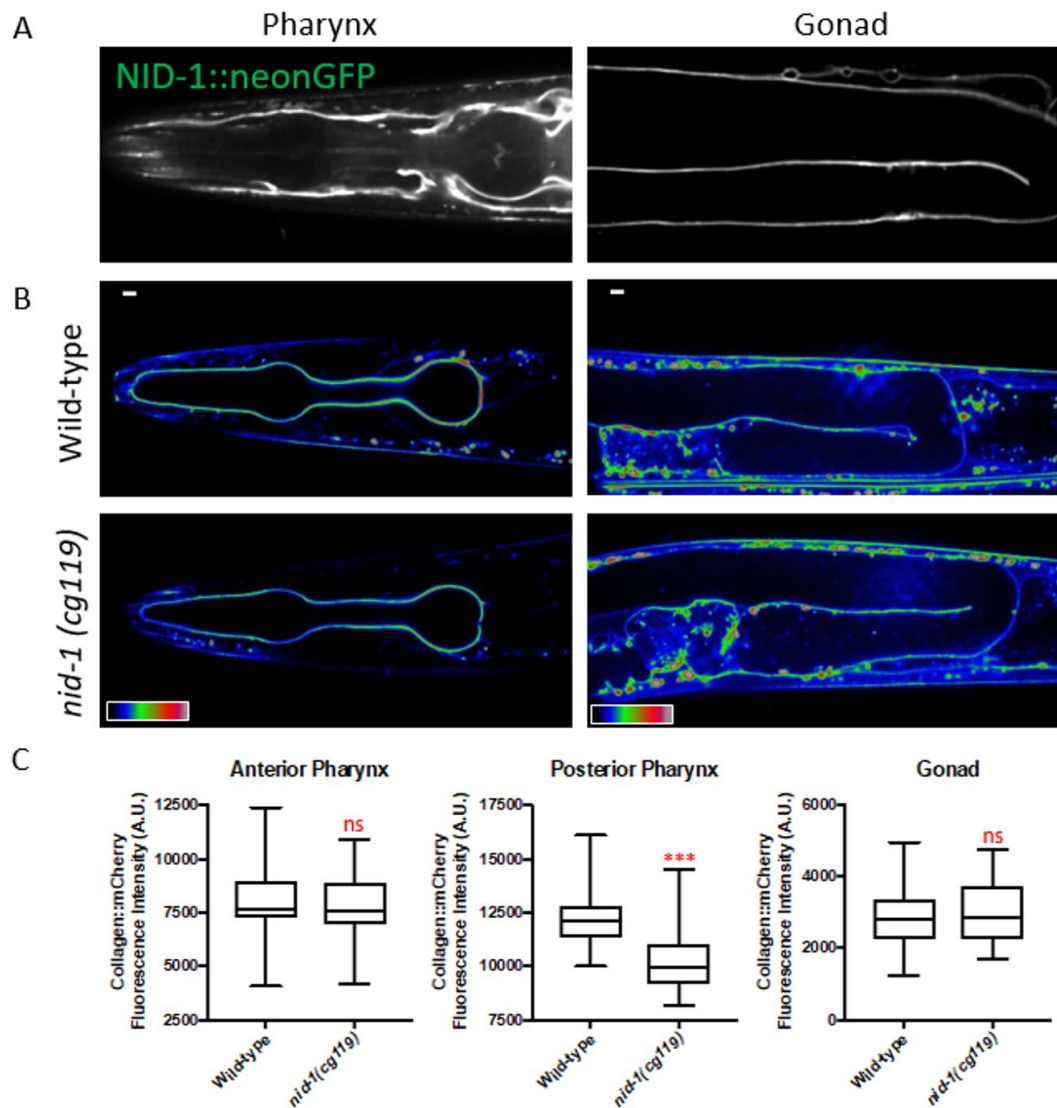


Figure 30: Nidogen is required for the recruitment of collagen to the posterior pharyngeal BM but not the gonadal BM.

(A) NID-1::mNG localizes in the vicinity of both the pharyngeal and gonadal BMs (B) Spectral representation of fluorescence intensity of collagen::mCherry at the pharyngeal (left) and gonadal (right) BMs in wild-type (top) and *nid-1(cg119)* (bottom) animals. (C) Quantification of collagen::mCherry fluorescence intensity at the anterior and posterior pharyngeal BMs (left) and the gonadal BM (right) ($n \geq 34$ for each treatment). *** $p < 0.001$, unpaired two-tailed Student's *t*-test; n.s., $p > 0.05$. Box edges in boxplots depict the 25th and 75th percentile, the line in the box indicates the median value, and whiskers mark the minimum and maximum values. Scale bars are $5 \mu\text{m}$.

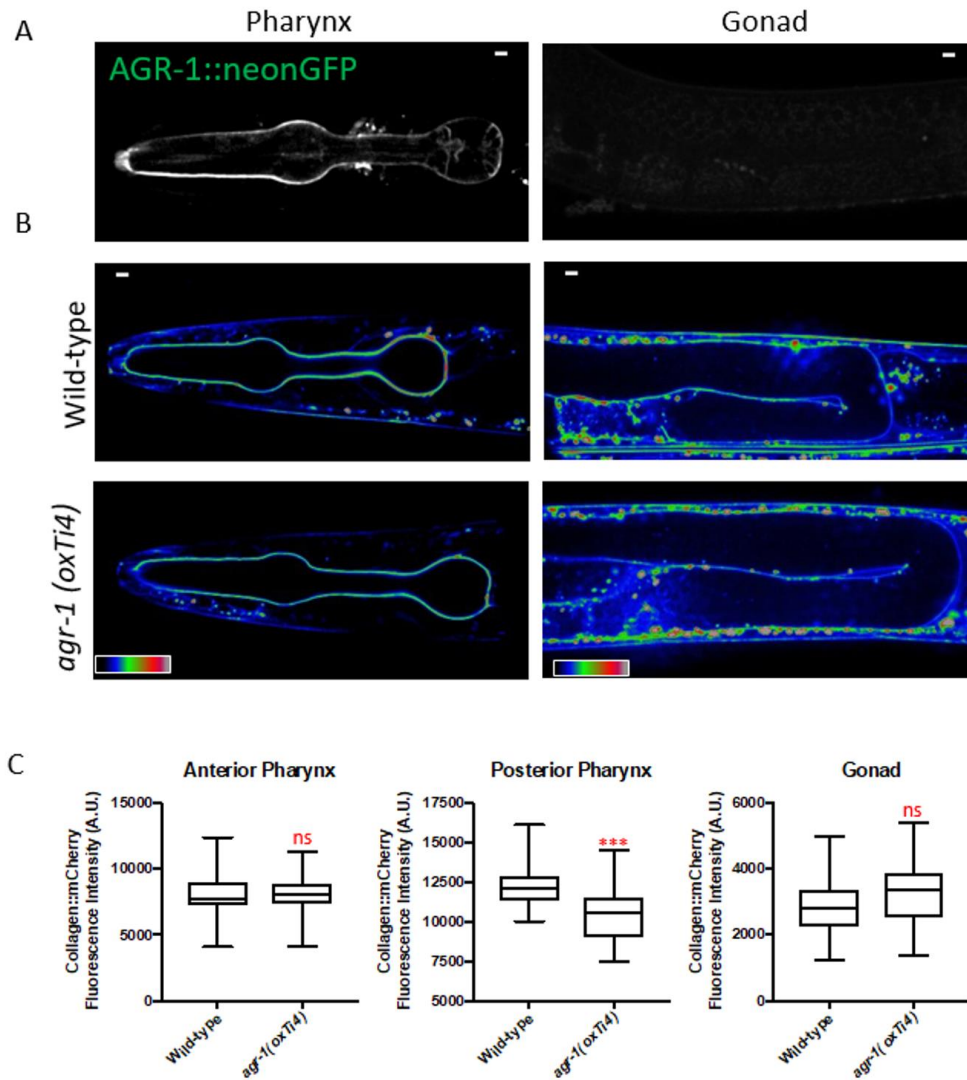


Figure 31: Agrin is required for collagen recruitment to the posterior pharyngeal BM, but not the gonadal BM.

(A) Agrin is detected in the pharyngeal but not gonadal BM. Interestingly, agrin seems to be enriched in the anterior pharynx. (B) Spectral representation of fluorescence intensity of collagen::mCherry at the pharyngeal (left) and gonadal (right) BMs in wild-type (top) and *agr-1(OxTi4)* (bottom) animals. (C) Quantification of collagen::mCherry fluorescence intensity at the anterior and posterior pharyngeal BMs (left) and the gonadal BM (right) ($n \geq 34$ for each treatment). *** $p < 0.001$, unpaired two-tailed Student's *t*-test; n.s., $p > 0.05$. Box edges in boxplots depict the 25th and 75th percentile, the line in the box indicates the median value, and whiskers mark the minimum and maximum values. Scale bars are $5 \mu\text{m}$.

and gonadal BMs appeared to be unaffected (Figure 31B and Figure 31C). These data indicate that agrin is required for recruiting type IV collagen specifically to the pharyngeal but not gonadal BM.

3.2.2 Nidogen and agrin function in a distinct pathway from perlecan in recruiting collagen to the posterior pharyngeal basement membrane

Given the implication from cell culture studies that agrin, nidogen, and perlecan could function redundantly, I decided to investigate whether these molecules have redundant functions in recruiting collagen to the BM (Clay and Sherwood 2015; Yurchenco and Patton 2009). I first examined type IV collagen levels in *agr-1(OxTi4); nid-1(cg119)* double mutant animals. I observed a ~14% decrease in collagen::mCherry levels at the posterior pharyngeal BM in these animals as compared to wild-type animals (Figure 32). This decrease was similar to that observed in the individual nidogen and agrin mutants. Furthermore, collagen::mCherry levels in the anterior pharyngeal BM of *agr-1(OxTi4); nid-1(cg119)* animals decreased ~12.5% (Figure 32), in contrast to the single mutants, where anterior pharyngeal collagen was not affected. Finally, collagen levels in the gonadal BM appeared to be unaffected in the double mutant animals (Figure 32). Taken together, these data suggest that agrin and nidogen likely function in the same pathway to recruit collagen specifically to the pharyngeal but not gonadal BM. Moreover, agrin and nidogen function redundantly/together to recruit

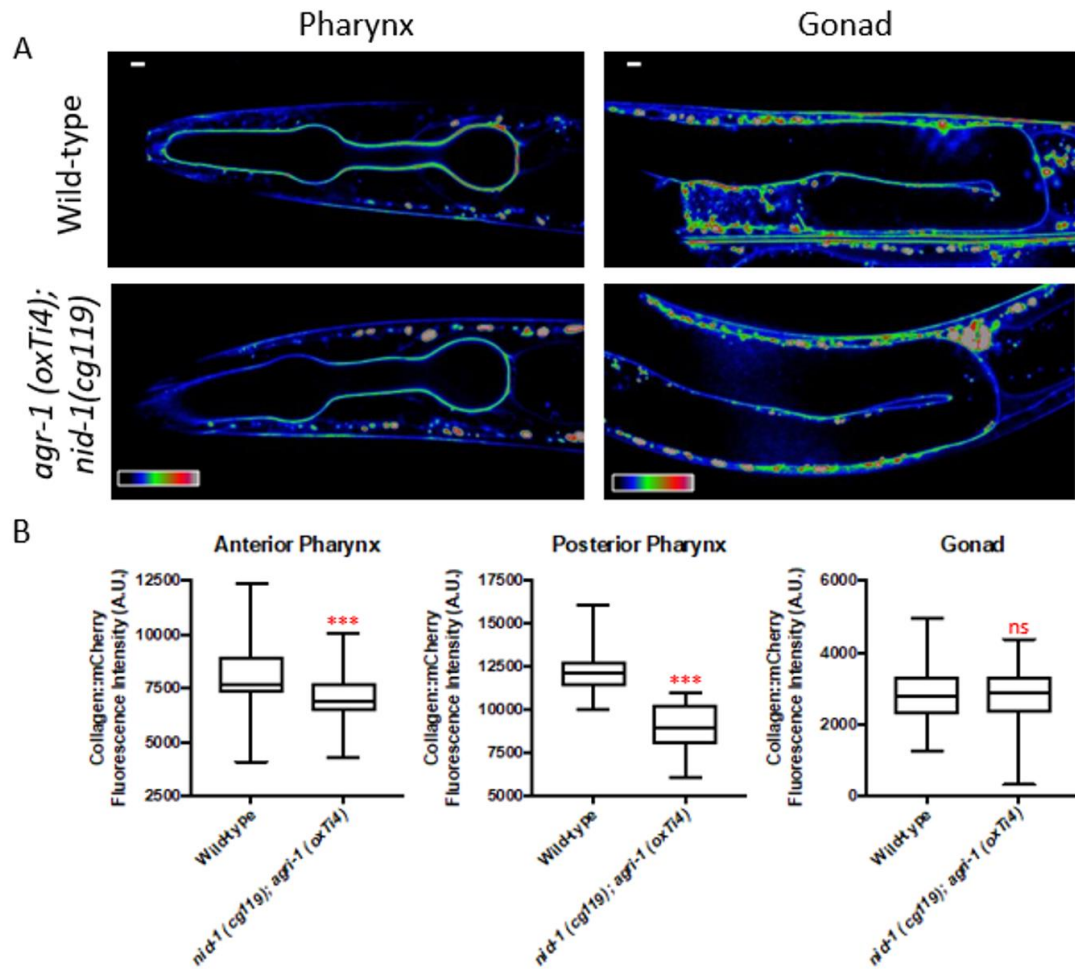


Figure 32: Agrin and nidogen function together to recruit collagen to the pharyngeal BM.

(A) Spectral representation of fluorescence intensity of collagen::mCherry at the pharyngeal (left) and gonadal (right) BMs in wild-type (top) and *agr-1(OxTi4); nid-1(cg119)* null (bottom) animals. (B) Quantification of collagen::mCherry fluorescence intensity at the anterior and posterior pharyngeal BMs (left) and the gonadal BM (right) ($n \geq 26$ for each treatment). *** $p < 0.001$, unpaired two-tailed Student's *t*-test; n.s., $p > 0.05$. Box edges in boxplots depict the 25th and 75th percentile, the line in the box indicates the median value, and whiskers mark the minimum and maximum values. Scale bars are 5 μ m.

collagen to the anterior pharyngeal BM, but have non-redundant functions in localizing collagen to the posterior pharyngeal BM.

To test whether nidogen, agrin, and perlecan function together to localize collagen to BMs, we reduced UNC-52 levels by RNAi in the *agr-1(OxTi4);nid-1(cg119)* double mutant animals and examined collagen::mCherry levels at the pharyngeal and gonadal BMs. Type IV collagen levels in the posterior pharyngeal BM of RNAi treated animals was ~25% lower than that in control animals (Figure 33). Moreover, knockdown of perlecan in the double mutant animals resulted in a ~23% reduction of collagen::mCherry levels in the anterior pharyngeal BM (Figure 33). However, gonadal BM collagen::mCherry levels in these animals appeared to be unaffected (Figure 33). Given that the magnitude of reduction in collagen levels at the pharyngeal BMs of *agr-1(OxTi4);nid-1(cg119)* animals treated with *unc-52* RNAi (~23%) was roughly the sum of the reduction seen in *agr-1(OxTi4);nid-1(cg119)* animals (~15%) and *unc-52* RNAi treated animals (~11%), I conclude that perlecan functions in a distinct pathway from nidogen and agrin to recruit type IV collagen to the pharyngeal BM.

3.2.3 SPARC is required for collagen recruitment to the pharyngeal but not gonadal basement membrane

SPARC is a collagen-binding matricellular glycoprotein thought to function as an extracellular chaperone to promote type IV collagen assembly into BMs (Chioran et al. 2017). In *C. elegans*, loss of SPARC causes embryonic lethality and fertility defects, but it

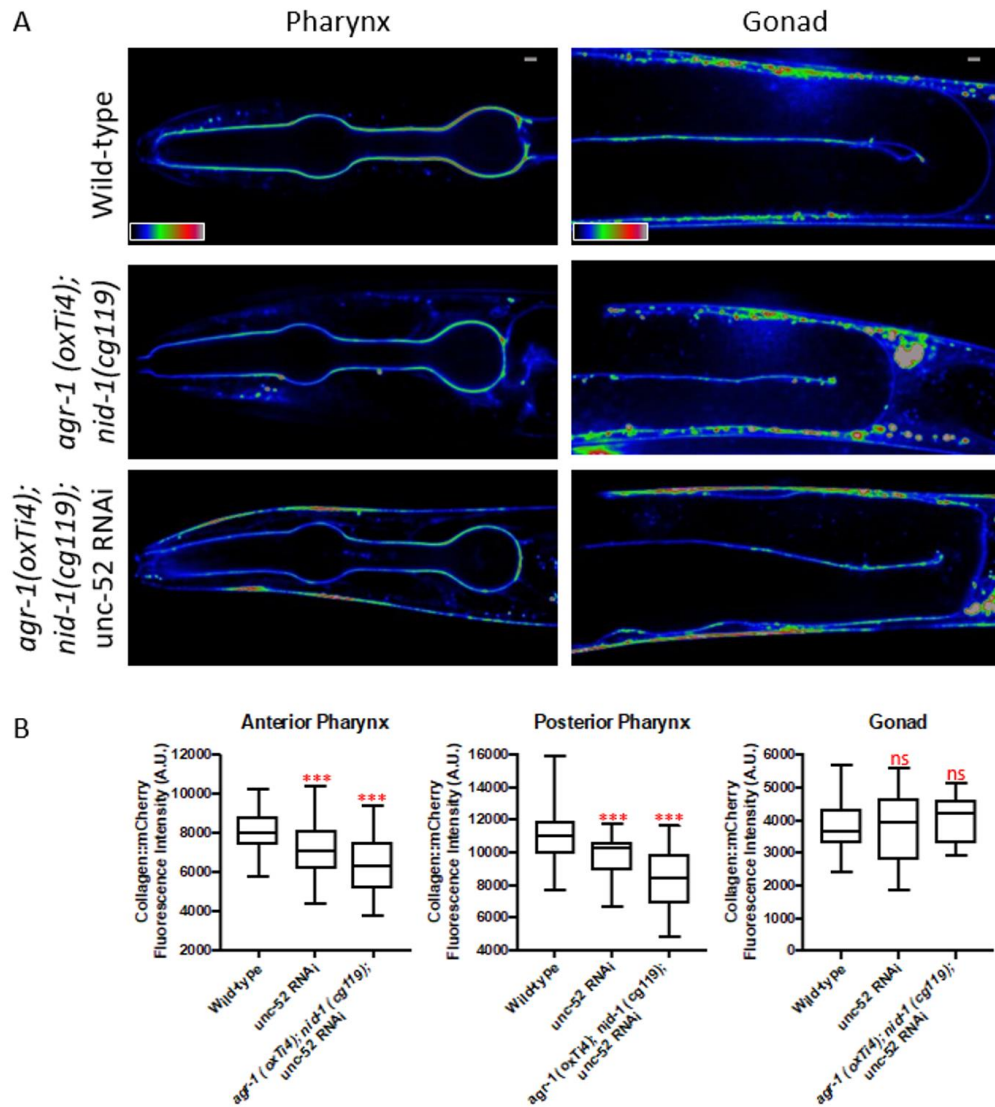


Figure 33: Nidogen and agrin function in a distinct pathway from perlecan in the recruitment of collagen to the pharyngeal BM.

(A) Spectral representation of fluorescence intensity of collagen::mCherry at the pharyngeal (left) and gonadal (right) BMs in wild-type (top) and *agr-1(OxTi4);nid-1(cg119)* animals treated with RNAi targeting *unc-52* (bottom). (B) Quantification of collagen::mCherry fluorescence intensity at the anterior and posterior pharyngeal BMs (left) and the gonadal BM (right) ($n \geq 38$ for each treatment). *** $p < 0.0001$, one-way ANOVA followed by post-hoc Dunnett's test. n.s., $p > 0.05$. Box edges in boxplots depict the 25th and 75th percentile, the line in the box indicates the median value, and whiskers mark the minimum and maximum values. Scale bars are 5 μ m.

is unclear whether it affects collagen deposition into BMs (Fitzgerald and Schwarzbauer 1998). To determine whether SPARC is required for collagen recruitment to the pharyngeal and gonadal BMs, I knocked SPARC down conditionally by RNAi beginning at the L1 larval stage. Reduction of SPARC levels resulted in a dramatic decrease in collagen levels at the pharyngeal BM (~60% reduction in collagen::mCh fluorescence intensity compared to control animals, Figure 34A). In addition, severe morphological defects were observed in the pharyngeal bulbs (n= 20/33 animals examined, Figure 34A), indicating that the mechanical integrity of the pharynx was compromised. Laminin::GFP levels in the pharyngeal BM were unaffected upon SPARC reduction, suggesting that SPARC functions specifically in the recruitment of collagen to the pharyngeal BM. Type IV collagen is predominantly synthesized and secreted from the body wall muscle, and then incorporated into distant BMs, including the pharyngeal BM, from the extracellular fluid (Clay and Sherwood 2015; Graham et al. 1997). Reduction of SPARC resulted in the accumulation of collagen levels at the surface of the body wall muscle (approximately two-fold increase in collagen::mCh fluorescence compared to control animals, Figure 34B). Surprisingly, reduction of SPARC did not affect collagen recruitment to the gonadal BM (Figure 35). Together, these results suggest that SPARC is required to transport type IV collagen from the body wall muscle surface to the pharyngeal BM, but is dispensable for collagen recruitment to the gonadal BM.

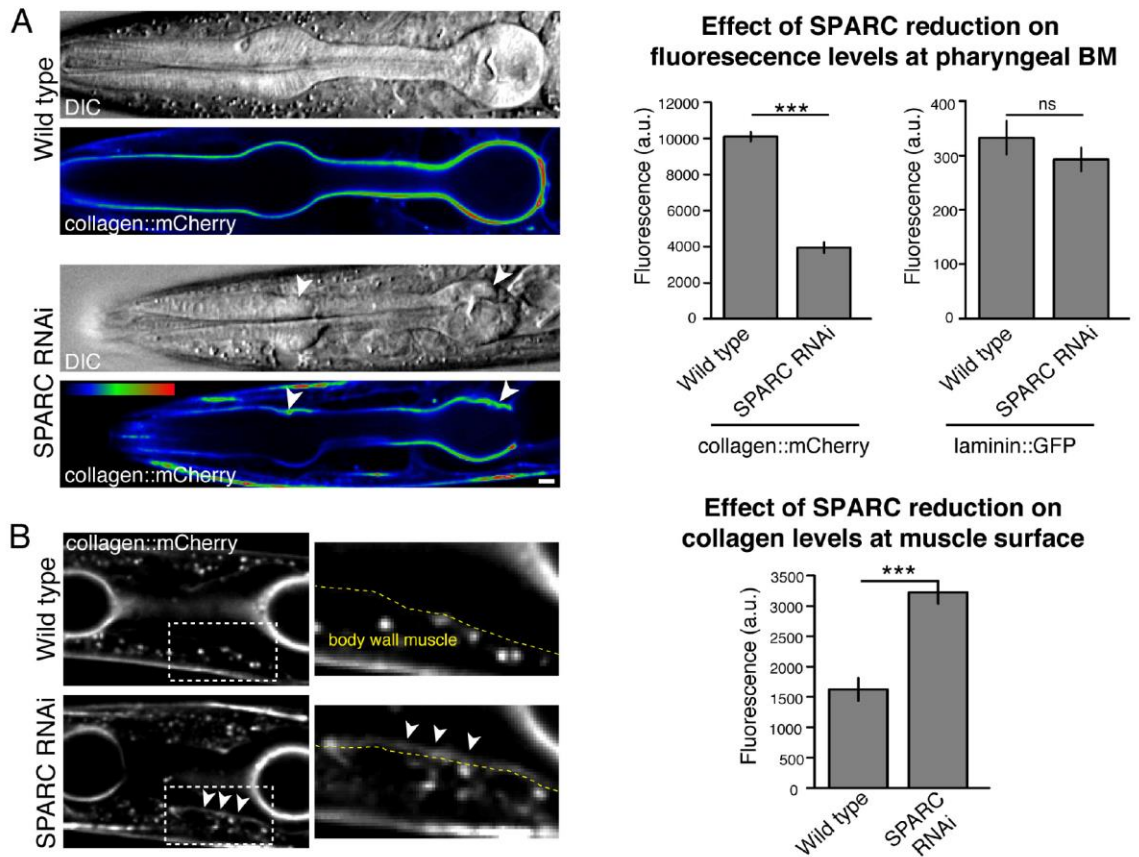


Figure 34: SPARC is required for collagen recruitment to the pharyngeal BM.

(A) DIC images and spectral representations of collagen::mCh fluorescence in the pharynxes of control and *SPARC* RNAi treated animals are shown on the left. Quantification of collagen::mCh and laminin::GFP levels is shown on the right (n=15 for each treatment). (B) Fluorescence images of collagen::mCh at body wall muscle surfaces of control and *SPARC* RNAi treated animals. Boxed regions are magnified on the right, and the body wall muscle surface is outline in yellow. Arrowheads indicate accumulation of collagen::mCh at the body wall muscle surface in *SPARC* RNAi treated animals. Quantification of collagen::mCh and laminin::GFP levels is shown on the right (n=15 for each treatment). *** $p < 0.001$, unpaired two-tailed Student's *t*-test; n.s., $p > 0.05$. Bar graphs show mean fluorescence intensity and error bars represent standard error of the mean. Scale bars are 5 μ m. Figure originally appeared in (Morrissey et al. 2016) and is adapted with permission.

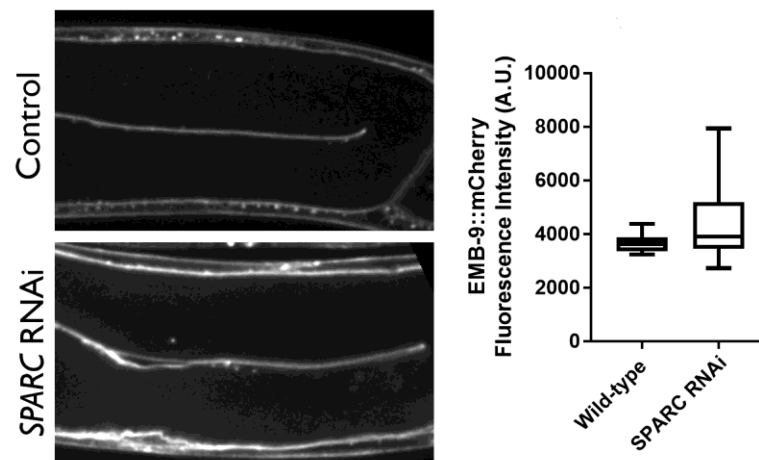


Figure 35: SPARC is not required for collagen recruitment to the gonadal BM.

Fluorescence images of gonadal BM collagen::mCherry in control and *SPARC* RNAi treated animals are shown on the left. Quantification of collagen::mCherry fluorescence intensity is shown on the right (n=15 for each treatment). n.s., $p>0.05$, unpaired two-tailed Student's *t*-test. Box edges in boxplots depict the 25th and 75th percentile, the line in the box indicates the median value, and whiskers mark the minimum and maximum values.

3.3 Discussion

In this study, I used genetic analysis and live-cell imaging in *C. elegans* to investigate the role of the matricellular proteins agrin, nidogen, perlecan, and SPARC in the targeting of type IV collagen to the pharyngeal and gonadal BMs of *C. elegans*. Through live-cell imaging, examination of endogenous localization, conditional RNAi knockdown, and genetic analysis, I discovered that all of these proteins functioned in the recruitment of type IV collagen specifically to the pharyngeal but not gonadal BMs, highlighting the existence of tissue-specific machinery that control BM collagen

localization. Furthermore, we found that nidogen and agrin functioned in a distinct pathway from perlecan in recruiting collagen to the pharyngeal BM, suggesting that these network-bridging molecules have non-redundant functions.

Genetic analysis of the network-bridging molecules nidogen, agrin, and perlecan revealed previously unappreciated roles for these proteins in localizing collagen to the BM. In particular, I found that all three proteins regulate collagen localization to the pharyngeal but not gonadal BM. This is a very surprising result, given my findings in Chapter 2 that the localization of collagen to the pharyngeal BM is laminin-independent. It is possible that nidogen, agrin, and perlecan can themselves bind to cell surfaces, thus facilitating collagen association. Alternatively, these molecules could bind to cell surface receptors, thus tethering collagen directly to the cell surface instead of connecting the collagen network to existing laminin networks as traditionally thought. Biochemical analysis of proteins complexed with these bridging molecules could distinguish between these possibilities.

My data also reveal that nidogen and agrin function in a distinct pathway from perlecan in recruiting collagen to the pharyngeal BM. Thus, these molecules have non-redundant functions, at least with regards to the recruitment of collagen to the BM, countering the prevailing model that nidogen, agrin, and perlecan function redundantly (Hohenester & Yurchenco, 2013) I also observed that agrin and nidogen function redundantly in recruiting collagen to the anterior pharyngeal BM, but that they have

non-redundant functions in the posterior pharyngeal BM. These observations highlight the compartmentalization of the pharyngeal BM (discussed further in Chapter 5). It is possible that the localization of agrin or nidogen is dependent on the other at the posterior pharyngeal BM. It would be informative to visualize AGR-1::mNG in *nid-1(cg119)* animals, and NID-1::mNG in *agr-1(OxTi4)* animals to determine if this is the case.

In agreement with studies in *Drosophila* (discussed in Chapter 3.1), I discovered that SPARC is required for the recruitment of collagen to the *C. elegans* pharyngeal BM. Our data suggests that it acts as an extracellular chaperone to transport collagen synthesized by the body wall muscle to distant sites of incorporation such as the pharyngeal BM. Interestingly, however, SPARC activity is not required for the recruitment of collagen to the gonadal BM. In addition to the body wall muscle, type IV collagen is also synthesized by the distal tip cell and spermathecal cells of the gonad, as well as the vulval muscle cells (Graham et al. 1997). As these cells are in direct contact with the gonadal BM, SPARC may not be required to transport the extracellular collagen. Alternatively, very low levels of SPARC might be sufficient for collagen transport to the gonadal BM.

Collectively, my findings begin to piece together the tissue-specific machinery that govern collagen recruitment to BMs. However, many open questions remain. The genetic perturbations of nidogen, agrin, and perlecan cause a maximal reduction in

pharyngeal collagen levels of only 30%. This suggests the existence of multiple other mechanisms contributing to the localization of collagen to the pharyngeal BM (as I similarly discussed in Chapter 2). Furthermore, while I have identified pharynx-specific collagen regulatory proteins, I did not identify any gonad-specific factors in this study, or in studies discussed in Chapter 2. In Chapter 4, I leverage a reverse genetic screening approach available in *C. elegans* to identify new components of the molecular machineries governing the recruitment of collagen to BMs. Understanding these tissue-specific mechanisms underlying collagen targeting will have profound implications in the development of targeted therapies for BM diseases.

3.4 Acknowledgements

Some strains were provided by the CGC, which is funded by the NIH Office of Research Infrastructure Programs (P40 OD010440). Varun Jain, an excellent undergraduate student who I mentored in the lab, assisted me with image acquisition and quantification for studies described in Chapter 3.2.1 and 3.2.2. Dan Keeley and Eric Hastie helped generate the UNC-52::mNG, AGR-1::mNG, and NID-1::mNG worm strains. I thank Meghan Morrissey and my advisor David Sherwood for helpful intellectual discussions on experiments detailed in Chapter 3.2.3.

4. A genome-scale RNAi screen to identify novel regulators of type IV collagen synthesis, trafficking, and incorporation into basement membranes

4.1 Introduction

Thus far, I have discussed the roles of the matrix receptor integrin (Chapter 2) and the matricellular proteins nidogen, agrin, and SPARC (Chapter 3) in directing type IV collagen to BMs. However, our understanding of the mechanisms by which these molecules regulate BM collagen incorporation is far from complete. For example, in chapter 2, I discovered that inside-out activation of integrin facilitates distinct modes of collagen recruitment to the *C. elegans* pharyngeal and gonadal BMs. I identified a small GTPase, RAP-3 (Rap1), as a specific activator of PAT-2/PAT-3 integrin in the pharynx. In lymphocytes, Rap1 activates the α L β 2 integrin through the effector RapL that binds to the α L subunit (Katagiri et al. 2004; Zhang and Wang 2012). Whether RAP-3 activates PAT-2/PAT-3 in a similar manner is unclear. Further, the identity of analogous activators of INA-1/PAT-3 in the gonad is not known.

In addition, in chapter 3, I outlined tissue-specific roles for the matricellular proteins SPARC, nidogen, agrin, and perlecan in targeting collagen to BMs. All of these proteins were required for collagen recruitment to the pharyngeal but not gonadal BMs. The requirement of the cross-bridging molecules nidogen, agrin, and perlecan for directing collagen to pharyngeal BMs is particularly intriguing, given my findings that

collagen targeting to the pharynx is not dependent on laminin (Chapter 2). It is possible that these proteins interact with either a molecule(s) in the matrix, or on the cell surface, to facilitate collagen recruitment to the BM. The identity of these molecules has not been determined.

Here, I describe a genome-scale RNAi screen initiated to tackle these open questions in an unbiased manner. As I discussed in Chapter 1.7, excellent reverse genetic tools are available in *C. elegans*. For this study I made use of the Ahringer RNAi library (Kamath et al. 2003). This library contains 19,762 clones, targeting about ~90% of the worm genes. In my pilot study, I designed and optimized a screening pipeline, and screened through ~30% of the library. Candidate genes from this round of screening were verified by two additional independent RNAi platings and by sequencing of the RNAi clones to confirm their identity. In this chapter, I present 27 candidate regulators of type IV collagen and discuss how they could mediate collagen synthesis, trafficking, secretion, or incorporation into BMs.

4.2 Results

4.2.1 Screen design

The strain I used for the screen carried a type IV collagen reporter described in chapters 2 and 3 (*collagen::mCherry*), the *rrf-3(pk1426)* mutation that enhances somatic RNAi (Simmer et al. 2002), and a pharyngeal muscle marker (*myo-2p::GFP*) to visualize

pharyngeal morphology. To increase the throughput of the screen, I used 6-well plates, where each well was seeded with bacteria carrying an individual RNAi clone. Further, as the collagen::mCherry marker is very bright, I decided to perform the screen visually on a fluorescent stereoscope, instead of using the confocal imaging technique I employed in Chapters 2 and 3. I verified the validity of this approach by including control wells containing *emb-9* or *let-268* RNAi in each screening batch. Visual inspection of worms in these wells showed that collagen::mCherry fluorescence was visibly far dimmer than control worms fed bacteria containing the L4440 empty vector. Moreover, in my pilot visual screen, I identified *let-2*, *let-268*, and *ina-1*, all of which I have previously implicated in collagen recruitment to BMs (Chapter 2).

4.2.2 Candidate novel regulators of type IV collagen

From my pilot screen, I identified 461 genes whose knockdown resulted in a variety of visually detectable defects. These included reduced collagen::mCherry signal in the pharyngeal or gonadal BMs, pharyngeal and gonadal morphology defects, and accumulation of collagen::mCherry in the body wall muscle (the predominant site of collagen production, discussed in Chapter 2). To exclude false positives, I performed two additional RNAi platings of these preliminary candidates. Genes whose knockdown did not produce the initially observed phenotype in at least two of the three RNAi experiments were not pursued further. Next, I excluded all proteins with general

functions clearly not related to BM collagen recruitment, such as those involved in DNA replication and repair, transcription, RNA processing, translation, cell cycle, and apoptosis. Finally, I verified the identity of the remaining genes by sequencing of respective RNAi clones. These quality control steps yielded a final list of 27 genes (true positive detection rate of ~0.5%), outlined in Table 2.

I classified these genes into two broad categories based on the phenotypes associated with their knockdown and their hypothesized function in relation to type IV collagen. RNAi against 10 of these 27 genes resulted in reduced BM collagen::mCh fluorescence signal, defects in the morphology of the pharynx and/or gonad, and an accumulation of collagen in the body wall muscle (Figure 36A). Based on these phenotypes, I hypothesized that these proteins facilitate intracellular collagen trafficking or secretion of collagen into the extracellular fluid. Indeed, four of these genes—*sec-24.2*, *uso-1*, *eas-1*, *agef-1*, and *use-1*—encode proteins that function in vesicle formation and vesicular transport. Two proteins, VPS-20 and VPS-28, are components of ESCRT complexes (Schmidt and Teis 2012) that function in membrane remodeling and vesicular transport of cargoes for degradation. CHP-1, a CHORD-domain containing protein, is thought to function as a co-chaperone with Hsp90 (Bohush et al. 2019; Ferretti et al. 2010) to stabilize protein folding. Two of the 10 genes, *pign-1* and *dpm-3*, both code for proteins involved in glycosylphosphatidylinositol (GPI) anchor biosynthesis. However, the accumulation of collagen in the body wall muscle upon knockdown of these genes

Table 2: Candidate novel regulators of type IV collagen synthesis, trafficking, secretion, and incorporation into basement membranes

Gene	Vertebrate ortholog	Functional annotation	Observed phenotype	Proposed function
<i>sec-24.2</i>	SEC24	COPII coat complex	Accumulation of collagen::mCh in body wall muscle	Intracellular collagen trafficking or collagen secretion
<i>uso-1</i>	USO1	ER-to-Golgi transport		
<i>eas-1</i>	GOLT1	Golgi transport		
<i>agef-1</i>	ARFGEF	Vesicle transport		
<i>use-1</i>	USE1	Unconventional SNARE protein	Reduced BM collagen levels	
<i>vps-28</i>	VPS28	ESCRT I Complex	Pharyngeal/gonadal morphology defects	
<i>vps-20</i>	CHMP6	ESCRT III Complex		
<i>chp-1</i>	CHORDC1	Chaperone?		
<i>pign-1</i>	PIGN	GPI anchor biosynthesis		
<i>dpm-3</i>	DPM3	GPI anchor biosynthesis		
<i>hpo-4</i>	PIGK	GPI anchor biosynthesis	Reduced BM collagen levels	Collagen synthesis or BM collagen incorporation
ZK792.7	MPPE1	GPI anchor biosynthesis		
<i>gon-2</i>	TRPM	TRP channel		
<i>gtl-1</i>	TRPM	TRP channel		
M57.2	RABGGTA	Prenylation		
<i>tag-335</i>	GMPPB	Mannose biosynthesis		
<i>ifo-1</i>	AC106799.1	Intermediate filament organizer		
<i>vab-10</i>	DST/MACF1	Spectraplaklin		
<i>riok-1</i>	RIOK1	Phosphorylation		
<i>kin-10</i>	CSNK2B	Phosphorylation		
<i>mvk-1</i>	MVK	Phosphorylation		
<i>let-92</i>	PPP2CA	Phosphatase		
ZK686.3	MAGT1/TUSC3	Magnesium transport; glycosylation		
<i>cua-1</i>	ATP7A	Copper transporter	Reduced BM collagen levels Gonadal morphology defects	
<i>mig-38</i>	BICRA	Copper binding		
<i>tln-1</i>	TLN1	Integrin activator		
<i>mlt-7</i>	PXDNL	Heme peroxidase	Reduced BM collagen levels Pharyngeal morphology defects	

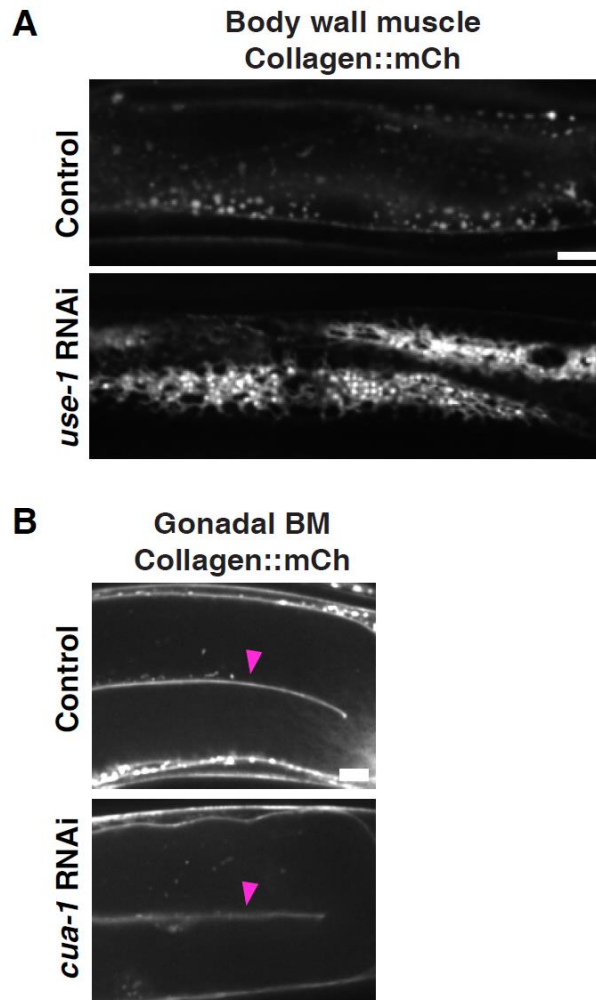


Figure 36: Representative phenotypes observed in the screen. (A) Fluorescence images of collagen::*mCherry* in the body wall muscle of control and *use-1* RNAi-treated 72h adult animals. (B) Fluorescence images of collagen::*mCherry* in the gonad of control and *cua-1* RNAi-treated 72h adult animals. Arrowheads indicate a reduction in gonadal BM collagen levels in the *cua-1* RNAi-treated animal compared to the control animal. Scale bars are 10 μ m.

suggests that these proteins may also regulate collagen trafficking and secretion.

Supporting this idea, a recent study found that PIGN-1 prevents the aggregation of type IV collagen in the endoplasmic reticulum (ER), independently of its function in GPI synthesis (Ihara et al. 2017). Whether DPM-3 performs a similar function has not been determined.

RNAi against the remaining 17 genes resulted in reduced BM collagen::mCherry fluorescence signal (Figure 36B), and defects in pharyngeal and/or gonadal morphology. Thus, I hypothesized that these proteins could either function directly in BM collagen recruitment, or indirectly through regulation of collagen synthesis. Two of these 17 genes, *hpo-4* and *ZK792.7*, encode proteins involved in GPI anchor biosynthesis. However, unlike *pign-1* and *dpm-3* described above, RNAi against *hpo-4* and *ZK792.7* resulted in reduced BM collagen levels without causing collagen accumulation in the secretory apparatus of body wall muscle. It is likely that their function in GPI assembly could contribute to either collagen synthesis or BM incorporation of collagen. I identified two TRP channel genes—*gon-2* and *gtl-1*—through this screen. In *C. elegans*, TRP channels regulate diverse physiological processes ranging from gene expression in response to environmental stimuli, to lysosome biogenesis (Xiao and Xu 2011). Thus, it is possible that GON-2 and GTL-1 could mediate either synthesis or secretion of type IV collagen. I also detected two genes encoding components of the intermediate filament cytoskeleton, *ifo-1* and *vab-10*, in my screen. Six proteins involved in post-translational

modifications were identified. M57.2 functions in prenylation, while TAG-335 is involved in mannose biosynthesis. *riok-1*, *kin-10*, and *mvk-1* code for genes that promote phosphorylation while LET-92 facilitates dephosphorylation. I also found three proteins involved in divalent cation binding. ZK686.3 functions in magnesium (Mg^{2+}) transport, CUA-1 is a copper (Cu^{2+}) transporter, and MIG-38 binds copper. Importantly, biochemical and cell culture studies have shown that Mg^{2+} binding to integrin promotes the association of integrin with matrix ligands (Zhang and Chen 2012). Further, Cu^{2+} promotes the upregulation of integrin $\beta 3$ mRNA levels and integrin $\beta 4$ protein levels *in vitro* (Fan et al. 2009; Savaris and Chies 2003). Thus, these three proteins could affect BM collagen incorporation by modulating integrin activity or levels. The integrin activator talin, which I detected in my screen, binds to integrin, triggering a conformational change that promotes high affinity binding of matrix ligands to integrin (Klapholz and Brown 2017). Thus, it is possible that TLN-1 activates INA-1/PAT-3 or PAT-2/PAT-3 or both heterodimers to promote collagen recruitment to the BM. Finally, I identified the heme peroxidase MLT-7 in my screen. RNAi against *mlt-7* resulted in reduced BM collagen levels and resulted in pharyngeal morphology defects. MLT-7 functions in the cross-linking of collagens in the nematode cuticle (Thein et al. 2009), but whether it can also cross-link type IV collagen in BMs is unknown.

4.3 Discussion

Type IV collagen is essential for the mechanical and signaling functions of BMs. Yet, the mechanisms targeting collagen to BMs *in vivo* have remained elusive. Here, I initiated a genome-scale RNAi screen in *C. elegans* to identify novel regulators of type IV collagen function. Through visual assessment of pharyngeal and gonadal collagen::mCherry fluorescence, I identified 27 genes whose knockdown resulted in reduced BM collagen levels. RNAi against 10 of these 27 genes also caused an abnormal buildup of collagen in the body wall muscle, the predominant site of collagen IV production in the worm. Together, these findings establish a high throughput screening strategy to uncover general mechanisms of type IV collagen synthesis, intracellular trafficking, secretion, and incorporation into BMs.

RNAi against the majority of the genes I identified in the pilot screen—17 out of 27—affected BM collagen levels without causing a buildup of collagen in the body wall muscle. I hypothesize that these proteins could affect collagen function in two ways: (1) by regulating BM collagen incorporation, or (2) regulating the transcription or translation of type IV collagen. Transcriptional and translational reporters could be used in the future to distinguish between these possibilities. If these proteins do not control collagen synthesis, then it is likely that they affect BM collagen incorporation. It would also be interesting to examine other matrix components—including laminin, nidogen, and perlecan—upon knockdown of these genes, to see if they are affected in

their synthesis or incorporation into BM, in order to determine whether these candidates are specific regulators of collagen, or general regulators of other BM components.

Four of these 17 genes—*riok-1*, *kin-10*, *mvk-1*, and *let-92*—encode proteins that regulate phosphorylation. It is possible that these three kinases and one phosphatase regulate the synthesis of type IV collagen. Alternatively, they might regulate the phosphorylation of collagen itself. In particular, type IV collagen is phosphorylated at its Goodpasture antigen-containing region near the C-terminus. Defective phosphorylation in this region is associated with Goodpasture's syndrome, where collagen deposition into the glomerular BM is disrupted, thus causing kidney disease (Revert et al. 2007; Mao et al. 2015). Furthermore, phosphorylation of matrix proteins promotes RGD-mediated cell attachment, and phosphorylation of a serine residue adjacent to the RGD sequence within the Goodpasture antigen region of type IV collagen is thought to expose the RGD to facilitate binding to integrin (Revert et al. 1995). Based on these observations, an intriguing possibility is that one or more of these kinases I identified could promote interactions between type IV collagen and the RGD-binding PAT-2/PAT-3 integrin heterodimer (detailed in Chapter 2).

I hypothesize that five of the 17 genes could affect BM collagen incorporation by regulating integrin function. The magnesium transporter ZK686.3, the copper transporter CUA-1, and the copper-binding protein MIG-38 could affect integrin activity or levels, while TLN-1 (talin) activates integrin, as discussed earlier. It would be

interesting to see where these proteins are expressed and localized using CRISPR/Cas9-based mNeonGreen knock-in studies. These might suggest tissue-specific functions and possibly activity at the cell-BM interface. Further, combined RNAi against each of these genes and either *ina-1* or *pat-2* could provide insight into which integrin heterodimer they activate. I also identified M57.2, an ortholog of mammalian RABGGTA, in my pilot screen. M57.2 functions in protein prenylation, the post-translational addition of lipid moieties to proteins (Wang and Casey 2016). Prenylation promotes the membrane-targeting and thus activation of Ras family GTPases, including Rap1 (Wilson et al. 2016). RAP-3, the *C. elegans* ortholog of Rap1, specifically activates the PAT-2/PAT-3 integrin in the pharynx (Chapter 2). Based on these observations, it is possible that M57.2 promotes the activity of RAP-3 or some other Ras family member to facilitate collagen recruitment to the BM. Collectively, my findings suggest that this screening approach is very useful in identifying new regulatory components of integrin-driven collagen targeting to BMs. In particular, I might find specific activators of INA-1/PAT-3 in the gonad, similar to RAP-3 the pharynx (see Chapter 2).

RNAi knockdown of *hpo-4* and ZK792.7, both genes involved in different aspects of GPI anchor biosynthesis, affected gonadal BM collagen levels. In chapter 2, I discussed the possible role of other receptor systems functioning with integrin to direct collagen to BMs. My observations here suggest that components of this unidentified receptor system could include GPI-anchored moieties. *C. elegans* encodes ~300 proteins

predicted to contain GPI anchors (Rao et al. 2011). A separate targeted RNAi screen of these GPI-anchored proteins could assess their roles in collagen incorporation into BMs.

RNAi against the remaining 10 of the 27 genes I identified in my screen resulted in a reduction in BM collagen levels, accompanied by an accumulation of collagen in the body wall muscle, the major source of collagen in the worm (Clay and Sherwood 2015). I hypothesize that these proteins probably do not directly affect BM collagen incorporation, but rather, facilitate intracellular collagen trafficking or exocytosis of collagen into the extracellular fluid. As type IV collagen molecules are 400nm long, they cannot be packaged into classical COPII type vesicles, which are typically between 60-90nm in size (Jensen and Schekman 2011). Studies in *Drosophila* and human cells suggest that the protein Tango1 facilitates the expansion of COPII vesicles into large tubular-shaped vesicles to allow for the packaging of large cargoes like type IV collagen (Chioran et al. 2017). Further, work in mice and cell culture have implicated the ER-resident Hsp47 as a molecular chaperone that promotes collagen IV stability and transit from the ER to Golgi (Marutani et al. 2004; Matsuoka et al. 2004). As *C. elegans* does not encode Hsp47 or Tango1 in its genome, the mechanisms facilitating collagen transport in the worm are not clear. The 10 genes I have identified in my screen, whose knockdown resulted in abnormal accumulation of collagen in body wall muscle cells, provide a first glimpse at these mechanisms. Five genes—*sec-24.2*, *uso-1*, *eas-1*, *agef-1*, and *use-1*—encode proteins that function in vesicular transport. To determine whether these

proteins function specifically in the transport of collagen or to traffic general secreted cargoes, it would be informative to examine the levels of other secreted proteins in the body wall muscle upon knockdown of these genes in animals expressing laminin::mNG, the metalloprotease MIG-17::Venus (Nishiwaki et al. 2000), or secreted soluble GFP (Fares and Greenwald 2001). It would also be interesting to tag *sec-24.2*, *uso-1*, *eas-1*, *agef-1*, and *use-1* endogenously with mNeongreen in order to determine where they localize in muscle cells (ER, Golgi, vesicles, etc), and whether they co-localize with collagen during its secretion.

In conclusion, I have established a screening pipeline for identifying new regulators of type IV collagen function and demonstrated its validity and efficacy. I identified 27 preliminary candidates in my pilot screen and have discussed how they could affect collagen function, and provided follow-up experiments to test these possibilities. I anticipate that the completion of this screen will provide new insight into cellular mechanisms that control type IV collagen synthesis, transport, secretion, and incorporation into BMs.

4.4 Acknowledgements

Qiuyi Chi managed and cultured the Ahringer library RNAi clones and prepared all screening plates used in this study. I also thank Alejandro Aballay, Dong Yan, and Lingfeng Meng for sharing Ahringer library RNAi clones.

5. Discussion

Basement membranes are thin, dense sheets of extracellular matrix that underlie most tissues and organs (Pozzi et al. 2017; Kalluri 2003). Type IV collagen is a scaffolding protein that is essential for the mechanical, barrier, and signaling functions of BMs (Khoshnoodi et al. 2008; Jayadev and Sherwood 2017). However, due to the large gene families of BM components and receptors in vertebrates, the difficulty of imaging cell-BM interactions *in situ* in vertebrate tissues, and the essential embryonic functions of BM receptors, the mechanisms that direct type IV collagen to BMs *in vivo* have been challenging to identify (Clay and Sherwood 2015; Kelley et al. 2014; Yurchenco and Patton 2009; Li et al. 2017). Here, I have established the nematode *C. elegans* as a simple and powerful model to study type IV collagen incorporation into BMs *in vivo* (see Chapter 1). In my work, I focused on two BM-encased tissues: the pharynx, a rigid and contractile feeding apparatus; and the gonad, a flexible, cylindrical reproductive organ.

I hypothesized that either molecules on the cell surface or within the BM could facilitate the recruitment of type IV collagen. I explored the former possibility in Chapter 2 and discovered that integrin is the predominant cell surface receptor system that facilitates collagen incorporation into the pharyngeal and gonadal BMs. Depletion of PAT-2/PAT-3 integrin in the pharynx and INA-1/PAT-3 integrin in the gonad resulted in ~50% reduction in BM collagen levels in each tissue, nearly matching RNAi-mediated

reduction of collagen, suggesting they are the main players. In Chapter 3, I investigated the roles of the BM components nidogen, agrin, perlecan, and SPARC in directing collagen to BMs. Surprisingly, I found that all four matricellular proteins were required for collagen incorporation into the pharyngeal BM, but not the gonadal BM, as their loss resulted in between 30-60% reduction in pharyngeal BM collagen levels. Thus, the targeting of collagen to BMs in the worm is controlled by both intracellular and extracellular systems that function in a tissue-specific manner.

Loss of none of these molecules completely removed collagen from the BM, implying the existence of additional mechanisms of BM collagen targeting. In Chapter 4, I investigated this possibility by initiating a genome-scale visual-based RNAi screen to discover novel regulators of type IV collagen function. I identified 27 candidate genes in my pilot study that could facilitate collagen synthesis, transport, secretion, or incorporation into BMs.

Collectively, my work provides new insight into the mechanisms controlling type IV collagen recruitment to BMs *in vivo*, and also implicates new players in the regulation of different aspects of collagen function. In this chapter, I discuss the implications of my findings.

5.1 Integrins mediate distinct modes of type IV collagen incorporation into basement membranes

The prevailing model of BM assembly, based largely on early embryonic and cell culture studies, suggests that the laminin network associates with cell surface molecules, including integrin, and that the collagen network then associates with laminin through interactions with cross-bridging molecules (Yurchenco 2011). However, I discovered that the PAT-2/PAT-3 integrin heterodimer directs collagen to the pharyngeal BM independent of laminin. This discrepancy can be resolved through two considerations. First, as I discussed in Chapter 1, cell culture work has shown that type IV collagen can bind to integrin, triggering downstream signaling. As type IV collagen contains several RGD sequences, and PAT-2/PAT-3 is a putative RGD-binding integrin, it is possible that PAT-2/PAT-3 promotes collagen incorporation directly (discussed in Chapter 2). This then raises the question of how laminin and collagen networks are both anchored to cell surfaces at the same time. Conventional transmission electron microscopy measurements have estimated the thickness of most BMs to be less than 100 nm (Halfter et al. 2015). As laminin and collagen molecules are 80nm and 400nm long respectively, they are thought to form flat, parallel lattices in the BM (Abrams et al. 2000, 2003; Yurchenco and Ruben 1987). However, these models are problematic as they are based on studies performed on desiccated BMs, and do not consider the abundance of proteoglycans and water in the BM. In fact, emerging evidence from work on hydrated chick, mouse, and human BMs suggests that they are over two times thicker (Halfter et

al. 2015). Thus, collagen and laminin networks do not necessarily have to form flat lattices within the BM. Instead, by adopting more diverse three-dimensional configurations, both networks could interact with cell surface molecules simultaneously. Super-resolution imaging of laminin and collagen in live worms, using a recently developed light-sheet microscopy technique that resolves single molecules (Gustavsson et al. 2018), could provide new insight into ultrastructural properties and orientations of BM networks.

It is unclear how laminin is recruited to the pharyngeal BM. Cell culture work suggests that cell surface integrins, dystroglycan, and sulfated glycolipids facilitate the targeting of laminin to BMs, potentially through redundant mechanisms (Li et al. 2005, 2017, 2002). Dystroglycan was not expressed in the pharynx, ruling out its potential role in laminin recruitment (Chapter 2). *C. elegans* does not produce sulfated glycolipids, which are made from galactose-ceramide moieties (Bai et al. 2018), but it assembles glucose-ceramide derived glycosphingolipids (Gerdt et al. 1997). In particular, phosphocholine-modified glycosphingolipids have been detected in contact with muscle BM through immunofluorescence studies (Gerdt et al. 1999). It would be interesting to determine whether this class of modified glycosphingolipid is present in the pharynx and if it could function in laminin recruitment. The laminin-binding integrin INA-1/PAT-3 is expressed in the pharynx, but is not required for laminin or collagen recruitment to the pharyngeal BM. It is possible that INA-1/PAT-3 functions

redundantly with another receptor system to facilitate laminin binding to the pharyngeal surface, or that an unidentified receptor other than integrin could be the predominant laminin-recruiting system in the pharynx. The screening approach I detailed in Chapter 4 could be used to identify candidate receptors.

Although laminin is not required for pharyngeal collagen recruitment, it is maintained in the pharyngeal BM through adulthood. However, RNAi-mediated reduction of BM laminin levels in the pharynx did not cause any overt defects to the BM or pharyngeal morphology. What is the function of laminin in the pharyngeal BM? During the formation of the pharynx in the embryo, laminin is essential for orienting and polarizing the pharyngeal epithelium correctly (Rasmussen et al. 2012). It is possible that laminin in the pharyngeal BM has post-embryonic signaling functions that were not detected after its RNAi-mediated reduction. Alternatively, since RNAi treatment does not remove all laminin from the pharyngeal BM, it is possible that a very small amount of laminin is sufficient to maintain BM structure, particularly as the pharynx grows nearly two orders of magnitude less than the gonad during larval development (detailed in Chapter 2).

Only one integrin heterodimer functions in each tissue to promote collagen recruitment, even though INA-1/PAT-3 and PAT-2/PAT-3 are expressed in both tissues (summarized in Figure 28). It is unclear what the function of the integrin heterodimer not involved in collagen recruitment in each tissue is. One possibility is that they are

maintained at the cell surface to respond to environmental changes. For example, the integrins $\alpha 2\beta 1$ and $\alpha 3\beta 1$ are both expressed in mouse keratinocytes but are not required for matrix adhesion. However, when the skin is wounded, both integrins are activated and trigger matrix adhesion and cell migration (Longmate and Dipersio 2014; Hegde and Raghavan 2013; Margadant et al. 2009). Another possibility is that these “inactive” integrins could function as mechanosensors, and are activated to signal by forces generated by the intracellular actomyosin machinery or extracellularly by the BM (Sun et al. 2019). It is thought that integrin heterodimers at the cell surface can exist in a dynamic equilibrium between the closed, inactive conformation and the open, active state (Askari et al. 2009). It is plausible that these mechanosensing functions of integrin could involve transient, low or intermediate affinity interactions with laminin or collagen in the BM, rather than the high-affinity interactions associated with BM anchorage to the cell surface. A third possibility involves ligand-independent mechanisms of integrin signaling. For example, in mice, the binding of the hepatocyte growth factor to the Met surface receptor triggers the phosphorylation of integrin $\beta 4$ near its C-terminus, inducing the association of integrin effectors to facilitate downstream signaling. Importantly, this process occurs normally even in integrin $\beta 4$ mutants incapable of binding matrix proteins (Comoglio et al. 2003). Given these observations, it is possible that INA-1/PAT-3 in the pharynx or PAT-2/PAT-3 in the gonad might have signaling functions that do not require BM binding.

As loss of integrin did not completely remove collagen from the pharyngeal or gonadal BMs, it suggests another receptor system functions alongside integrin to promote collagen recruitment. A sensitized RNAi screening approach, similar to what I have described in Chapter 4, could be used to investigate this. In particular, hypomorphic mutants of *ina-1* are viable (Baum and Garriga 1997). RNAi screens with these mutants could identify other receptors in the gonad that also facilitate laminin and collagen recruitment together with integrin.

5.2 The matricellular proteins nidogen, agrin, and perlecan, have tissue-specific functions in collagen recruitment to basement membranes

Collagen recruitment to the gonadal BM is dependent on laminin, and I expected to find that the known network-bridging molecules nidogen, agrin, or perlecan mediate the connection. However, I discovered that these proteins are all required to target collagen to the pharyngeal BM, but not gonadal BM (detailed in Chapter 3). One possible implication of my findings is that laminin and collagen networks can associate directly, precluding the need for network-bridging proteins. Biochemical analyses have shown that laminin and type IV collagen bind together in the presence of Zn^{2+} cations (Ancsin and Kisilevsky 1996). Furthermore, electron microscopy experiments on co-incubated laminin and type IV collagen demonstrated that laminin can bind to the C-terminal region of collagen *in vitro* (Laurie et al. 1986). Thus, it is possible that the

gonadal BM laminin and collagen networks are directly associated. Alternatively, an unidentified cross-bridging protein might function redundantly with nidogen and perlecan in collagen recruitment (as agrin is not detected in the gonadal BM). A sensitized RNAi screening approach could be used to investigate this possibility, as the null mutant of *nid-1* (nidogen) is viable (Kang and Kramer 2000) and several hypomorphic mutations in *unc-52* (perlecan) are available.

Paradoxically, agrin, nidogen, and perlecan were required for the targeting of collagen to the pharyngeal BM, even though collagen incorporation is not dependent on laminin in this tissue (see Chapter 2). In particular, nidogen and agrin were required redundantly for collagen recruitment to the anterior pharyngeal BM, but had non-redundant functions in directing collagen to the posterior pharyngeal BM. It is possible that distinct pathways facilitate collagen recruitment to the anterior and posterior pharyngeal BMs, as collagen is enriched in the posterior compared to the anterior pharynx. The functional significance of this collagen gradient in the pharynx is not known. A recent study on the *Drosophila* egg chamber demonstrated that a collagen gradient in the anterior-posterior axis specified a mechanical gradient where the poles of the egg containing less collagen were softer than the stiff, central collagen-rich regions. This collagen-based force gradient controls the final, ellipsoid shape of the egg chamber (Crest et al. 2017). It is plausible that the collagen gradient in the pharynx similarly influences the mechanical properties of the tissue. The posterior of the pharynx contains

a grinding apparatus that breaks apart the bacteria that the worm feeds on (Mango 2007). The enrichment of collagen might increase the rigidity of the posterior pharynx to protect against the mechanical stresses of food grinding. Atomic force microscopy studies on extruded pharynxes could determine whether the posterior of the pharynx is indeed stiffer than its anterior.

5.3 A genome-scale RNAi screen to uncover novel regulators of collagen targeting to basement membranes

In Chapter 4, I established a visual-based genome-scale RNAi screening pipeline to discover novel regulators of different aspects of type IV collagen function. In addition to identifying new regulators of collagen incorporation into BMs and proteins facilitating intracellular transport and exocytosis of collagen, the screening pipeline I have outlined can also be used to discover proteins that regulate type IV collagen turnover. Type IV collagen networks are covalently cross-linked (outlined in Chapter 1), and these networks have to be remodeled to facilitate the growth of BMs and expansion of tissues during development. Both peroxidase and lysyl oxidase like 2 mediate formation of sulfilimine and lysyl-derived crosslinks respectively in type IV collagen networks (Añazco et al. 2016; Bhave et al. 2017). However, it is unclear if hydrolases and/or reductases are involved in breaking these crosslinks, or if proteases are involved in pruning collagen networks to facilitate tissue expansion. I hypothesize that RNAi-mediated knockdown of such factors could lead to abnormal accumulation or

aggregation of collagen in BMs. While I did not detect these phenotypes in the pilot screen, I have now identified a positive control for future iterations, as knockdown of *pat-2* resulted in increased collagen levels in the gonadal BM (discussed in Chapter 2).

Interestingly, preliminary photobleaching studies in our laboratory indicate that type IV collagen in the gonadal BM turns over much faster than the pharyngeal BM (R. Jayadev, data not shown; and Keeley et al. 2019, manuscript in preparation). These observations suggest that the systems controlling collagen turnover, and perhaps BM turnover in general, could be different in each tissue. Future RNAi screens could incorporate worm strains expressing photoconvertible BM components, including Dendra-tagged collagen (Ihara et al. 2011) and laminin (Hagedorn et al. 2013). Visual comparisons of photoconverted pharyngeal and gonadal BMs in RNAi-treated animals could uncover factors that mediate BM turnover in these tissues.

6. Conclusion

BMs are cell-associated extracellular matrices that provide mechanical support to tissues, have barrier properties, and facilitate cell signaling processes. Type IV collagen is a scaffolding protein that is crucial for BM functions, and mutations in collagen cause diseases in nearly every organ system in humans. Despite its physiological importance, how collagen is targeted to BMs *in vivo* is poorly understood. In this dissertation, I have presented work that advances our understanding of how collagen is incorporated into BMs, using the nematode *C. elegans* as a model.

Through examination of endogenous localization, conditional knockdown, and misexpression studies, I identified distinct integrin heterodimers that promote collagen recruitment to the pharyngeal and gonadal BMs via distinct modes. The putative laminin-binding integrin INA-1/PAT-3 is selectively activated in the gonad and directs laminin and collagen to the gonadal BM, while the putative RGD-binding PAT-2/PAT-3 is activated in the pharynx and facilitates collagen incorporation into the pharyngeal BM independent of laminin. Through a targeted RNAi screen, I identified the Rap1 GTPase ortholog RAP-3 as a specific activator of PAT-2/PAT-3 integrin in the pharynx. While interactions between integrin and collagen have been observed *in vitro*, my work provides the first *in vivo* evidence implicating integrin in directing type IV collagen to BMs. Using genetic analysis, RNAi-mediated knockdown, and CRISPR/Cas9 genome editing to visualize endogenous expression, I found that the matricellular proteins

nidogen, agrin, perlecan, and SPARC were required for collagen incorporation into the pharyngeal BM, but not the gonadal BM. Finally, I established a genome-scale visual-based RNAi screen for novel regulators of type IV collagen function and identified 27 potential candidates involved in collagen synthesis, transport, secretion, or incorporation into BMs.

Type IV collagen emerged at the dawn of multicellularity and its function in BMs is associated with diverse physiological processes. Understanding how collagen is directed to BMs is vital to the development of new therapies against pathologies of defective BM collagen incorporation, such as cancer, Alzheimer's disease, and multiple sclerosis. *C. elegans* is a simple but powerful model system to genetically dissect and visualize mechanisms of collagen recruitment to BMs *in vivo*.

Appendix A

A.1 Materials and Methods

A.1.1 *C. elegans* strains

C. elegans strains used in this study are listed in Table 3. Worms were reared on NGM plates seeded with OP50 *Escherichia coli* at 16°C, 18°C, or 20°C according to standard procedures (Stiernagle 2006).

Table 3: *C. elegans* strains used in this study

Strain	Genotype ^a	Reference
N2	Wild-type (ancestral)	
NK364	<i>unc-119(ed3)</i> III; qyls46 [<i>emb-9p::emb-9::mCherry, unc-119(+)</i>] X	Ihara et al., 2011
NK1911	<i>rrf-3(pk1426)</i> II; <i>qyls46</i> X	This study
NK2335	qy20 [<i>lam-2::mNeonGreen</i>] X	This study
NK2351	<i>lin-35(n745)</i> I; <i>rrf-3(pk1426)</i> II; ruls38 [<i>myo-2p::gfp, unc-119 (+)</i>] III; <i>qyls46</i> X	This study
NK2334	<i>rrf-3(pk1426)</i> II; <i>qy20</i> X	This study
NK2429	<i>lin-35(n745)</i> I; <i>qy20</i> X	This study
NK2318	qy18 [<i>dgn-1::mNG</i>] X	This study
NK2469	<i>rrf-3(pk1426)</i> II; <i>qy18</i> X	This study
NK2436	qy36 [<i>pat-3::mNG</i>] III	This study
NK2324	qy23 [<i>ina-1::mNG</i>] III	This study
NK2479	qy49 [<i>pat-2::2xmNG</i>] III	This study
NK2339	<i>rrf-3(pk1426)</i> II; <i>qy23</i> III	This study
NK2064	<i>rrf-3(pk1426)</i> II; <i>ruls38</i> III; <i>qyls46</i> X	This study
NK2446	qy41 [<i>lam-2::mKate2</i>] X	This study
NK2503	qy57 [<i>rap-3::mNG</i>] IV	This study
NK2538	qy67 [<i>rap-3 deletion + mNG</i>] IV; <i>qyls46</i> X	This study
NK2430	<i>lin-35(n745)</i> I; qy26 [<i>pat-2::mNG</i>] III	This study
NK2472	<i>lin-35(n745)</i> I; <i>qy36</i> III	This study
NK1885	<i>agr-1(OxTi4)</i> II; <i>qyls46</i> X	This study
NK1872	<i>nid-1(cg119)</i> V; <i>qyls46</i> X	This study
NK2343	<i>agr-1(OxTi4)</i> II; <i>nid-1(cg119)</i> V; <i>qyls46</i> X	This study
NK2500	qy53 [<i>unc-52::mNG</i>] II	Keeley et al., manuscript in preparation
NK2443	qy38 [<i>nid-1::mNG</i>] V	Keeley et al., manuscript in preparation
NK2353	qy27 [<i>agr-1::mNG</i>] II	Keeley et al., manuscript in preparation

^aWhen a transgene is listed for the first time, it is bolded, and the entire genotype is displayed.

A.1.2 Transgene construction

A.1.2.1 mNeonGreen (mNG)/mKate2 knock-ins

To generate the following functional, genome-edited mNG/mKate2 knock-ins *lam-2(qy20[lam-2::mNG + LoxP])*, *lam-2(qy41[lam-2::mKate2 + LoxP])*, *pat-3(qy36[pat-3::mNG + LoxP])*, *ina-1(qy23[ina-1::mNG + LoxP])*, *pat-2(qy26[pat-2::mNG + LoxP])*, *pat-2(qy49[pat-2::2xmNG + LoxP])*, and *rap-3(qy57[rap-3::mNG + LoxP])*, we used CRISPR/Cas9 genome

editing with a self-excising drug (hygromycin) selection cassette (SEC) as described previously (Dickinson et al. 2015), with some modifications. Briefly, we generated new starter repair plasmids lacking the 3xFlag tag downstream of the SEC cassette sequence, and we attached an 18 amino acid (glycine-alanine-serine) flexible linker (flexlink) in-frame and directly upstream of mNG, mKate2, or two tandem mNG fluorophores. ~700bp-1kb left and right homology arms for each target were amplified from N2 genomic DNA (gDNA), mutated to introduce six silent point mutations adjacent to the Cas9 cut site, and inserted into the appropriate repair plasmid using Gibson assembly. We generated 1 or 2 guide RNA (sgRNA) plasmids for each target by inserting the respective sgRNA sequences into the pDD122 plasmid. To direct cleavage near the C-terminus, the following sgRNA sequences were used:

(5'-GTCATCAATTTGGAGCAAGA-3') and (5'-ATTGATGACATTGAAGCATT-3') for *lam-2*; (5'-TTGGCTTTTCCAGCGTATAC-3') and (5'-TTTAAAATCCAGTATACGC-3') for *pat-3*; (5'-CGAGAAGAATGGGCTGATAC -3') and (5'-ACGAGAAGAATGGGCTGATA-3') for *ina-1*;

(5'-CAGTACAATCAGGGACGTCA-3') for *pat-2*; and (5'-ATCTAATCGTGTGCAAAACA-3') for *rap-3*. For each tagging experiment, we injected a mixture of 50ng/μl Cas9-sgRNA plasmids (25ng/μl of each guide plasmid in cases where two sgRNAs were available), 100ng/μl repair template plasmid, and red co-injection markers [2.5ng/μl pCFJ90(*myo-2p::mCherry*) and 5ng/μl pCFJ104(*myo-*

3p::mCherry)] into the gonads of ~30-40 young adult N2 animals. The injected animals were singled onto fresh OP50 plates and allowed to lay eggs for 3-4 days at 20°C in the absence of selection. Then, 500µl of 2mg/ml hygromycin solution was added to each plate, and the plates were returned to 20°C for 4-5 days. Candidate knock-in animals were roller [*sqt-1(e1350)*, dominant Rol mutation] worms that survived the hygromycin treatment and lacked the red fluorescent extrachromosomal array markers. We were able to isolate ~2-5 independent lines for each construct. All initial insertion strains were homozygous viable and segregated 100% Rol progeny. To excise the SEC, we heat-shocked plates containing ~6 L3/L4 rollers each at 34°C in a water bath for 4h, and then grew the animals at 20°C for 3-4 days. We then singled adult wild-type animals (worms that lost both copies of the SEC) and verified successful genome editing by visualizing mNG/mKate2 fluorescence, PCR genotyping, and sequencing of the fluorophore insertion site.

A.1.2.2 rap-3 knock-out

To generate *rap-3(qy67[mNG + LoxP])*, we used CRISPR/Cas9 genome editing with the SEC as described above to delete the endogenous *rap-3* coding sequence and replace it with mNG. We directed cleavage near the N- and C-terminus of *rap-3* using the following sgRNAs: (5'-TTTTGGGAAATGGAGGAGTT-3') and

(5'-ATCTAATCGTGTGCAAAACA-3'). We modified the starter repair template plasmid described above to include 1kb left and right homology arms for *rap-3*.

A.1.2.3 *myo-2p::pat-2::mNG::unc-54 3'utr*

myo-2p::pat-2::mNG::unc-54 3'utr was built by Gibson assembling the following fragments in order: a ~1kb *myo-2p* fragment from the pCFJ90 vector, full-length *pat-2* amplified from N2 gDNA, and *flexlink::mNG::unc-54 3'utr*.

A.1.2.4 *myo-2p::ina-1[EX]::pat-2[CTMD]::mNG::unc-54 3'utr*

To generate *myo-2p::ina-1[EX]::pat-2[CTMD]::mNG::unc-54 3'utr*, I first amplified full-length *ina-1* and *pat-2* from N2 gDNA and cloned these fragments into separate TOPO vectors. Then I used Gibson assembly to ligate the following fragments in order: a ~1kb *myo-2p* fragment from the pCFJ90 vector; *ina-1* fragment containing only the extracellular, transmembrane, and intracellular membrane-proximal regions; *pat-2* fragment containing only the CTMD; and *flexlink::mNG::unc-54 3'utr*.

A.1.2.5 *myo-2p::rap-3^{G12V}::mNG::unc-54 3'utr*

To construct *myo-2p::rap-3^{G12V}::mNG::unc-54 3'utr*, we first used Gibson assembly to connect the following fragments in order: a ~1kb *myo-2p* fragment from the pCFJ90

vector, full-length *rap-3* amplified from N2 gDNA, and *flexlink::mNG::unc-54 3'utr*. We then introduced the G12V mutation in *rap-3* by site-directed mutagenesis.

A.1.2.6 *inx-8p::rap-3::mNG::unc-54 3'utr*

To build *inx-8p::rap-3::mNG::unc-54 3'utr*, we replaced (by Gibson assembly) the *myo-2p* fragment in the *myo-2p::rap-3::mNG::unc-54 3'utr* construct created above with a 1.5kb fragment upstream of *inx-8* amplified from N2 gDNA.

A.1.3 Transgenic strains

All CRISPR/Cas9 genome-edited mNG/mKate2 knock-in strains were created by injecting the relevant constructs into the germline of young adult N2 worms as described earlier. All knock-in alleles were functional, and viability and growth rates of knock-in strains were similar to N2 animals. The *rap-3(qy67)* knock-out strain was generated by injecting the relevant CRISPR/Cas9 constructs into the gonads of young adult NK364 animals. I was unable to isolate homozygous *rap-3(qy67)* animals as the null mutation caused embryonic lethality. Transgenic worms expressing *myo-2p::pat-2::mNG::unc-54 3'utr* or *myo-2p::INA-1/PAT-2::mNG::unc-54 3'utr* were created by injecting these constructs (1.5ng/μl) together with full-length *pat-3* gDNA amplified from N2, EcoRI-digested salmon sperm DNA (50ng/μl), and pBluescript II (50ng/μl) into the gonads of young adult NK364 or NK2446 animals respectively. Animals expressing

myo-2p::rap-3^{G12V}::mNG::unc-54 3'utr were created by co-injecting the construct (1.5ng/μl) with EcoRI-digested salmon sperm DNA (50ng/μl) and pBluescript II (50ng/μl) into the gonads of young adult NK364 animals. Worms carrying *inx-8p::rap-3::mNG::unc-54 3'utr* were made by co-injecting the construct (50ng/μl), EcoRI-digested salmon sperm DNA (50ng/μl), pBluescript II (50ng/μl), and a green co-injection marker (*myo-2p::gfp*, 2.5ng/μl) into the gonads of NK364 or NK2446 animals. As F1 progeny expressed the above constructs mosaically and did not transmit them to subsequent generations, I collected and imaged F1s directly for the relevant experiments.

A.1.4 RNAi

All RNAi constructs were obtained from the Vidal (Rual et al. 2004) and Ahringer (Kamath et al. 2003) libraries, except for the following clones: *csk-1*, *kin-32*, *pix-1*, *rsu-1*, *unc-97*, *unc-112*, and *pat-3*. To build these RNAi clones, we PCR-amplified fragments corresponding to the longest transcripts of these genes from N2 gDNA, and inserted them into the L4440 (pPD129.36) vector (Timmons and Fire 1998) by Gibson assembly. RNAi constructs were then transformed into *Escherichia coli* strain HT115, and all RNAi experiments were performed using the feeding method (Timmons et al. 2001). Briefly, I grew RNAi bacterial cultures in selective media for 12-14h at 37°C, and then for an additional hour following addition of 1mM Isopropyl b-D-1-thiogalactopyranoside (IPTG) to induce dsRNA expression. For co-depletion experiments, I mixed the relevant

induced bacterial cultures at a 1:1 ratio. NGM agar plates containing topically applied 1M IPTG and 100mg/ml ampicillin (9µl each) were then seeded with these RNAi bacterial cultures, and then left at room temperature overnight for further induction. Synchronized L1 worms were placed on RNAi plates and allowed to feed for 24-96h at 20°C, depending on the experiment. The L4440 empty vector was used as a negative control for all RNAi experiments. To improve RNAi knockdown efficiency in the pharyngeal tissue, I used worms harboring the *lin-35(n745)* mutant allele (Shiu and Hunter 2017); and for the gonadal sheath and other tissues the *rrf-3(pk1426)* genetic background (Simmer et al. 2002). I verified knockdown efficiency for all RNAi experiments, with the exception of the targeted RNAi screen and *pat-2; pat-3* double RNAi experiments, by including a control with the relevant mNG/mCherry/mKate2-tagged target protein. I achieved between ~70-100% reduction for all RNAi experiments. For the co-depletion of PAT-2 and RAP-3, I verified knockdown efficiency by plate-level assessment of worm paralysis: RNAi initiated at the L1 larval stage against *pat-2* alone, or *pat-2* and *rap-3* in combination, resulted in 100% paralysis of animals by early adulthood.

A.1.5 Imaging

Confocal DIC and fluorescence images were acquired at 20°C on an AxioImager A1 microscope (Carl Zeiss) controlled by µManager software (Edelstein et al. 2010), and

equipped with an EMCCD camera (Hamamatsu Photonics), a 40x Plan-Apochromat (1.4NA) objective, a spinning disc confocal scan head (CSU-10;Yokogawa Electric Corporation), and 488-nm and 561-nm laser lines. Worms were mounted on 5% noble agar pads containing 0.01M sodium azide for imaging. For all experiments except those detailed in Figure 5 and Figure 13, I captured single-slice images at the middle focal plane of animals where most or all of the gonadal and pharyngeal tissue cross-sections were in focus. For Figure 5, I acquired z-stacks at 1 μ m intervals spanning the entirety of the pharynx or gonad. For Figure 13, I captured single-slice images at a superficial focal plane, where the body wall muscle was in focus.

A.1.6 Image analysis, processing, and quantification

All quantifications of mean fluorescence intensity were done on raw images in FIJI 2.0 (Schindelin et al. 2012). I drew ~5-8-pixel long linescans along the BM to obtain raw values of mean fluorescence intensity. Background intensity values were obtained by averaging two linescans of similar length in regions adjacent to the BM with no visible fluorescence signal. DIC and fluorescence images in all figures were processed in FIJI. The unsharp mask filter was applied to DIC images. 3D isosurface renderings of the pharyngeal and gonadal BMs were constructed using Imaris 7.4 software (Bitplane). Briefly, we acquired z-stacks of pharyngeal and gonadal collagen::mCherry in early L1 and young adult worms. Young adult gonads were imaged in sections, and z-stacks of

individual sections were stitched together with the FIJI pairwise stitching method (Preibisch et al. 2009). 3D isosurfaces were constructed from these z-stacks by manually tracing the outline of BM collagen::mCherry in every z-slice, and surface area measurements were automatically calculated from these isosurfaces by Imaris.

A.1.7 Statistical analysis

Statistical analysis was performed in GraphPad Prism 7. To blind analysis of fluorescence intensity in all datasets, I used a filename-randomizing ImageJ macro (courtesy of Martin Höhne). Sample sizes were validated *a posteriori* through assessments of normality by log-transforming all datasets and then using the Shapiro-Wilk test. For comparisons of mean fluorescence intensities between two populations, I used an unpaired two-tailed Student's *t*-test (with Welch's correction in cases of unequal variance between samples). To compare mean fluorescence intensities between three or more populations, I performed one-way analysis of variance followed by either a post-hoc Dunnett's or Tukey's multiple comparison test. For comparisons of fluorescence intensity ratios, I used a paired two-tailed Student's *t*-test (with Welch's correction in cases of unequal variance between samples). Bar graphs and boxplots were prepared in GraphPad Prism 7. Figure legends indicate sample sizes, statistical tests used, and *p*-values.

References

- Abrams GA, Goodman SL, Nealey PF, Franco M, Murphy CJ. 2000. Nanoscale topography of the basement membrane underlying the corneal epithelium of the rhesus macaque. *Cell Tissue Res* **299**: 39–46.
- Abrams GA, Murphy CJ, Wang Z-Y, Nealey PF, Bjorling DE. 2003. Ultrastructural basement membrane topography of the bladder epithelium. *Urol Res* **31**: 341–346.
- Añazco C, López-Jiménez AJ, Rafi M, Vega-Montoto L, Zhang M-Z, Hudson BG, Vanacore RM. 2016. Lysyl Oxidase-like-2 Cross-links Collagen IV of Glomerular Basement Membrane. *J Biol Chem* **291**: 25999–26012.
- Ancsin JB, Kisilevsky R. 1996. Laminin interactions important for basement membrane assembly are promoted by zinc and implicate laminin zinc finger-like sequences. *J Biol Chem* **271**: 6845–6851.
- Askari JA, Buckley PA, Mould AP, Humphries MJ. 2009. Linking integrin conformation to function. *J Cell Sci* **122**: 165–170.
- Aumailley M, Bruckner-Tuderman L, Carter WG, Deutzmann R, Edgar D, Ekblom P, Engel J, Engvall E, Hohenester E, Jones JCR, et al. 2005. A simplified laminin nomenclature. *Matrix Biol* **24**: 326–332.
- Bader BL, Smyth N, Nedbal S, Miosge N, Baranowsky A, Mokkaapati S, Murshed M, Nischt R. 2005. Compound genetic ablation of nidogen 1 and 2 causes basement membrane defects and perinatal lethality in mice. *Mol Cell Biol* **25**: 6846–6856.
- Baeten KM, Akassoglou K. 2011. Extracellular matrix and matrix receptors in blood-brain barrier formation and stroke. *Dev Neurobiol* **71**: 1018–1039.
- Bai M, Vozdek R, Hnízda A, Jiang C, Wang B, Kuchar L, Li T, Zhang Y, Wood C, Feng L, et al. 2018. Conserved roles of *C. elegans* and human MANFs in sulfatide binding and cytoprotection. *Nat Commun* **9**: 897.
- Ballabh P, Braun A, Nedergaard M. 2004. The blood-brain barrier: an overview: structure, regulation, and clinical implications. *Neurobiol Dis* **16**: 1–13.
- Baum PD, Garriga G. 1997. Neuronal migrations and axon fasciculation are disrupted in *ina-1* integrin mutants. *Neuron* **19**: 51–62.

- Behrens DT, Villone D, Koch M, Brunner G, Sorokin L, Robenek H, Bruckner-Tuderman L, Bruckner P, Hansen U. 2012. The epidermal basement membrane is a composite of separate laminin- or collagen IV-containing networks connected by aggregated perlecan, but not by nidogens. *J Biol Chem* **287**: 18700–18709.
- Bhave G, Colon S, Ferrell N. 2017. The sulfilimine cross-link of collagen IV contributes to kidney tubular basement membrane stiffness. *Am J Physiol Renal Physiol* **313**: F596–F602.
- Boettner B, Van Aelst L. 2009. Control of cell adhesion dynamics by Rap1 signaling. *Curr Opin Cell Biol* **21**: 684–693.
- Bohush A, Niewiadomska G, Weis S, Filippek A. 2019. HSP90 and Its Novel Co-Chaperones, SGT1 and CHP-1, in Brain of Patients with Parkinson’s Disease and Dementia with Lewy Bodies. *J Parkinsons Dis* **9**: 97–107.
- Borradori L, Sonnenberg A. 1999. Structure and function of hemidesmosomes: more than simple adhesion complexes. *J Invest Dermatol* **112**: 411–418.
- Bouvard D, Pouwels J, De Franceschi N, Ivaska J. 2013. Integrin inactivators: balancing cellular functions in vitro and in vivo. *Nat Rev Mol Cell Biol* **14**: 430–442.
- Breitkreutz D, Koxholt I, Thiemann K, Nischt R. 2013. Skin basement membrane: the foundation of epidermal integrity--BM functions and diverse roles of bridging molecules nidogen and perlecan. *Biomed Res Int* **2013**: 179784.
- Brenner S. 1974. The genetics of *Caenorhabditis elegans*. *Genetics* **77**: 71–94.
- Brown NH. 2000. Cell-cell adhesion via the ECM: integrin genetics in fly and worm. *Matrix Biol* **19**: 191–201.
- Bunt S, Hooley C, Hu N, Scahill C, Weavers H, Skaer H. 2010. Hemocyte-secreted type IV collagen enhances BMP signaling to guide renal tubule morphogenesis in *Drosophila*. *Dev Cell* **19**: 296–306.
- Carmona G, Göttig S, Orlandi A, Scheele J, Bäuerle T, Jugold M, Kiessling F, Henschler R, Zeiher AM, Dimmeler S, et al. 2009. Role of the small GTPase Rap1 for integrin activity regulation in endothelial cells and angiogenesis. *Blood* **113**: 488–497.

- Carney TJ, Feitosa NM, Sonntag C, Slanchev K, Kluger J, Kiyozumi D, Gebauer JM, Coffin Talbot J, Kimmel CB, Sekiguchi K, et al. 2010. Genetic analysis of fin development in zebrafish identifies furin and hemicentin1 as potential novel fraser syndrome disease genes. *PLoS Genet* **6**: e1000907.
- Chioran A, Duncan S, Catalano A, Brown TJ, Ringuette MJ. 2017. Collagen IV trafficking: The inside-out and beyond story. *Dev Biol* **431**: 124–133.
- Clay MR, Sherwood DR. 2015. Basement Membranes in the Worm: A Dynamic Scaffolding that Instructs Cellular Behaviors and Shapes Tissues. *Curr Top Membr* **76**: 337–371.
- Comoglio PM, Boccaccio C, Trusolino L. 2003. Interactions between growth factor receptors and adhesion molecules: breaking the rules. *Curr Opin Cell Biol* **15**: 565–571.
- Conte D, MacNeil LT, Walhout AJM, Mello CC. 2015. RNA Interference in *Caenorhabditis elegans*. *Curr Protoc Mol Biol* **109**: 26.3.1–30.
- Copp AJ, Carvalho R, Wallace A, Sorokin L, Sasaki T, Greene NDE, Ybot-Gonzalez P. 2011. Regional differences in the expression of laminin isoforms during mouse neural tube development. *Matrix Biol* **30**: 301–309.
- Corsi AK. 2006. A biochemist's guide to *Caenorhabditis elegans*. *Anal Biochem* **359**: 1–17.
- Crest J, Diz-Muñoz A, Chen D-Y, Fletcher DA, Bilder D. 2017. Organ sculpting by patterned extracellular matrix stiffness. *Elife* **6**.
- Desgrosellier JS, Cheresch DA. 2010. Integrins in cancer: biological implications and therapeutic opportunities. *Nat Rev Cancer* **10**: 9–22.
- Dickinson DJ, Pani AM, Heppert JK, Higgins CD, Goldstein B. 2015. Streamlined Genome Engineering with a Self-Excising Drug Selection Cassette. *Genetics* **200**: 1035–1049.
- Edelstein A, Amodaj N, Hoover K, Vale R, Stuurman N. 2010. Computer control of microscopes using μ Manager. *Curr Protoc Mol Biol* **Chapter 14**: Unit14.20.

- Fan C, Zhao J, Zhao B, Zhang S, Miao J. 2009. Novel complex of copper and a salicylaldehyde pyrazole hydrazone derivative induces apoptosis through up-regulating integrin beta 4 in vascular endothelial cells. *Chem Res Toxicol* **22**: 1517–1525.
- Fares H, Greenwald I. 2001. Regulation of endocytosis by CUP-5, the *Caenorhabditis elegans* mucolipin-1 homolog. *Nat Genet* **28**: 64–68.
- Feitosa NM, Zhang J, Carney TJ, Metzger M, Korzh V, Bloch W, Hammerschmidt M. 2012. Hemicentin 2 and Fibulin 1 are required for epidermal-dermal junction formation and fin mesenchymal cell migration during zebrafish development. *Dev Biol* **369**: 235–248.
- Ferretti R, Palumbo V, Di Savino A, Velasco S, Sbroggiò M, Sportoletti P, Micale L, Turco E, Silengo L, Palumbo G, et al. 2010. Morgana/chp-1, a ROCK inhibitor involved in centrosome duplication and tumorigenesis. *Dev Cell* **18**: 486–495.
- Fidler AL, Boudko SP, Rokas A, Hudson BG. 2018. The triple helix of collagens - an ancient protein structure that enabled animal multicellularity and tissue evolution. *J Cell Sci* **131**.
- Fidler AL, Darris CE, Chetyrkin SV, Pedchenko VK, Boudko SP, Brown KL, Gray Jerome W, Hudson JK, Rokas A, Hudson BG. 2017. Collagen IV and basement membrane at the evolutionary dawn of metazoan tissues. *Elife* **6**.
- Fitzgerald MC, Schwarzbauer JE. 1998. Importance of the basement membrane protein SPARC for viability and fertility in *Caenorhabditis elegans*. *Curr Biol* **8**: 1285–1288.
- Gautam J, Zhang X, Yao Y. 2016. The role of pericytic laminin in blood brain barrier integrity maintenance. *Sci Rep* **6**: 36450.
- Gerdt S, Dennis RD, Borgonie G, Schnabel R, Geyer R. 1999. Isolation, characterization and immunolocalization of phosphorylcholine-substituted glycolipids in developmental stages of *Caenorhabditis elegans*. *Eur J Biochem* **266**: 952–963.
- Gerdt S, Lochnit G, Dennis RD, Geyer R. 1997. Isolation and structural analysis of three neutral glycosphingolipids from a mixed population of *Caenorhabditis elegans* (Nematoda: Rhabditida). *Glycobiology* **7**: 265–275.

- Giannelli G, Falk-Marzillier J, Schiraldi O, Stetler-Stevenson WG, Quaranta V. 1997. Induction of cell migration by matrix metalloprotease-2 cleavage of laminin-5. *Science* **277**: 225–228.
- Glentis A, Gurchenkov V, Matic Vignjevic D. 2014. Assembly, heterogeneity, and breaching of the basement membranes. *Cell Adh Migr* **8**: 236–245.
- Goldberg S, Harvey SJ, Cunningham J, Tryggvason K, Miner JH. 2009. Glomerular filtration is normal in the absence of both agrin and perlecan-heparan sulfate from the glomerular basement membrane. *Nephrol Dial Transplant* **24**: 2044–2051.
- Graham PL, Johnson JJ, Wang S, Sibley MH, Gupta MC, Kramer JM. 1997. Type IV collagen is detectable in most, but not all, basement membranes of *Caenorhabditis elegans* and assembles on tissues that do not express it. *J Cell Biol* **137**: 1171–1183.
- Grau-Bové X, Torruella G, Donachie S, Suga H, Leonard G, Richards TA, Ruiz-Trillo I. 2017. Dynamics of genomic innovation in the unicellular ancestry of animals. *Elife* **6**.
- Gupta MC, Graham PL, Kramer JM. 1997. Characterization of alpha1(IV) collagen mutations in *Caenorhabditis elegans* and the effects of alpha1 and alpha2(IV) mutations on type IV collagen distribution. *J Cell Biol* **137**: 1185–1196.
- Gustavsson A-K, Petrov PN, Lee MY, Shechtman Y, Moerner WE. 2018. 3D single-molecule super-resolution microscopy with a tilted light sheet. *Nat Commun* **9**: 123.
- Hagedorn EJ, Yashiro H, Ziel JW, Ihara S, Wang Z, Sherwood DR. 2009. Integrin acts upstream of netrin signaling to regulate formation of the anchor cell's invasive membrane in *C. elegans*. *Dev Cell* **17**: 187–198.
- Hagedorn EJ, Ziel JW, Morrissey MA, Linden LM, Wang Z, Chi Q, Johnson SA, Sherwood DR. 2013. The netrin receptor DCC focuses invadopodia-driven basement membrane transmigration in vivo. *J Cell Biol* **201**: 903–913.
- Halfter W, Oertle P, Monnier CA, Camenzind L, Reyes-Lua M, Hu H, Candiello J, Labilloy A, Balasubramani M, Henrich PB, et al. 2015. New concepts in basement membrane biology. *FEBS J* **282**: 4466–4479.

- Harunaga JS, Doyle AD, Yamada KM. 2014. Local and global dynamics of the basement membrane during branching morphogenesis require protease activity and actomyosin contractility. *Dev Biol* **394**: 197–205.
- Hegde S, Raghavan S. 2013. A skin-depth analysis of integrins: role of the integrin network in health and disease. *Cell Commun Adhes* **20**: 155–169.
- Hinck L, Silberstein GB. 2005. Key stages in mammary gland development: the mammary end bud as a motile organ. *Breast Cancer Res* **7**: 245–251.
- Hohenester E, Yurchenco PD. 2013. Laminins in basement membrane assembly. *Cell Adh Migr* **7**: 56–63.
- Horton ER, Byron A, Askari JA, Ng DHJ, Millon-Frémillon A, Robertson J, Koper EJ, Paul NR, Warwood S, Knight D, et al. 2015. Definition of a consensus integrin adhesome and its dynamics during adhesion complex assembly and disassembly. *Nat Cell Biol* **17**: 1577–1587.
- Horton ER, Humphries JD, James J, Jones MC, Askari JA, Humphries MJ. 2016. The integrin adhesome network at a glance. *J Cell Sci* **129**: 4159–4163.
- Huang C-C, Hall DH, Hedgecock EM, Kao G, Karantza V, Vogel BE, Hutter H, Chisholm AD, Yurchenco PD, Wadsworth WG. 2003. Laminin alpha subunits and their role in *C. elegans* development. *Development* **130**: 3343–3358.
- Ihara S, Hagedorn EJ, Morrissey MA, Chi Q, Motegi F, Kramer JM, Sherwood DR. 2011. Basement membrane sliding and targeted adhesion remodels tissue boundaries during uterine-vulval attachment in *Caenorhabditis elegans*. *Nat Cell Biol* **13**: 641–651.
- Ihara S, Nakayama S, Murakami Y, Suzuki E, Asakawa M, Kinoshita T, Sawa H. 2017. PIGN prevents protein aggregation in the endoplasmic reticulum independently of its function in the GPI synthesis. *J Cell Sci* **130**: 602–613.
- Iozzo RV. 2005. Basement membrane proteoglycans: from cellar to ceiling. *Nat Rev Mol Cell Biol* **6**: 646–656.
- Iozzo RV, Zoeller JJ, Nyström A. 2009. Basement membrane proteoglycans: modulators Par Excellence of cancer growth and angiogenesis. *Mol Cells* **27**: 503–513.

- Isabella AJ, Horne-Badovinac S. 2015a. Building from the Ground up: Basement Membranes in *Drosophila* Development. *Curr Top Membr* **76**: 305–336.
- Isabella AJ, Horne-Badovinac S. 2015b. Dynamic regulation of basement membrane protein levels promotes egg chamber elongation in *Drosophila*. *Dev Biol* **406**: 212–221.
- Isabella AJ, Horne-Badovinac S. 2016. Rab10-Mediated Secretion Synergizes with Tissue Movement to Build a Polarized Basement Membrane Architecture for Organ Morphogenesis. *Dev Cell* **38**: 47–60.
- Jayadev R, Sherwood DR. 2017. Basement membranes. *Curr Biol* **27**: R207–R211.
- Jensen D, Schekman R. 2011. COPII-mediated vesicle formation at a glance. *J Cell Sci* **124**: 1–4.
- Jeon TJ, Lee D-J, Merlot S, Weeks G, Firtel RA. 2007. Rap1 controls cell adhesion and cell motility through the regulation of myosin II. *J Cell Biol* **176**: 1021–1033.
- Johnson RP, Kang SH, Kramer JM. 2006. *C. elegans* dystroglycan DGN-1 functions in epithelia and neurons, but not muscle, and independently of dystrophin. *Development* **133**: 1911–1921.
- Kalluri R. 2003. Basement membranes: structure, assembly and role in tumour angiogenesis. *Nat Rev Cancer* **3**: 422–433.
- Kamath RS, Fraser AG, Dong Y, Poulin G, Durbin R, Gotta M, Kanapin A, Le Bot N, Moreno S, Sohrmann M, et al. 2003. Systematic functional analysis of the *Caenorhabditis elegans* genome using RNAi. *Nature* **421**: 231–237.
- Kang SH, Kramer JM. 2000. Nidogen is nonessential and not required for normal type IV collagen localization in *Caenorhabditis elegans*. *Mol Biol Cell* **11**: 3911–3923.
- Karsdal MA, Genovese F, Madsen EA, Manon-Jensen T, Schuppan D. 2016. Collagen and tissue turnover as a function of age: Implications for fibrosis. *J Hepatol* **64**: 103–109.
- Katagiri K, Ohnishi N, Kabashima K, Iyoda T, Takeda N, Shinkai Y, Inaba K, Kinashi T. 2004. Crucial functions of the Rap1 effector molecule RAPL in lymphocyte and dendritic cell trafficking. *Nat Immunol* **5**: 1045–1051.

- Kedinger M, Lefebvre O, Duluc I, Freund JN, Simon-Assmann P. 1998. Cellular and molecular partners involved in gut morphogenesis and differentiation. *Philos Trans R Soc Lond B, Biol Sci* **353**: 847–856.
- Keeley DP, Sherwood DR. 2019. Tissue linkage through adjoining basement membranes: The long and the short term of it. *Matrix Biol* **75-76**: 58–71.
- Kelley LC, Lohmer LL, Hagedorn EJ, Sherwood DR. 2014. Traversing the basement membrane in vivo: a diversity of strategies. *J Cell Biol* **204**: 291–302.
- Kessenbrock K, Plaks V, Werb Z. 2010. Matrix metalloproteinases: regulators of the tumor microenvironment. *Cell* **141**: 52–67.
- Khoshnoodi J, Pedchenko V, Hudson BG. 2008. Mammalian collagen IV. *Microsc Res Tech* **71**: 357–370.
- Klapholz B, Brown NH. 2017. Talin - the master of integrin adhesions. *J Cell Sci* **130**: 2435–2446.
- Kramer JM. 2005. Basement membranes. *WormBook* 1–15.
- Kubota Y, Nagata K, Sugimoto A, Nishiwaki K. 2012. Tissue architecture in the *Caenorhabditis elegans* gonad depends on interactions among fibulin-1, type IV collagen and the ADAMTS extracellular protease. *Genetics* **190**: 1379–1388.
- Lagarrigue F, Kim C, Ginsberg MH. 2016. The Rap1-RIAM-talin axis of integrin activation and blood cell function. *Blood* **128**: 479–487.
- Laurie GW, Bing JT, Kleinman HK, Hassell JR, Aumailley M, Martin GR, Feldmann RJ. 1986. Localization of binding sites for laminin, heparan sulfate proteoglycan and fibronectin on basement membrane (type IV) collagen. *J Mol Biol* **189**: 205–216.
- Leitinger B. 2014. Discoidin domain receptor functions in physiological and pathological conditions. *Int Rev Cell Mol Biol* **310**: 39–87.
- Li S, Edgar D, Fässler R, Wadsworth W, Yurchenco PD. 2003. The role of laminin in embryonic cell polarization and tissue organization. *Dev Cell* **4**: 613–624.

- Li S, Harrison D, Carbonetto S, Fassler R, Smyth N, Edgar D, Yurchenco PD. 2002. Matrix assembly, regulation, and survival functions of laminin and its receptors in embryonic stem cell differentiation. *J Cell Biol* **157**: 1279–1290.
- Li S, Liquari P, McKee KK, Harrison D, Patel R, Lee S, Yurchenco PD. 2005. Laminin-sulfatide binding initiates basement membrane assembly and enables receptor signaling in Schwann cells and fibroblasts. *J Cell Biol* **169**: 179–189.
- Li S, Qi Y, McKee K, Liu J, Hsu J, Yurchenco PD. 2017. Integrin and dystroglycan compensate each other to mediate laminin-dependent basement membrane assembly and epiblast polarization. *Matrix Biol* **57-58**: 272–284.
- Lilja J, Zacharchenko T, Georgiadou M, Jacquemet G, Franceschi ND, Peuhu E, Hamidi H, Pouwels J, Martens V, Nia FH, et al. 2017. SHANK proteins limit integrin activation by directly interacting with Rap1 and R-Ras. *Nat Cell Biol* **19**: 292–305.
- Liu J, Wang Z, Thinn AMM, Ma Y-Q, Zhu J. 2015. The dual structural roles of the membrane distal region of the α -integrin cytoplasmic tail during integrin inside-out activation. *J Cell Sci* **128**: 1718–1731.
- Longmate WM, Dipersio CM. 2014. Integrin regulation of epidermal functions in wounds. *Adv Wound Care (New Rochelle)* **3**: 229–246.
- Lu P, Weaver VM, Werb Z. 2012. The extracellular matrix: a dynamic niche in cancer progression. *J Cell Biol* **196**: 395–406.
- Ma M, Cao X, Dai J, Pastor-Pareja JC. 2017. Basement membrane manipulation in drosophila wing discs affects dpp retention but not growth mechanoregulation. *Dev Cell* **42**: 97–106.e4.
- Mango SE. 2007. The C. elegans pharynx: a model for organogenesis. *WormBook* 1–26.
- Mao M, Alavi MV, Labelle-Dumais C, Gould DB. 2015. Type IV collagens and basement membrane diseases: cell biology and pathogenic mechanisms. *Curr Top Membr* **76**: 61–116.
- Margadant C, Raymond K, Kreft M, Sachs N, Janssen H, Sonnenberg A. 2009. Integrin $\alpha3\beta1$ inhibits directional migration and wound re-epithelialization in the skin. *J Cell Sci* **122**: 278–288.

- Marshall CB. 2016. Rethinking glomerular basement membrane thickening in diabetic nephropathy: adaptive or pathogenic? *Am J Physiol Renal Physiol* **311**: F831–F843.
- Martinek N, Shahab J, Saathoff M, Ringuette M. 2008. Haemocyte-derived SPARC is required for collagen-IV-dependent stability of basal laminae in *Drosophila* embryos. *J Cell Sci* **121**: 1671–1680.
- Marutani T, Yamamoto A, Nagai N, Kubota H, Nagata K. 2004. Accumulation of type IV collagen in dilated ER leads to apoptosis in Hsp47-knockout mouse embryos via induction of CHOP. *J Cell Sci* **117**: 5913–5922.
- Matsubayashi Y, Louani A, Dragu A, Sánchez-Sánchez BJ, Serna-Morales E, Yolland L, Gyoergy A, Vizcay G, Fleck RA, Heddleston JM, et al. 2017. A moving source of matrix components is essential for de novo basement membrane formation. *Curr Biol* **27**: 3526–3534.e4.
- Matsuoka Y, Kubota H, Adachi E, Nagai N, Marutani T, Hosokawa N, Nagata K. 2004. Insufficient folding of type IV collagen and formation of abnormal basement membrane-like structure in embryoid bodies derived from Hsp47-null embryonic stem cells. *Mol Biol Cell* **15**: 4467–4475.
- McAteer JA, Dougherty GS, Gardner KD, Evan AP. 1988. Polarized epithelial cysts in vitro: a review of cell and explant culture systems that exhibit epithelial cyst formation. *Scanning Microsc* **2**: 1739–1763.
- McClatchey ST, Wang Z, Linden LM, Hastie EL, Wang L, Shen W, Chen A, Chi Q, Sherwood DR. 2016. Boundary cells restrict dystroglycan trafficking to control basement membrane sliding during tissue remodeling. *Elife* **5**.
- Miner JH. 2011. Glomerular basement membrane composition and the filtration barrier. *Pediatr Nephrol* **26**: 1413–1417.
- Miner JH. 2012. The glomerular basement membrane. *Exp Cell Res* **318**: 973–978.
- Miner JH, Li C, Mudd JL, Go G, Sutherland AE. 2004. Compositional and structural requirements for laminin and basement membranes during mouse embryo implantation and gastrulation. *Development* **131**: 2247–2256.
- Miner JH, Yurchenco PD. 2004. Laminin functions in tissue morphogenesis. *Annu Rev Cell Dev Biol* **20**: 255–284.

- Morris AWJ, Carare RO, Schreiber S, Hawkes CA. 2014. The Cerebrovascular Basement Membrane: Role in the Clearance of β -amyloid and Cerebral Amyloid Angiopathy. *Front Aging Neurosci* **6**: 251.
- Morrissey MA, Jayadev R, Miley GR, Blebea CA, Chi Q, Ihara S, Sherwood DR. 2016. SPARC promotes cell invasion in vivo by decreasing type IV collagen levels in the basement membrane. *PLoS Genet* **12**: e1005905.
- Morrissey MA, Keeley DP, Hagedorn EJ, McClatchey STH, Chi Q, Hall DH, Sherwood DR. 2014. B-LINK: a hemidentin, plakin, and integrin-dependent adhesion system that links tissues by connecting adjacent basement membranes. *Dev Cell* **31**: 319–331.
- Morrissey MA, Sherwood DR. 2015. An active role for basement membrane assembly and modification in tissue sculpting. *J Cell Sci* **128**: 1661–1668.
- Naba A, Clauser KR, Lamar JM, Carr SA, Hynes RO. 2014. Extracellular matrix signatures of human mammary carcinoma identify novel metastasis promoters. *Elife* **3**: e01308.
- Naegeli KM, Hastie E, Garde A, Wang Z, Keeley DP, Gordon KL, Pani AM, Kelley LC, Morrissey MA, Chi Q, et al. 2017. Cell Invasion In Vivo via Rapid Exocytosis of a Transient Lysosome-Derived Membrane Domain. *Dev Cell* **43**: 403–417.e10.
- Nishiwaki K, Hisamoto N, Matsumoto K. 2000. A metalloprotease disintegrin that controls cell migration in *Caenorhabditis elegans*. *Science* **288**: 2205–2208.
- Norman KR, Moerman DG. 2000. The let-268 locus of *Caenorhabditis elegans* encodes a procollagen lysyl hydroxylase that is essential for type IV collagen secretion. *Dev Biol* **227**: 690–705.
- Page-McCaw A, Ewald AJ, Werb Z. 2007. Matrix metalloproteinases and the regulation of tissue remodelling. *Nat Rev Mol Cell Biol* **8**: 221–233.
- Pastor-Pareja JC, Xu T. 2011. Shaping cells and organs in *Drosophila* by opposing roles of fat body-secreted Collagen IV and perlecan. *Dev Cell* **21**: 245–256.

- Pedchenko V, Zent R, Hudson BG. 2004. Alpha(v)beta3 and alpha(v)beta5 integrins bind both the proximal RGD site and non-RGD motifs within noncollagenous (NC1) domain of the alpha3 chain of type IV collagen: implication for the mechanism of endothelial cell adhesion. *J Biol Chem* **279**: 2772–2780.
- Pöschl E, Schlötzer-Schrehardt U, Brachvogel B, Saito K, Ninomiya Y, Mayer U. 2004. Collagen IV is essential for basement membrane stability but dispensable for initiation of its assembly during early development. *Development* **131**: 1619–1628.
- Pozzi A, Yurchenco PD, Iozzo RV. 2017. The nature and biology of basement membranes. *Matrix Biol* **57-58**: 1–11.
- Preibisch S, Saalfeld S, Tomancak P. 2009. Globally optimal stitching of tiled 3D microscopic image acquisitions. *Bioinformatics* **25**: 1463–1465.
- Ramos-Lewis W, LaFever KS, Page-McCaw A. 2018. A scar-like lesion is apparent in basement membrane after wound repair in vivo. *Matrix Biol* **74**: 101–120.
- Randles MJ, Humphries MJ, Lennon R. 2017. Proteomic definitions of basement membrane composition in health and disease. *Matrix Biol* **57-58**: 12–28.
- Rao W, Isaac RE, Keen JN. 2011. An analysis of the *Caenorhabditis elegans* lipid raft proteome using geLC-MS/MS. *J Proteomics* **74**: 242–253.
- Rasmussen JP, Reddy SS, Priess JR. 2012. Laminin is required to orient epithelial polarity in the *C. elegans* pharynx. *Development* **139**: 2050–2060.
- Rasmussen NR, Dickinson DJ, Reiner DJ. 2018. Ras-Dependent Cell Fate Decisions Are Reinforced by the RAP-1 Small GTPase in *Caenorhabditis elegans*. *Genetics* **210**: 1339–1354.
- Reiner DJ, Lundquist EA. 2018. Small GTPases. *WormBook* **2018**: 1–65.
- Revert F, Merino R, Monteagudo C, Macias J, Peydró A, Alcácer J, Muniesa P, Marquina R, Blanco M, Iglesias M, et al. 2007. Increased Goodpasture antigen-binding protein expression induces type IV collagen disorganization and deposit of immunoglobulin A in glomerular basement membrane. *Am J Pathol* **171**: 1419–1430.

- Revert F, Penadés JR, Plana M, Bernal D, Johansson C, Itarte E, Cervera J, Wieslander J, Quinones S, Saus J. 1995. Phosphorylation of the Goodpasture antigen by type A protein kinases. *J Biol Chem* **270**: 13254–13261.
- Roy S, Ha J, Trudeau K, Beglova E. 2010. Vascular basement membrane thickening in diabetic retinopathy. *Curr Eye Res* **35**: 1045–1056.
- Rual J-F, Ceron J, Koreth J, Hao T, Nicot A-S, Hirozane-Kishikawa T, Vandenhautte J, Orkin SH, Hill DE, van den Heuvel S, et al. 2004. Toward improving *Caenorhabditis elegans* phenome mapping with an ORFeome-based RNAi library. *Genome Res* **14**: 2162–2168.
- Savaris R, Chies JAB. 2003. Copper ions dynamically regulate beta3 integrin subunit expression in Ishikawa cells. *Contraception* **67**: 247–249.
- Schindelin J, Arganda-Carreras I, Frise E, Kaynig V, Longair M, Pietzsch T, Preibisch S, Rueden C, Saalfeld S, Schmid B, et al. 2012. Fiji: an open-source platform for biological-image analysis. *Nat Methods* **9**: 676–682.
- Schmidt O, Teis D. 2012. The ESCRT machinery. *Curr Biol* **22**: R116–20.
- Sekiguchi R, Yamada KM. 2018. Basement membranes in development and disease. *Curr Top Dev Biol* **130**: 143–191.
- Shahab J, Baratta C, Scuric B, Godt D, Venken KJT, Ringuette MJ. 2015. Loss of SPARC dysregulates basal lamina assembly to disrupt larval fat body homeostasis in *Drosophila melanogaster*. *Dev Dyn* **244**: 540–552.
- Sherwood DR, Plastino J. 2018. Invading, Leading and Navigating Cells in *Caenorhabditis elegans*: Insights into Cell Movement in Vivo. *Genetics* **208**: 53–78.
- Shiu PK, Hunter CP. 2017. Early Developmental Exposure to dsRNA Is Critical for Initiating Efficient Nuclear RNAi in *C. elegans*. *Cell Rep* **18**: 2969–2978.
- Simmer F, Tijsterman M, Parrish S, Koushika SP, Nonet ML, Fire A, Ahringer J, Plasterk RHA. 2002. Loss of the putative RNA-directed RNA polymerase RRF-3 makes *C. elegans* hypersensitive to RNAi. *Curr Biol* **12**: 1317–1319.

- Starich TA, Hall DH, Greenstein D. 2014. Two classes of gap junction channels mediate soma-germline interactions essential for germline proliferation and gametogenesis in *Caenorhabditis elegans*. *Genetics* **198**: 1127–1153.
- Stiernagle T. 2006. Maintenance of *C. elegans*. *WormBook* 1–11.
- Suh JH, Miner JH. 2013. The glomerular basement membrane as a barrier to albumin. *Nat Rev Nephrol* **9**: 470–477.
- Sun Z, Costell M, Fässler R. 2019. Integrin activation by talin, kindlin and mechanical forces. *Nat Cell Biol* **21**: 25–31.
- Tanjore H, Kalluri R. 2006. The role of type IV collagen and basement membranes in cancer progression and metastasis. *Am J Pathol* **168**: 715–717.
- Thein MC, Winter AD, Stepek G, McCormack G, Stapleton G, Johnstone IL, Page AP. 2009. Combined extracellular matrix cross-linking activity of the peroxidase MLT-7 and the dual oxidase BLI-3 is critical for post-embryonic viability in *Caenorhabditis elegans*. *J Biol Chem* **284**: 17549–17563.
- Thinn AMM, Wang Z, Zhu J. 2018. The membrane-distal regions of integrin α cytoplasmic domains contribute differently to integrin inside-out activation. *Sci Rep* **8**: 5067.
- Timmons L, Court DL, Fire A. 2001. Ingestion of bacterially expressed dsRNAs can produce specific and potent genetic interference in *Caenorhabditis elegans*. *Gene* **263**: 103–112.
- Timmons L, Fire A. 1998. Specific interference by ingested dsRNA. *Nature* **395**: 854.
- Tsiper MV, Yurchenco PD. 2002. Laminin assembles into separate basement membrane and fibrillar matrices in Schwann cells. *J Cell Sci* **115**: 1005–1015.
- Urbano JM, Torgler CN, Molnar C, Tepass U, López-Varea A, Brown NH, de Celis JF, Martín-Bermudo MD. 2009. *Drosophila* laminins act as key regulators of basement membrane assembly and morphogenesis. *Development* **136**: 4165–4176.
- Uspenskaia O, Liebetrau M, Herms J, Danek A, Hamann GF. 2004. Aging is associated with increased collagen type IV accumulation in the basal lamina of human cerebral microvessels. *BMC Neurosci* **5**: 37.

- van Horssen J, Bö L, Vos CMP, Virtanen I, de Vries HE. 2005. Basement membrane proteins in multiple sclerosis-associated inflammatory cuffs: potential role in influx and transport of leukocytes. *J Neuropathol Exp Neurol* **64**: 722–729.
- van Horssen J, Dijkstra CD, de Vries HE. 2007. The extracellular matrix in multiple sclerosis pathology. *J Neurochem* **103**: 1293–1301.
- Vanacore R, Ham A-JL, Voehler M, Sanders CR, Conrads TP, Veenstra TD, Sharpless KB, Dawson PE, Hudson BG. 2009. A sulfilimine bond identified in collagen IV. *Science* **325**: 1230–1234.
- Walko G, Castañón MJ, Wiche G. 2015. Molecular architecture and function of the hemidesmosome. *Cell Tissue Res* **360**: 363–378.
- Wang M, Casey PJ. 2016. Protein prenylation: unique fats make their mark on biology. *Nat Rev Mol Cell Biol* **17**: 110–122.
- Wang X, Harris RE, Bayston LJ, Ashe HL. 2008. Type IV collagens regulate BMP signalling in *Drosophila*. *Nature* **455**: 72–77.
- Weber KS, Klickstein LB, Weber C. 1999. Specific activation of leukocyte beta2 integrins lymphocyte function-associated antigen-1 and Mac-1 by chemokines mediated by distinct pathways via the alpha subunit cytoplasmic domains. *Mol Biol Cell* **10**: 861–873.
- Wilson JM, Prokop JW, Lorimer E, Ntantie E, Williams CL. 2016. Differences in the Phosphorylation-Dependent Regulation of Prenylation of Rap1A and Rap1B. *J Mol Biol* **428**: 4929–4945.
- Wiradjaja F, DiTommaso T, Smyth I. 2010. Basement membranes in development and disease. *Birth Defects Res C Embryo Today* **90**: 8–31.
- Wolfenson H, Lavelin I, Geiger B. 2013. Dynamic regulation of the structure and functions of integrin adhesions. *Dev Cell* **24**: 447–458.
- Xiao R, Xu XZS. 2011. *C. elegans* TRP channels. *Adv Exp Med Biol* **704**: 323–339.
- Xu J, Rodriguez D, Petitclerc E, Kim JJ, Hangai M, Moon YS, Davis GE, Brooks PC. 2001. Proteolytic exposure of a cryptic site within collagen type IV is required for angiogenesis and tumor growth in vivo. *J Cell Biol* **154**: 1069–1079.

- Xu L, Nirwane A, Yao Y. 2018. Basement membrane and blood–brain barrier. *Stroke Vasc Neurol* svn–2018–000198.
- Yan Q, Blake D, Clark JI, Sage EH. 2003. Expression of the matricellular protein SPARC in murine lens: SPARC is necessary for the structural integrity of the capsular basement membrane. *J Histochem Cytochem* **51**: 503–511.
- Yurchenco PD. 2011. Basement membranes: cell scaffoldings and signaling platforms. *Cold Spring Harb Perspect Biol* **3**.
- Yurchenco PD. 2015. Integrating Activities of Laminins that Drive Basement Membrane Assembly and Function. *Curr Top Membr* **76**: 1–30.
- Yurchenco PD, Patton BL. 2009. Developmental and pathogenic mechanisms of basement membrane assembly. *Curr Pharm Des* **15**: 1277–1294.
- Yurchenco PD, Ruben GC. 1987. Basement membrane structure in situ: evidence for lateral associations in the type IV collagen network. *J Cell Biol* **105**: 2559–2568.
- Zarow C, Barron E, Chui HC, Perlmutter LS. 1997. Vascular basement membrane pathology and Alzheimer's disease. *Ann N Y Acad Sci* **826**: 147–160.
- Zhang K, Chen J. 2012. The regulation of integrin function by divalent cations. *Cell Adh Migr* **6**: 20–29.
- Zhang Y, Wang H. 2012. Integrin signalling and function in immune cells. *Immunology* **135**: 268–275.

Biography

Ranjay Jayadev attended the National University of Singapore (NUS) where he completed his Bachelor of Science in Life Sciences with honors in 2012. At NUS, Ranjay worked in the laboratory of Dr. Maki Murata-Hori, studying the role of α -actinin in mammalian cell division. After completing his undergraduate studies, Ranjay worked as a research intern in the laboratory of Dr. Snezhana Oliferenko, where he studied endoplasmic reticulum biology in fission yeast. Ranjay was named a Duke University Chancellor's Scholar in 2013. Ranjay is an author on the following publications:

Jayadev R, Chi Q, Keeley DP, Hastie EL, Sherwood DR. 2019. α -integrins dictate distinct modes of type IV collagen recruitment to basement membranes. *In press*.

Jayadev R, Sherwood DR. 2017. Morphogenesis: Shaping tissues through extracellular force gradients. *Curr Biol* 27(17):R850-R852.

Jayadev R, Sherwood DR. 2017. Basement membranes. *Curr Biol* 27(6):R207-R211.

Jayadev R, Sherwood DR. 2016. Tissue sculpting by fibrils. *Dev Cell* 38(1):1-3.

Morrissey MA, **Jayadev R**, Miley GR, Blebea CA, Chi Q, Ihara S, Sherwood DR. 2016. SPARC promotes cell invasion in vivo by decreasing type IV collagen levels in the basement membrane. *PLoS Genet* 12(2):e1005905.

Lohmer LL, Clay MR, Naegeli KM, Chi Q, Ziel JW, Hagedorn EJ, Park JE, **Jayadev R**, Sherwood DR. 2016. A sensitized screen for genes promoting invadopodia function in vivo: CDC-42 and Rab GDI-1 direct distinct aspects of invadopodia formation. *PLoS Genet* 12(1):e1005786.

Jayadev R, Kuk CY, Low SH, Murata-Hori M. 2012. Calcium sensitivity of α -actinin is required for equatorial actin assembly during cytokinesis. *Cell Cycle* 11(10):1929-1937. PMID: 22544326